

# **The influence of iron (Fe) nutritional status on plant-pathogen interactions**

Dissertation

zur Erlangung des  
Doktorgrades der Agrarwissenschaften (Dr. agr.)

an der

Naturwissenschaftlichen Fakultät III  
der Martin-Luther-Universität  
Halle-Wittenberg

vorgelegt

von Herrn Fanghua Ye

geb. am 04.05.1975 in Zhejiang, China

Gutachter

1. Prof. Dr. Nicolaus von Wirén
2. Prof. Dr. Holger B. Deising
3. Prof. Dr. Ralph Hüchelhoven

Verteidigt am 21.12.2015



# Table of contents

1	Introduction .....	7
1.1	Iron in living organisms.....	7
1.2	Fe nutrition of higher plants.....	8
1.2.1	Fe uptake from soil .....	8
1.2.2	Fe translocation and subcellular compartmentalization .....	10
1.3	Fe acquisition in pathogenic fungi .....	12
1.3.1	The reductive Fe assimilation (RIA) pathway .....	13
1.3.2	The siderophore-mediated Fe acquisition (SIA) pathway .....	14
1.4	Fe in plant-pathogen interaction.....	15
1.5	Plant-pathogen systems with <i>Colletotrichum</i> .....	16
1.5.1	The maize- <i>Colletotrichum graminicola</i> pathosystem .....	16
1.5.2	The Arabidopsis- <i>Colletotrichum higginsianum</i> pathosystem .....	18
1.6	Aims of this study .....	18
2	Fe in the maize- <i>Colletotrichum graminicola</i> interaction.....	21
2.1	Material and methods.....	21
2.1.1	Plant material and growth conditions.....	21
2.1.2	Fungal culture and plant inoculation .....	21
2.1.3	Infection assays.....	22
2.1.3.1	Detection of lesion areas.....	22
2.1.3.2	Quantification of fungal DNA .....	22
2.1.4	Histological staining and microscopy.....	23
2.1.4.1	Light microscopy .....	23
2.1.4.2	Prussian blue staining.....	23
2.1.4.3	DAB staining .....	23
2.1.4.4	Scanning electron microscopy (SEM) .....	24
2.1.4.5	Transmission electron microscopy (TEM) .....	24
2.1.5	Gene expression analysis .....	24

2.1.6	Quantification of the plant Fe nutritional status .....	25
2.1.6.1	Determination of chlorophyll concentration .....	25
2.1.6.2	Determination of total Fe concentration .....	25
2.1.7	Fe fractionation in maize leaves during <i>C. graminicola</i> infection .....	25
2.2	Results .....	27
2.2.1	The influence of the Fe nutritional status on the susceptibility of maize plants to <i>C. graminicola</i> infection .....	27
2.2.1.1	Infection of WT UH002 with <i>C. graminicola</i> .....	27
2.2.1.2	Infection of the maize mutant <i>ys1</i> with <i>C. graminicola</i> .....	29
2.2.2	Iron resupply restores the tolerance of Fe-deficient maize plants to <i>C. graminicola</i> .....	32
2.2.3	Fungal growth and development in dependence of the Fe nutritional status of maize leaves.....	33
2.2.4	Influence of the Fe nutritional status on Fe distribution in maize leaves during <i>C. graminicola</i> infection.....	35
2.2.4.1	Fe accumulation at infection sites of <i>C. graminicola</i> .....	35
2.2.4.2	Analysis of different Fe fractions in maize leaves during <i>C. graminicola</i> infection.....	37
2.2.5	The Fe nutritional status of maize leaves affects H <sub>2</sub> O <sub>2</sub> production during <i>C. graminicola</i> infection.....	39
2.2.6	The Fe nutritional status in maize influence Fe homeostasis-related gene expression during <i>C. graminicola</i> infection.....	41
2.2.7	Influence of the Fe nutritional status of maize plants on the infection by fungal mutants defective in Fe acquisition.....	44
2.2.7.1	Infection assay with fungal mutants .....	44
2.2.7.2	Influence of the Fe nutritional status of maize leaves on the development of <i>Colletotrichum</i> mutants with disabled Fe acquisition.....	46
2.2.7.3	Influence of fungal Fe acquisition pathways on local Fe accumulation at the infection sites.....	48
2.2.7.4	Influence of fungal Fe acquisition pathways on local H <sub>2</sub> O <sub>2</sub> formation at the infection sites.....	49
2.2.8	Fe deficiency affects maize leaf structure.....	50
3	Fe in Arabidopsis- <i>Colletotrichum higginsianum</i> interaction.....	52
3.1	Material and methods.....	52

3.1.1	Plant material and growth conditions .....	52
3.1.1.1	Hydroponic culture .....	52
3.1.1.2	Soil culture .....	53
3.1.2	Fungal culture and plant inoculation .....	53
3.1.3	Infection assays .....	54
3.1.3.1	Determination of disease scores .....	54
3.1.3.2	Determination of lesion areas.....	54
3.1.3.3	Quantification of fungal RNA .....	54
3.1.4	Quantification of the Fe nutritional status in Arabidopsis plants.....	55
3.1.4.1	Determination of chlorophyll concentration .....	55
3.1.4.2	Determination of total Fe concentration .....	55
3.1.5	Histological staining and microscopy .....	55
3.1.5.1	Light microscopy .....	55
3.1.5.2	Prussian blue staining.....	55
3.1.5.3	DAB staining .....	56
3.2	Results .....	57
3.2.1	Influence of the iron nutritional status on the susceptibility of Arabidopsis plants to <i>C. higginsianum</i> .....	57
3.2.2	Fungal growth and development are accelerated on Fe-deficient Arabidopsis leaves .....	60
3.2.3	Assessment of the sensitivity to <i>C. higginsianum</i> in Arabidopsis lines affected in the expression of Fe homeostasis-related genes .....	62
3.2.4	Influence of the expression of Fe homeostasis-related genes on Fe accumulation and H <sub>2</sub> O <sub>2</sub> production after infection with <i>C. higginsianum</i> .....	64
3.2.4.1	Confirmation of disease susceptibility of the lines 35S: <i>FIT1</i> , 35S: <i>FER1</i> , 35S: <i>F6'H1</i> , 35S: <i>NAS k8</i> and <i>vit1-1</i> .....	64
3.2.4.2	Influence of the expression of Fe homeostasis-related genes on Fe accumulation after infection with <i>C. higginsianum</i> .....	66
3.2.4.3	Influence of the expression of Fe homeostasis-related genes on H <sub>2</sub> O <sub>2</sub> accumulation after infection with <i>C. higginsianum</i> .....	68
4	Discussion.....	70
4.1	An adequate Fe nutritional status suppresses infection and biotrophic growth of <i>Colletotrichum</i> .....	71

4.1.1	Fe-sufficient maize and Arabidopsis plants are more tolerant than Fe-deficient plants to the hemibiotrophic pathogen <i>Colletotrichum</i> .....	71
4.1.2	The Fe nutritional status does not affect the severity of <i>C. graminicola</i> infection in wounded leaves .....	74
4.1.3	The benefit of an adequate Fe nutritional status in maize leaves is independent on the Fe acquisition pathways of <i>C. graminicola</i> .....	74
4.1.4	The impact of Fe deficiency on the ultrastructure of maize leaves ...	74
4.2	A protective role of Fe against fungal infection by H <sub>2</sub> O <sub>2</sub> production .....	76
4.2.1	Fe accumulates at infection sites in maize or Arabidopsis leaves infected by <i>Colletotrichum</i> .....	76
4.2.2	The relation between Fe recruitment and H <sub>2</sub> O <sub>2</sub> production at pathogen infection sites .....	78
4.3	Fe homeostasis-related genes influence the susceptibility of maize and Arabidopsis to <i>Colletotrichum</i> .....	79
5	Summary .....	84
6	References.....	86
7	Supplementary data .....	98
8	Abbreviations .....	100
9	Acknowledgements .....	102
10	Curriculum Vitae.....	103
11	Affirmation.....	105

# 1 Introduction

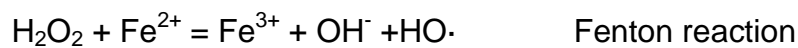
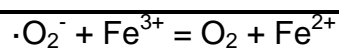
## 1.1 Iron in living organisms

As a transition element, iron (Fe) possesses two major aqueous oxidation states, ferrous ( $\text{Fe}^{2+}$ ) and ferric ( $\text{Fe}^{3+}$ ) ions which are able to form six-coordinate complexes with various ligands like oxygen, nitrogen and sulfur (Marschner, 1995). These physiochemical properties enable Fe to be considered as an indispensable element for living organisms as it is involved in fundamental biochemical reactions in particular those involving electron transport. In plants, Fe-dependent processes include photosynthesis, respiration, nitrogen fixation, chlorophyll and DNA synthesis. Paradoxically, free Fe can generate hydroxyl radicals which possess a huge potential as oxidizing agents via Fenton/Haber Weiss reaction:

---

Toxicity of iron caused by generation of oxidizing agents

---



(modified from Guerinot and Yi, 1994)

These Reactive Oxygen Species (ROS) are highly reactive and toxic for living organisms causing protein oxidation, lipid peroxidation and DNA mutations, and finally leading to cell death (Briat, 2002). In order to avoid the generation of toxic ROS and balance Fe homeostasis, free Fe in living organisms is tightly controlled by binding it into various proteins/chelators during transport and storage (Ratledge and Dover, 2000; Arosio and Levi, 2002). The Fe chelator nicotianamine (NA) for example functions in protecting plants from oxidative damage, since once complexed by NA, Fe becomes Fenton-inactive (von Wirén et al., 1999). Excess Fe can also be inactivated by binding to Fe storage proteins, in particular to ferritin, a 24-subunit plastidic protein which is able to store up to 4500  $\text{Fe}^{(\text{III})}$  ions

and has pivotal significance in protecting plants from oxidative stress (Ravet et al., 2009; Briat et al., 2010). These metabolic principles in Fe homeostasis are also valid in fungi, where mycoferritin has been found in zygomycetes and was detected in some ascomycetes (Seckback, 1982; Vakdevi and Deshpande, 2009). For Fe acquisition in filamentous fungi, siderophores play a major role as iron scavengers (Haas et al., 2008) and ROS protectors (Eisendle et al., 2006; Oide et al., 2007).

## 1.2 Fe nutrition of higher plants

### 1.2.1 Fe uptake from soil

Although Fe is the fourth most abundant element in the Earth crust, its solubility is extremely low with only  $10^{-17}$  M Fe(III) at pH 7 in an oxygenated medium (Lindsay and Schwab, 1982). In contrast, the required Fe concentration for a plant in order to complete its life cycle ranges from  $10^{-9}$  to  $10^{-8}$  M (Guerinot and Yi, 1994). In order to overcome the discrepancy between available and required Fe, plants have evolved mechanisms to control Fe acquisition, internal distribution and storage to ensure a best possible growth by preventing both, Fe deficiency and toxicity (Colangelo and Guerinot, 2006). Based on their Fe acquisition mechanisms, plants have been grouped into two classes, Strategy I and Strategy II (Marschner and Römheld, 1994).

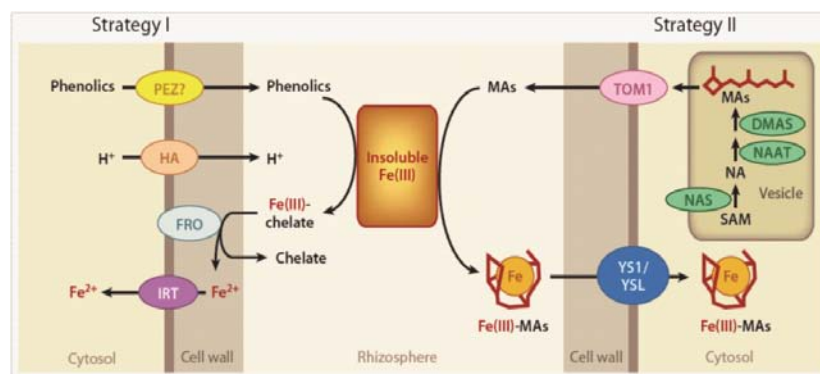


**Fig. 1. Fe acquisition strategies in higher plants.** Strategy I in nongraminaceous plants and Strategy II in graminaceous plants. DMAS, deoxymugineic acid synthase; FRO, ferric-chelate reductase oxidase; HA, H<sup>+</sup>-ATPase; IRT, iron-regulated transporter; MAs, mugineic acid family phytosiderophores; NA, nicotianamine; NAAT, nicotianamine aminotransferase; NAS, nicotianamine synthase; PEZ, phenolics exporter; SAM, S-adenosyl-methionine; TOM1, transporter of mugineic acid family phytosiderophores 1; YS1/YSL, yellow stripe 1/yellow stripe 1-like (modified from Kobayashi et al. 2012).



Strategy I (Fig. 1) relies on the reduction of insoluble ferric Fe to soluble ferrous Fe. Dicots and non-graminaceous monocots such as Arabidopsis, tomato and tobacco belong to this group. The major processes of the Fe deficiency response take place at the plasma membrane of outer root cells and include: a) activation of a plasmalemma P-Type H<sup>+</sup>-ATPase to acidify the surrounding medium, b) an enhanced reduction capacity of Fe(III) by induction of ferric-chelate reductase oxidase (FRO), and c) an increased uptake capacity for Fe<sup>2+</sup> via the iron-regulated transporter (IRT) (Schmidt, 2003). In addition, releasing phenolic compounds (Olsen et al., 1981; Jin et al., 2007) and phenylpropanoids (Schmid et al., 2014) can improve Fe mobilization by reduction and/or chelation. Many transcriptional factors have been reported in the regulation of Fe deficiency-induced genes. While *FIT* (FER-like iron deficiency–induced transcription factor) positively regulates various Fe deficiency–inducible genes like *FRO* and *IRT* in the rhizodermis and cortex (Colangelo and Guerinot, 2004; Bauer et al., 2007), the bHLH transcription factor POPEYE (PYE) negatively regulates Fe homeostasis-related genes in the stele (Long et al., 2010).

In contrast, graminaceous plants including important crop plants such as maize, wheat, barley and rice have developed another strategy (strategy II) (Fig. 1) based on Fe(III) chelation (Römheld and Marschner, 1986). The chelating agents, which are synthesized and secreted by graminaceous roots, are so-called phytosiderophores (PS). PSs represent different forms of mugineic acids (MAs) which are hexadentate ligands that coordinate ferric Fe with their amino and hydroxyl groups (Mino et al., 1983; Takagi et al., 1984; von Wirén et al., 2000). The biosynthesis pathway of PSs (Fig. 1) starts from *S*-adenosyl-L-methionine (SAM) (Shojima et al., 1990; Bashir et al., 2006, Ueno et al., 2007). Three sequential enzymes are included in this pathway: nicotianamine synthase (NAS), nicotianamine aminotransferase (NAAT), and deoxymugineic acid synthase (DMAS) (Higuchi et al., 1999; Takahashi et al., 1999; Bashir et al., 2006). The transporter of mugineic acid family phytosiderophores 1 (TOM1) as the responsible MAs efflux transporter has also been characterized (Nozoye et al., 2011). After mobilization and chelation, Fe(III)-MA complexes can be taken up via Yellow Stripe 1/Yellow Stripe 1-Like (YS1/YSL) transporters into root cells (Curie et al., 2001; Murata et al., 2006; Inoue et al., 2009). Two transcriptional factors, IDE-binding factor 1 (IDEF1) and IDEF2, have been identified in graminaceous

plants (Kobayashi et al., 2007; Ogo et al., 2008). *IDEF1* and *IDEF2* bind specifically to the *cis*-acting Iron Deficiency–responsive Element 1 (*IDE1*) and *IDE2*, respectively, which were the first identified elements related to micronutrient deficiencies in plants (Kobayashi et al., 2003). However, both *IDEF1* and *IDEF2* are constitutively expressed in vegetative and reproductive tissues without induction by Fe deficiency (Kobayashi and Nishizawa, 2012).

Due to the lower sensitivity of phytosiderophore-mediated Fe mobilization by elevated pH, strategy II can be considered more efficient than strategy I and thus allows graminaceous plants to cope with Fe acquisition also in calcareous and alkaline soils (Mori, 1999).

### 1.2.2 Fe translocation and subcellular compartmentalization

Due to the poor solubility and high reactivity of Fe, Fe trafficking in plants as well as its subcellular compartmentalization and remobilization must be associated with suitable chelating molecules and a proper control of redox states between the ferrous and ferric forms (Marschner, 1995; Hell and Stephan, 2003). Among some principal chelators indicated by physiological and molecular studies, nicotianamine (NA) seems to have a privileged role. It is present in all tissues of both strategy I and strategy II plants and is able to complex Fe at both oxidative states (Scholz et al., 1992). The Fe(II)-NA complex is kinetically stable and Fenton inactive (von Wirén et al., 1999). Citrate has long been thought to play a dominant role in the chelating and trafficking of Fe(III) in the xylem where the pH is usually between 5.5 and 6 (Brown and Chaney, 1971). Moreover, the occurrence of phytosiderophores (PSs) in the xylem sap of graminaceous plants suggested that PSs participate in the long-distance Fe translocation from roots to shoots (Kawei et al., 2001).

Since the xylem and phloem consist of dead and living cells, respectively, xylem loading therefore is assumed to require efflux transporters, whereas phloem loading needs Fe influx transporters. To date, many transporters have been identified to be involved either in xylem loading, such as Ferric Reductase Defective 3 (*FRD3*) (Rogers and Guerinot, 2002), *YSL2* (DiDonato et al., 2004), and *PEZ1* (Ishimaru et al., 2011), or in phloem loading, such as *YSL3* (Gendre et al., 2007).

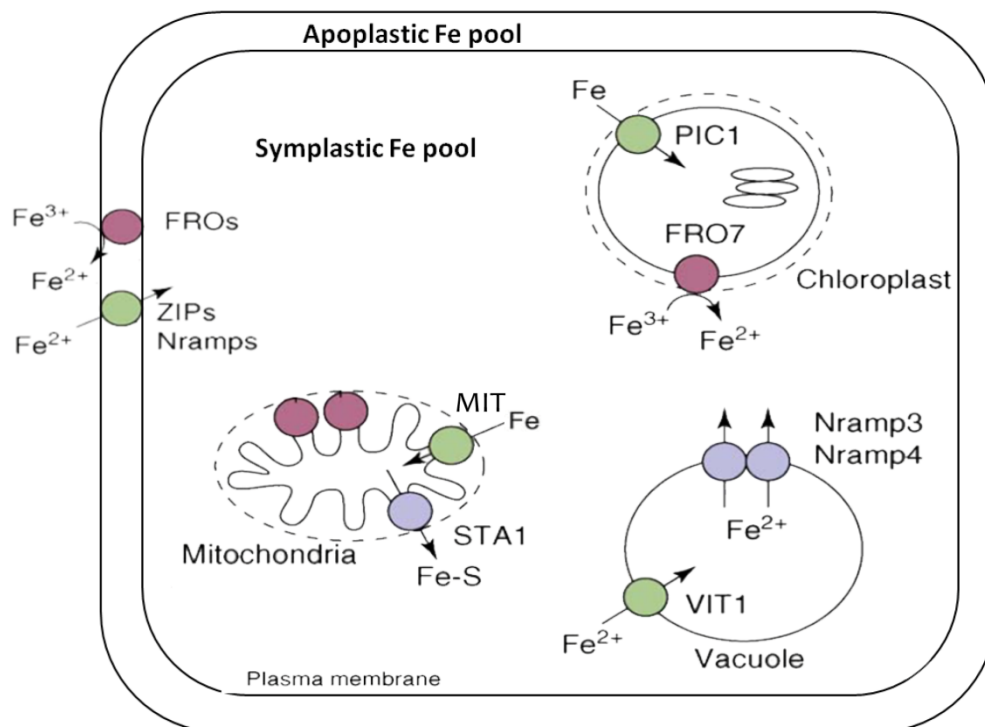


**Fig. 2. Subcellular iron trafficking in plant cells.** At the plasma membrane, Fe is taken up into the cytosol via reductases (FROs) and transporters of the ZIP and NRAMP families. PIC1 and FRO7 have been reported to be involved in chloroplast Fe uptake. MIT1 is the mitochondrial Fe importer and STA1 exports Fe-S clusters out of mitochondria. In the vacuole, Fe is taken up by VIT1 and is exported by NRAMP3 and NRAMP4 (modified from Jeong and Guerinot, 2009).

Once Fe enters a leaf cell (Fig. 2), while considerable amounts can remain in the apoplast (Nicolic and Römheld, 2002; 2003), approximately 80% - 90% is delivered to the chloroplasts (Marschner, 1995) to fulfill the high demand of Fe for photosynthetic electron transport, chlorophyll biosynthesis, Fe-S cluster assembly, and heme biosynthesis (Briat et al., 2007). Arabidopsis Permease In Chloroplasts 1 (PIC1) has been proposed to transport Fe into the chloroplast (Duy et al., 2007). A study with Arabidopsis ferric-chelate reductase *fro7* loss-of-function mutants suggested the implication of this reductase in Fe import into chloroplasts (Jeong et al., 2008). The other dominant Fe-requiring site inside a cell is the mitochondrion, where Fe is used as a cofactor in the respiratory electron transport chain and where Fe-S clusters are assembled like in chloroplasts (Briat et al., 2007). As soon as Fe is transported into these organelles, a part of it will be stored. Ferritins serve as major Fe storage proteins and buffer Fe inside plastids and mitochondria (Hintze and Theil, 2006). The vacuole generally serves as another pool and storage compartment for sequestration within plant cells. Vacuolar Iron

Transporter 1 (VIT1) transports Fe from the cytosol into vacuole (Kim et al., 2006), whereas two metal transporters of the Natural Resistance-Associated Macrophage Protein (NRAMP) family, NRAMP3 and NRAMP4, function counteractively to efflux Fe from the vacuole into the cytosol (Lanquar et al., 2005).

### **1.3 Fe acquisition in pathogenic fungi**

To successfully complete their life cycle, most microorganisms need Fe concentrations in the range of  $10^{-7}$  -  $10^{-6}$  M Fe (Schaible and Kaufmann, 2004), which means at even higher levels than plants do ( $10^{-9}$  -  $10^{-8}$  M). Compared to the soluble pool of Fe found in oxygenated environments, the labile Fe pool in living tissues is even much lower, since the majority of Fe is bound to proteinous (Fe-S-, haem-, or Fe-proteins) and non-proteinous molecules (organic acids, nicotianamine, phytosiderophores etc.). Whereas the concentration of free Fe in human serum is around  $10^{-24}$  M (Miethke and Marahiel, 2007), it is supposed to be ten times lower in plants (Expert, 1999). This situation forces pathogenic fungi to develop Fe sequestration strategies in order to overcome the limitation of Fe in host plants. Thus, they have evolved two high-affinity Fe acquisition strategies, reductive iron assimilation (RIA) and siderophore-mediated iron acquisition (SIA), which implement similar principles as strategy I and II, respectively, in plants. However, unlike plants are divided into two groups, fungi mostly possess both strategies, RIA and SIA, at same time (Fig. 3).

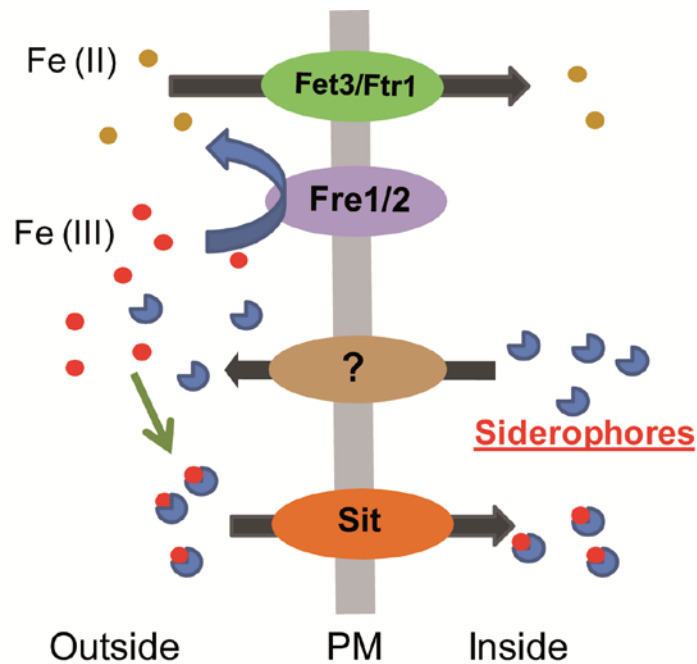


**Fig. 3. Fe acquisition strategies in pathogenic fungi.** Fre, ferric reductase; Fet, ferroxidase; Ftr, permease; Sit, siderophore uptake transporter; PM, plasma membrane.

### 1.3.1 The reductive Fe assimilation (RIA) pathway

The RIA strategy has been well documented in the eukaryotic model yeast *Saccharomyces cerevisiae* (Askwith et al., 1994; Stearman et al., 1996; Van Ho et al., 2002; Wang et al., 2003; Kwok et al., 2006). The pathway entails a two-step process that begins with the reduction of insoluble ferric Fe to soluble ferrous Fe by ferric reductase (Fre1/2) at the plasma membrane followed by the uptake of ferrous Fe by a high-affinity, ferrous-specific transporter complex, consisting of a multicopper ferroxidase (Fet3) and a permease (Ftr1) (Fig. 3). Since ferric Fe is not a substrate for the oxidation/permease (Fet3/Ftr1) complex, it must be first oxidized by Fet3 before being transferred into the cytosol as ferric Fe (Eide, 1997; Shi et al., 2003; Wang et al., 2003; Philpott, 2006). It has been reported that RIA is essential for full virulence of many animal and plant pathogenic fungi. For instance, in the dimorphic human pathogen *Candida albicans*, the *ptr1* mutants exhibited severe growth defects in Fe-deficient medium and were unable to establish systemic infection in mice (Ramanan and Wang, 2000). The importance of this Fe acquisition pathway was also demonstrated in the biotrophic corn smut fungus *Ustilago maydis* by studies of two components of this system, i.e. the Fe multicopper oxidase Fer1 and the high-affinity Fe permease Fer2 (Eichhorn et al.,

2006). Both, *fer1* as well as *fer2* deletion mutants were strongly affected in virulence.

### 1.3.2 The siderophore-mediated Fe acquisition (SIA) pathway

Most fungi synthesize and secrete siderophores, which are small organic molecules with tremendous affinity and specificity to ferric Fe (Hider, 1984; Neilands, 1995). Depending on the Fe-binding moieties, siderophores can be classified into three different groups: catecholates, hydroxamates and carboxylates (Boukhalfa and Crumbliss, 2002). Most siderophores from pathogenic fungi characterized so far are of the hydroxamate type (Haas et al., 2008). The biosynthetic pathway of hydroxamate siderophore begins with the hydroxylation of the amino acid ornithine to  $N^{\beta}$ -hydroxy-ornithine by ornithine  $N^{\beta}$ -oxygenase, which was initially characterized as the product of *Sid1* in *U. maydis* (Mei et al., 1993; Philpott, 2006). After the formation of the hydroxamate group which is accomplished by acylation of the  $N^{\beta}$ -hydroxyornithine, the hydroxamates are finally linked by nonribosomal peptide synthetases to form a variety of siderophore types.

The principle of the SIA system is presented in Fig. 3. Little is known regarding the mechanism of siderophore excretion. The uptake of siderophore-Fe(III) complexes is mediated by the plasma membrane-located transporter Sit (Pao et al., 1998), which is able to take up also Fe(III)-siderophores secreted by other species of fungi or bacteria (Philpott, 2006), even including phytosiderophores (Albarouki and Deising, 2013). Pathogenic siderophores are among the strongest Fe(III)-binding agents known, with Fe binding constants of  $> 10^{-30}$  M (Neilands, 1995), ensuring an effective competition with Fe-binding ligands of the host. Defects in the SIA pathway usually cause a strong decrease in growth under Fe deficiency and reduction of infection indicating that the SIA pathway is indispensable for vegetative growth and full virulence of many pathogenic fungi (Mei et al., 1993; Oide et al., 2006; Greenshields et al., 2007; Schrettl et al., 2007; Haas et al., 2008; Hof, 2009; Albarouki et al., 2014).

## 1.4 Fe in plant-pathogen interaction

Due to the two problematic properties of Fe, i.e. low availability of insoluble ferric Fe and toxicity of excess free Fe, control over Fe homeostasis is of central importance in host–pathogen interactions (Nairz et al., 2010). Since both opponents compete for this micronutrient, the outcome of this competition might decide over the success of a pathogenic infection or the pathogen resistance of a host. Thus, one effective strategy for host plants to suppress a pathogen infection is to reduce Fe availability to pathogens. This Fe-withholding strategy is well documented in animal-pathogen (Weinberg and Miklossy, 2008) but also in plant-pathogen interactions. For instance, it has been shown that plant-produced polyphenols reduce the availability of Fe to pathogens (Mila et al., 1996). Alternatively, the infection of potato leaves by the late blight pathogen *Phytophthora infestans* was drastically reduced by adding desferrioxamine (DFO), a bacterial Fe(III) chelator (Mata et al., 2001). In the same study, the expression of a ferritin-encoding gene was upregulated in the infected host plant, and induction of ferritin was also detected during infection of *Arabidopsis* by *Erwinia chrysanthemi* (Dellagi et al., 2005), suggesting the involvement of Fe sequestration by ferritin in the basal defense of plants. In line with this view, it has been shown that transgenic tobacco plants ectopically expressing alfalfa ferritin had a higher tolerance to viral and fungal infections (Deak et al., 1999).

While an Fe-deficient nutritional status may hinder pathogen infection of hosts, Fe is also required for various innate host defense mechanisms (Schaible and Kaufmann, 2004). In animals, Fe serves as a cofactor for the enzymatic generation of antimicrobial oxygen radicals by neutrophils and macrophages and is essential for the clonal expansion of T-cells (Nairz et al., 2010). Treatment of *Salmonella*-infected mice with the Fe chelator DFO dramatically exacerbated the infection by inhibiting the host NADPH oxidase-dependent respiratory burst due to a decreased availability of reactive Fe (Collins et al., 2002). A similar role of Fe may hold true for plants, where the sensitivity of bean to *Fusarium solani* (Guerra and Anderson, 1985) or of tomato to *Verticillium dahlia* (Macur et al., 1991) was enhanced when plants were Fe deficient, indicating a requirement for Fe in plant defense responses. A direct involvement of Fe in the defense response was observed in *Arabidopsis* (Segond et al., 2009; Chen et al., 2014) and wheat (Liu et

al., 2007) by a cellular relocation of Fe to infection sites which coincided with local ROS production (relocating strategy). These two studies have suggested a working model that plants can redistribute Fe to the apoplast by pathogen attack where an oxidative burst takes place and leads to Fe deficiency in the cytosol of attacked cells. This further stimulates a reprogramming of Fe homeostasis in the cells involving Fe storage, internal Fe allocation and Fe uptake.

However, it remains so far unclear how plants regulate these two antagonistic strategies in their defense responses, which role Fe plays in ROS production in response to certain pathogens and to what extent ROS formation depends on the plant Fe nutritional status.

## 1.5 Plant-pathogen systems with *Colletotrichum*

*Colletotrichum* is one of the most common and important genera of plant pathogenic fungi and has been classified as one of the 10 top fungal pathogens in agricultural plant production (Dean et al., 2012). *C. graminicola* and *C. higginsianum* belong to this genus and show different host specificities. As model for the study of hemibiotrophic fungal lifestyles, the genomes of both fungi have been already sequenced (O'Connell et al., 2012).

### 1.5.1 The maize-*Colletotrichum graminicola* pathosystem

*C. graminicola* is the causing agent of maize anthracnose leaf blight and stock rot (Fig. 4A). The infection process of the fungus starts with germination of conidia (Fig. 4B, C). After forming a melanized appressorium, this fungus invades the plant cell and forms a biotrophic infection vesicle and primary hyphae. This stage of infection is referred to as the biotrophic growth stage, since the host cell remains viable (Bergstrom and Nicholson, 1999). Following biotrophic growth, the fungus differentiates thin, fast-growing secondary hyphae actively killing the host cells by secreting toxins or generating ROS (Perpetua et al., 1996; Howlett, 2006), thus entering the necrotrophic growth stage (Bergstrom and Nicholson, 1999; Wharton et al., 2001; Mims and Vaillancourt, 2002). Through the proliferation of the fungus in the plant tissue, first symptoms are to be recognized as chlorotic spots. In further development, necrotic spots occur, in which the pathogen forms



acervuli and conidia for disease spreading (Fig. 4C) (Bergstrom and Nicholson, 1999).

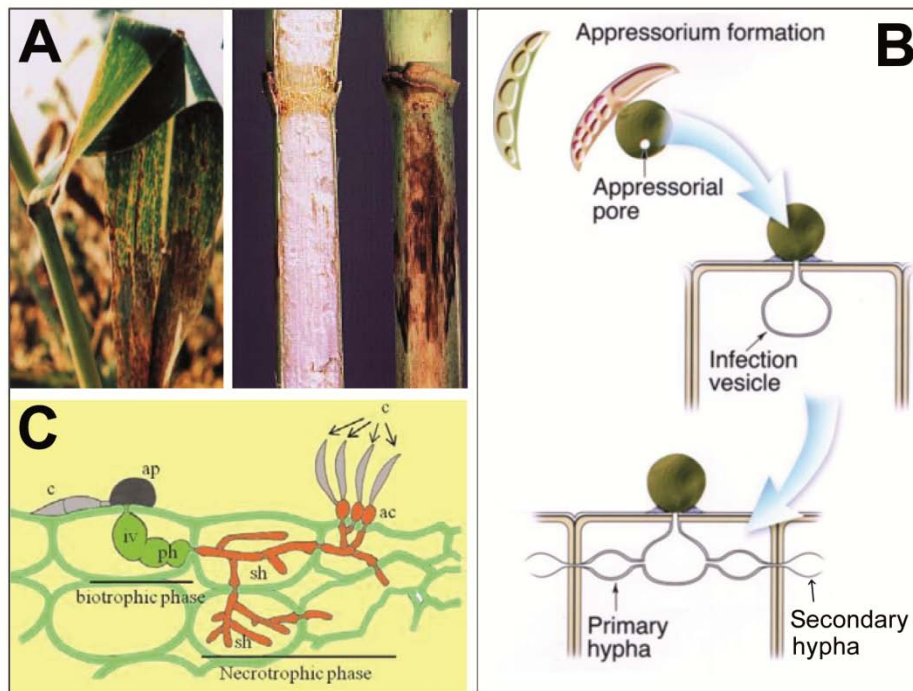


**Fig. 4. Biology of *Colletotrichum graminicola*.** (A) Anthracnose leaf blight and stalk rot. (B) Life cycle of *C. graminicola* (see text). (C) Infection structures formed on a maize leaf. c, conidium; ap, appressorium; iv, infection vesicle; ph, primary hypha; sh, secondary hypha; ac, acervulus. (A and B were modified from Bergstrom and Nicholson (1999), C is an artwork by D. Deising).

The maize-*C. graminicola* pathosystem has been widely used as model system to study hemibiotrophic fungal lifestyles (Bergstrom and Nicholson, 1999; Mims and Vaillancourt, 2002; Munch et al., 2008; Bechinger et al., 1999). Recently, the functions of two Fe acquisition pathways (RIA and SIA) of *C. graminicola* have been studied in this pathosystem. Two ferroxidase genes, *FET3-1* and *FET3-2*, were identified (Albarouki and Deising, 2013). The *fet3-1* and the double mutant *fet3-1/2* showed increased sensitivity to ROS and reduced virulence, but not the *fet3-2* mutant. Interestingly, *FET3-1* is expressed in infection structures specifically formed during fungal development on the cuticle and during biotrophic development on the leaf tissue, indicating that the RIA pathway is required for appressorial penetration, biotrophic development, and full virulence of fungus. In contrast, the study of the two siderophore biosynthesis genes *SID1* and *NPS6* (non-ribosomal peptide synthetase) revealed that siderophore biosynthesis in *C. graminicola* is biotrophy-specifically downregulated for modulation of defense responses of maize (Albarouki et al., 2014). Both *sid1* and *nps6* mutants were not

affected in biotrophic development, but spreading of necrotrophic hyphae was impaired resulting in a reduced virulence.

### 1.5.2 The *Arabidopsis-Colletotrichum higginsianum* pathosystem

Like many other *Colletotrichum* species, *C. higginsianum* invades host plants using a typical multi-stage hemibiotrophic infection process (Fig. 5B), which starts with biotrophic growth on living host cells, before switching to necrotrophic growth on dead cells (O'Connell et al., 2004; Shimada et al., 2006; Sun and Zhang, 2009).

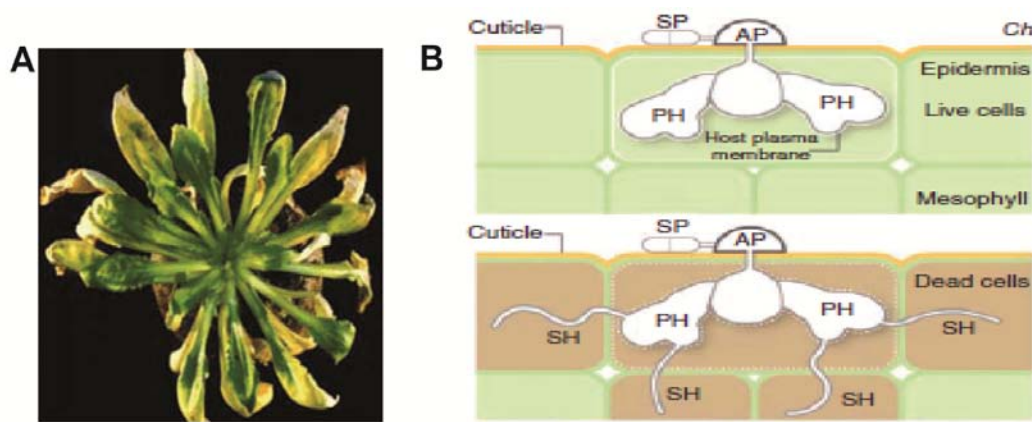


**Fig. 5. *Arabidopsis-Colletotrichum higginsianum* pathosystem.** (A) Symptoms of fungal infection on an *Arabidopsis* plant. (B) Infection process of *C. higginsianum* (Ch). SP, spore; AP, appressorium; PH, biotrophic primary hyphae; SH, necrotrophic secondary hyphae (modified from O'Connell et al., 2004; 2012).

*C. higginsianum* has a wide host range, attacking many cultivated forms of *Brassica* and *Raphanus* as well as wild *Brassicaceae* (Narusaka et al., 2004). The *Arabidopsis-C. higginsianum* pathosystem (Fig. 5) was first described by O'Connell et al., (2004), and soon became an attractive model for the study of plant-pathogen interactions, as it not only offers the advantage to use the genetic resources available for the host, but also the experimental advantages of the pathogen.

## 1.6 Aims of this study

Whereas fungal and host mechanisms of iron acquisition in mammalian-microbial interactions have already been intensively studied, the roles of iron in the immune

system of the plant and in its defense against pathogens are still far away from known. In particular the role of Fe during different stages of the fungal lifestyle is not yet clear. Therefore, the overall aims of this work were i) to investigate the role of Fe during different phases of the fungal infection process, and ii) to identify Fe homeostasis-related genes that contribute to resistance against *Colletotrichum* pathogens. Such knowledge may ultimately allow to develop strategies for enhanced pathogen resistance by plant breeding or improved nutritional management.

Limiting Fe availability to pathogens is a successful strategy of hosts to defend themselves. Fe homeostasis, determined by the Fe nutritional status of plant, is therefore a central battle field controlled by plants and pathogens. To investigate the influence of the plant Fe nutritional status in plant-pathogen interactions is of significant interest. Thus, one approach in this thesis was to manipulate the Fe nutritional status of maize or *Arabidopsis* plants and to examine their susceptibility to the corresponding pathogens (chapters 2.2.1 and 3.2.1).

To overcome the limitation of Fe in host plants, fungal pathogens may employ reduction- and siderophore-based Fe acquisition at same time. An open question is which of these Fe acquisition strategies is required when plants are adequately supplied with Fe or deficient of Fe. Therefore, fungal mutants defective in individual components of RIA- or SIA-mediated Fe acquisition have been employed to study the role of Fe during the infection process (chapter 2.2.7).

In order to protect themselves, plants have evolved different basal defense responses, including ROS production, during pathogen infection. Limited Fe availability in plant tissues may correspond to a ROS-generating power during pathogen attack, which may increase the susceptibility of host cells. Therefore, the Fe redistribution and ROS production in plants was investigated during pathogen infection using established staining procedures for Fe and ROS (chapter 2.2.4, 2.2.5 and 3.2.4).

Furthermore, the Fe homeostasis in plant tissues is tightly controlled by a complex network of homeostasis-related genes to avoid Fe deficiency or toxicity. Any changes in this complex network may not only influence Fe balances in plant tissues, but also the response of plant cells to pathogen infection and thereby host susceptibility. Therefore, the present study used reverse genetic approaches

(transgenic *Arabidopsis* lines) to investigate the potential contribution of plant Fe homeostasis-related genes to the defense against fungal pathogens (chapter 3.2.3 and 3.2.4).

## 2 Fe in the maize-*Colletotrichum graminicola* interaction

### 2.1 Material and methods

#### 2.1.1 Plant material and growth conditions

In this study the maize (*Zea mays*) inbred line UH002 was used as a reference line (WT) together with the maize mutant *ys1*, which is defective in phytosiderophore uptake by roots (von Wirén et al., 1994; Schaaf et al., 2004).

For hydroponic culture, seeds were dark-germinated in moistened filter paper. Two days after germination, seedlings were transferred to half-strength nutrient solution. After 3 days, full nutrient solution containing 2.0 mM Ca(NO<sub>3</sub>), 0.7 mM K<sub>2</sub>SO<sub>4</sub>, 0.5 mM MgSO<sub>4</sub>, 0.1 mM KCl, 0.1 mM KH<sub>2</sub>PO<sub>4</sub>, 1.0 µM H<sub>3</sub>BO<sub>3</sub>, 0.5 µM MnSO<sub>4</sub>, 0.5 µM ZnSO<sub>4</sub>, 0.2 µM CuSO<sub>4</sub>, and 0.01 µM (NH<sub>4</sub>)<sub>6</sub>Mo<sub>7</sub>O<sub>24</sub> was supplied. Fe was supplied at the beginning as Fe(III)-EDTA ranging in concentrations from 10 to 250 µM to vary the Fe nutritional status in plants. Nutrient solutions were continuously aerated and changed every 2 to 3 days. Plants were grown in a climate chamber under controlled environmental conditions in a 25°/20°C and 16/8h light/dark regime, a light intensity of 240 µmol photons m<sup>-2</sup> s<sup>-1</sup> and a relative humidity of 60%.

For soil culture, *ys1* plants were grown in a peat-based substrate (Substrat 2, Klasmann-Deilmann, Geeste, Germany) in a greenhouse at 60% relative humidity in a 22°/20°C and 16/8h light/dark regime for 3 weeks. As Fe treatments, 10 or 20 mg Fe-EDDHA (6% Sequestrene 138 Fe-Granulat, Syngenta, Germany) were directly supplied to the pots every two days and water was supplied as in the control.

#### 2.1.2 Fungal culture and plant inoculation

The wild-type (WT) strain CgM2 of *Colletotrichum graminicola* (Ces.) G. W. Wilson (teleomorph *Glomereella graminicola* D. J. Politis) (Anderson and Nicholson, 1996; Bergstrom and Nicholson, 1999) and all mutant strains used in this study were obtained from Prof. H. B. Deising's lab (Halle University, Germany).

In order to collect conidia for infection assays, the WT strain was grown on oat meal agar (OMA) (Werner et al., 2007), while the mutants deleted in one ( $\Delta fet3-1$ ) or two ( $\Delta fet3-1/2$ ) ferroxidase genes or defective in siderophore biosynthesis ( $\Delta nps6$  or  $\Delta sid1$ ) were grown on OMA medium supplemented with 100  $\mu$ M Fe(III)-EDTA (Albarouki and Deising, 2013; Albarouki et al., 2014). Conidia were collected from 2 to 4 week-old OMA plates by rinsing with 0.03% (v/v) Tween 20. After 3 times of washing, conidia suspensions were adjusted to certain concentrations with a hemocytometer (LO-Laboroptik, Friedrichsdorf, Germany).

Two week-old maize plants were used for infection assays. In general, the fourth fully expanded leaf was used for determination of the Fe nutritional status and for infection assays. Leaf segments (10 to 12 cm) were inoculated with 10  $\mu$ l droplets either containing  $10^5$  conidia  $ml^{-1}$  or no conidia as mock treatment. Alternatively, a sterile pipette tip was used to wound leaves immediately before inoculation. Leaf segments were placed into square Petri dishes (23 x 23 cm, Corning Inc., Corning, NY) containing two layers of moist filter paper and incubated in darkness at 25°C.

### **2.1.3 Infection assays**

#### **2.1.3.1 Determination of lesion areas**

Symptoms on maize leaves were photographed at 4 days post inoculation (dpi) and lesion areas were quantified using the ImageJ software (<http://rsbweb.nih.gov/ij/>).

#### **2.1.3.2 Quantification of fungal DNA**

Quantitative PCR (qPCR) was employed for quantifying fungal mass as described by Albarouki and Deising (2013). Briefly, infected areas were collected at 4 dpi using a cork borer (diameter 0.8 cm). Samples were homogenized using a mixer mill (MM400, Retsch, Haan, Germany) for 1 minute at 30 Hz. DNA was extracted following the manufacturer's protocol using the pegGOLD Fungal DNA Mini Kit (PEQLAB Biotechnologie GmbH, Erlangen, Germany). Plasmid pUC18 (50  $\mu$ g; Fermentas, St. Leon-Rot, Germany) was added at the beginning of DNA isolation as an external normalization reference. To determine the amount of fungal DNA,

qPCR was performed with a Mastercycler realplex (Eppendorf, Hamburg, Germany) and the iQ SYBR Green Supermix (Bio-Rad Laboratories, Hercules, CA, USA) using the primers ITS2-qPCR-Fw and ITS2-qPCR-Rv specific to the internal transcribed space region of rDNA of *C. graminicola*. The pUC18 concentration was measured using the primers M13-qPCR-Fw and M13-qPCR-Rv. All primers used are listed in the supplemental Table 1 (page 98).

## **2.1.4 Histological staining and microscopy**

### **2.1.4.1 Light microscopy**

Light microscopy was performed using a Zeiss Axio Imager M2 microscope (Zeiss, Oberkochen, Germany), equipped with a camera (Axio Cam MRC). After removing chlorophyll with 96% ethanol, infected leaf segments were mounted and directly observed under the microscope.

### **2.1.4.2 Prussian blue staining**

For Fe staining, leaf segments were taken from sites where fungal suspensions had been placed on. Prussian blue staining was modified from Cvitanich et al. (2010). Briefly, after removing chlorophyll by extraction with methanol: chloroform: acetic acid (6:3:1, v/v/v), samples were stained with 1 volume of 4% HCl mixed with 1 volume of 8% (w/v) fresh potassium hexacyanoferrate (II) trihydrate (Merck, Darmstadt, Germany) at 28°C for 24 h. After washing several times with bidistilled water, samples were mounted and observed under a light microscope.

### **2.1.4.3 DAB staining**

To localize the occurrence of hydrogen peroxide, 3,3'-diaminobenzidine (DAB) (Sigma-Aldrich, Steinheim, Germany) staining was conducted according to Hückelhoven et al. (1999). After briefly dipping leaf samples in 0.1% (v/v) Tween 20, they were vacuum infiltrated with freshly prepared 0.1% (w/v) DAB solution (pH 3.8, HCl) and incubated overnight in the dark at room temperature. After removing chlorophyll with 96% ethanol, samples were mounted and observed under a light microscope.

#### **2.1.4.4 Scanning electron microscopy (SEM)**

Specimens in sizes of 8 x 16 mm were taken from the middle section of the fourth youngest and fully expanded leaves of maize plants precultured under deficient (-Fe) or sufficient (+Fe) Fe supply in hydroponic culture. After fixation with 2% glutaraldehyde in 50 mM phosphate buffer (pH 7.0) for 2 h the leaf specimens were washed with buffer and dehydrated in an ethanol series from 30% to 100% for 15 min each. Then, samples were dried in a Bal-Tec critical point dryer (Bal-Tec AG, Balzers, Switzerland). Dried specimens were attached onto carbon-coated aluminium sample blocks and gold coated in an Edwards S150B sputter coater (Edwards High Vacuum Inc., Crowley, West Sussex, UK). Samples were examined in a Hitachi S4100 SEM (Hisco Europe, Ratingen, Germany) at 5 kV acceleration voltages.

#### **2.1.4.5 Transmission electron microscopy (TEM)**

Sample preparation for TEM was as described by Gernand et al. (2006) with slight modifications. Briefly, the specimens collected as described before in 2.1.4.4. were chemically fixed with 2% glutaraldehyde and 2% formaldehyde in 50 mM phosphate buffer (pH 7.0) for 2 h. After three 20 min washes with the same buffer, the samples were fixed with 1% OsO<sub>4</sub> for 2 h, followed by three washes in distilled water, dehydration in a graded ethanol series and subsequent embedding in Spurr's low viscosity resin. Ultrathin sections (75 nm) were made on a Reichert-Jung Ultracut S (Leica, Vienna, Austria) and collected on 75 mesh hexagonal grids. After staining with 2% uranyl acetate, samples were studied in a FEI Tecnai 20 electron microscope (Fei Company, Eindhoven, Netherlands) at 120 kV acceleration voltages.

#### **2.1.5 Gene expression analysis**

The samples from either infected or non-infected leaves were collected and homogenized as described in 2.1.3.2. Total RNA was extracted with Trizol<sup>®</sup> agent (Life Technologies, Darmstadt, Germany) according to the manufacturer's instructions. RNA concentrations were normalized and reverse transcribed using a RevertAid First Strand cDNA Synthesis Kit (Fermentas, St. Leon-Rot, Germany).



The cDNA samples were then used to investigate gene expression by quantitative real-time PCR (qRT-PCR) with a Mastercycler ep realplex (Eppendorf, Hamburg, Germany) and the iQ SYBR Green Supermix (Bio-Rad Laboratories, Hercules, CA, USA). Specific primers were designed and used for the target genes. In addition, the expression of the house-keeping genes *ZmGAPDH* (glyceraldehyde-3-phosphate dehydrogenase, X07156.1) and *ZmTUA4* (alpha tubulin 4, AJ420856.1) was determined as reference. Relative expression was calculated according to Pfaffl (2001). All primers used are listed in supplemented Table 1 (page 98).

## **2.1.6 Quantification of the plant Fe nutritional status**

### **2.1.6.1 Determination of chlorophyll concentration**

Chlorophyll concentrations in maize leaves were determined after extraction of fresh leaf material grinded in liquid N<sub>2</sub> with *N,N*-dimethylformamid (Sigma-Aldrich, Steinheim, Germany) at 4°C for 48 h. The absorbance at 647 and 664 nm was then measured in extracts according to Moran and Porath (1980) and Moran (1982).

### **2.1.6.2 Determination of total Fe concentration**

After homogenization by a mixer mill (2.1.3.2.), the samples were dried at 65°C for 3 days. The Fe concentrations were measured by Inductively-Coupled Plasma Optic Emission Spectrometry (ICP-OES; iCAP, Thermo Scientific, Dreieich, Germany) after wet digestion of grinded leaf material in HNO<sub>3</sub> in a microwave (Eggert and von Wirén, 2013).

## **2.1.7 Fe fractionation in maize leaves during *C. graminicola* infection**

Infected leaf samples were collected (2.1.3.2.) in a time course from 0 to 72 hpi during fungal infection. Deep-frozen samples were homogenized in liquid N<sub>2</sub> using a mortar and pestle and extracted in bidistilled water according to Shi et al. (2012). After centrifugation at 3500 g for 30 min at 4°C, the supernatant was collected as the water-soluble fraction. The pellet, containing the water-insoluble

fraction, was dried at 65°C for 3 days and wet-digested in the microwave. In both fractions Fe was determined by Inductively Coupled Plasma Mass Spectrometry (ICP-MS) (Elan 6000, Perkin Elmer, Boston, USA).

## 2.2 Results

### 2.2.1 The influence of the iron nutritional status on the susceptibility of maize plants to *C. graminicola* infection

#### 2.2.1.1 Infection of WT UH002 with *C. graminicola*

In order to examine the overall influence of the Fe nutritional status on the susceptibility of maize plants to *C. graminicola*, plants were precultured hydroponically with the supply of 10 to 250  $\mu\text{M}$  Fe(III)-EDTA. After two weeks, Fe deficiency symptoms as expressed by chlorosis in younger leaves appeared in plants with Fe supplies from 10 to 50  $\mu\text{M}$ , whereas no chlorosis was observed in plants with higher Fe supplies (Fig. 6A). As expected, plants supplied with only 10  $\mu\text{M}$  Fe appeared most chlorotic and showed lowest concentrations of chlorophyll and total Fe in youngest and fully expanded leaves (Fig. 6B). With increasing Fe supply, chlorophyll and total Fe concentrations increased steadily but reached adequate levels only when  $\geq 100$   $\mu\text{M}$  Fe was provided. Compared to plants grown at 100  $\mu\text{M}$  Fe, the growth of plants supplied with 250  $\mu\text{M}$  Fe was slightly inhibited, most likely indicating an excess of Fe.

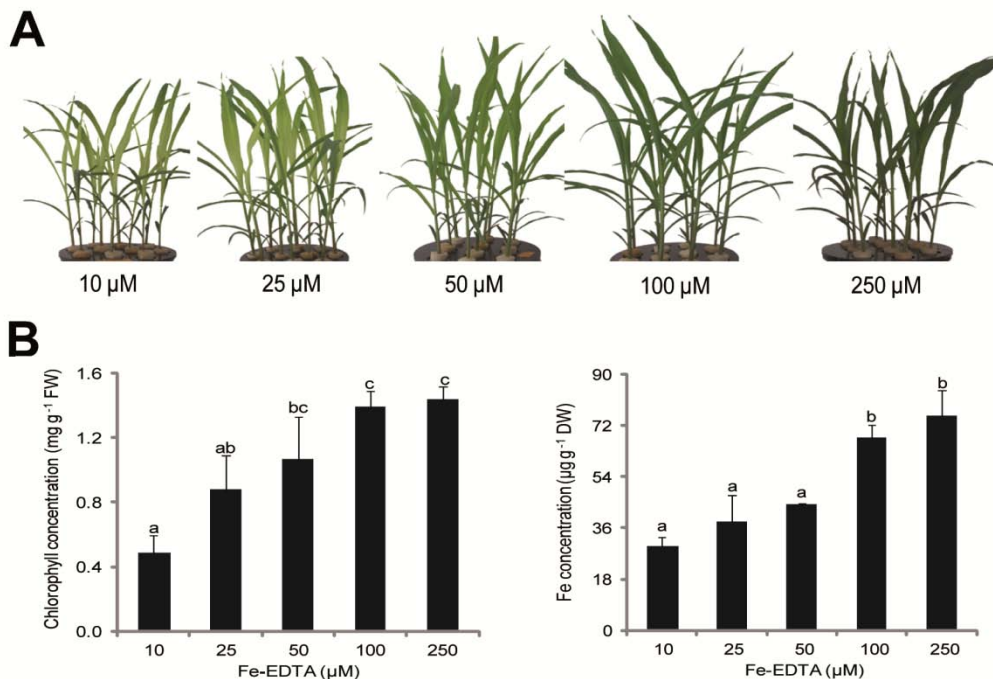


**Fig. 6. Characterization of the Fe nutritional status in wild-type maize UH002.** (A) Phenotype of two week-old maize plants grown in hydroponic culture with supply of 10 to 250  $\mu\text{M}$  Fe(III)-EDTA. (B) Chlorophyll and total Fe concentrations of youngest fully expanded leaves. Bars indicate means  $\pm$  SD,  $n = 4$ , and significant differences are indicated by different letters.

A subsequent infection assay was conducted on wounded and non-wounded leaf segments. Wounding allows immediate infection and progression of the fungus into the necrotrophic growth phase, while on non-wounded leaves a biotrophic growth phase precedes the necrotrophic growth phase (Horbach et al., 2009). On non-wounded leaves, the most severe disease symptoms occurred on leaves supplied with 10  $\mu\text{M}$  Fe (Fig. 7A). This was accompanied by a large lesion area of the infected tissue and a considerable amount of fungal DNA (Fig. 7B). As Fe supply increased up to 100  $\mu\text{M}$ , the lesion area and fungal DNA decreased by > 80% and 65%, respectively. Relative to adequately supplied plants (100  $\mu\text{M}$  Fe), leaves from plants with highest Fe supply showed a higher infection level. Compared to non-wounded leaves, the infection was dramatically enhanced by wounding, resulting in a higher fungal proliferation and corresponding DNA levels (Fig. 7B). As indicated by the lesion area (Fig. 7A), severely Fe-deficient leaves suffered most from the infection, while Fe supplies between 50 and 250  $\mu\text{M}$  were somewhat less affected. Taken together, this experiment showed that the Fe nutritional status strongly affects the susceptibility of non-wounded maize leaf segments to *C. graminicola*. Fe-deficient maize plants were more susceptible than Fe-sufficient plants to this fungus, while excess Fe supplies tended to increase susceptibility. This experiment also allowed choosing 100 and 10  $\mu\text{M}$  Fe as the two most contrasting Fe treatments for the subsequent experiments, from here on referred to as Fe-sufficient (+Fe) and Fe-deficient (–Fe), respectively.

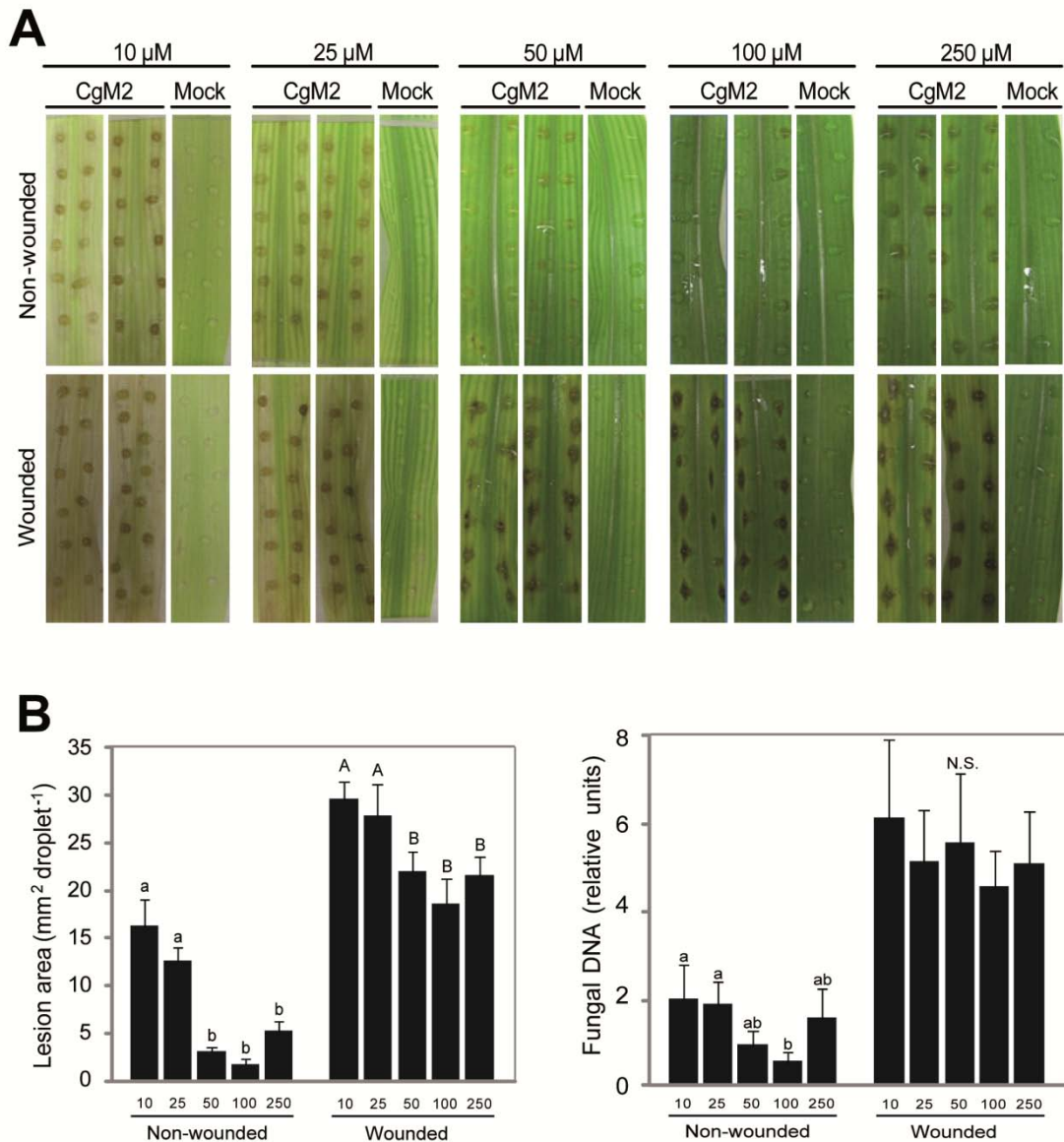


**Fig. 7. Influence of the Fe nutritional status of maize UH002 on its susceptibility to *C. graminicola*.** (A) Infection assay. Plants were grown in hydroponic culture with supply of 10 to 250 µM Fe(III)-EDTA. Excised leaf blades were either wounded or not wounded and inoculated with 10 µl of *C. graminicola* suspension containing either 10<sup>5</sup> spores ml<sup>-1</sup> (CgM2) or no spores (Mock). (B) Lesion area and relative fungal DNA amount. At 96 hpi lesion areas were measured by using ImageJ software and fungal DNA was quantified by qPCR. Bars indicate means ± SD, n = 4, and significant differences at p < 0.001 for lesion areas and at p < 0.05 for fungal DNA analysis are indicated by different letters. N.S., not significant.

### 2.2.1.2 Infection of the maize mutant *ys1* with *C. graminicola*

In an alternative approach to investigate the influence of iron on the pathogen response, the *ys1* mutant which is defective in uptake of phytosiderophores was used for infection assays. Plants grown without Fe fertilization showed Fe-deficiency symptoms in the form of chlorosis in younger leaves, whereas plants supplied with 10 or 20 mg Fe-EDDHA showed no chlorosis (Fig. 8A). A non-

deficient Fe nutritional status was also reflected by measurements of the chlorophyll and total Fe concentrations in youngest fully expanded leaves (Fig. 8B).

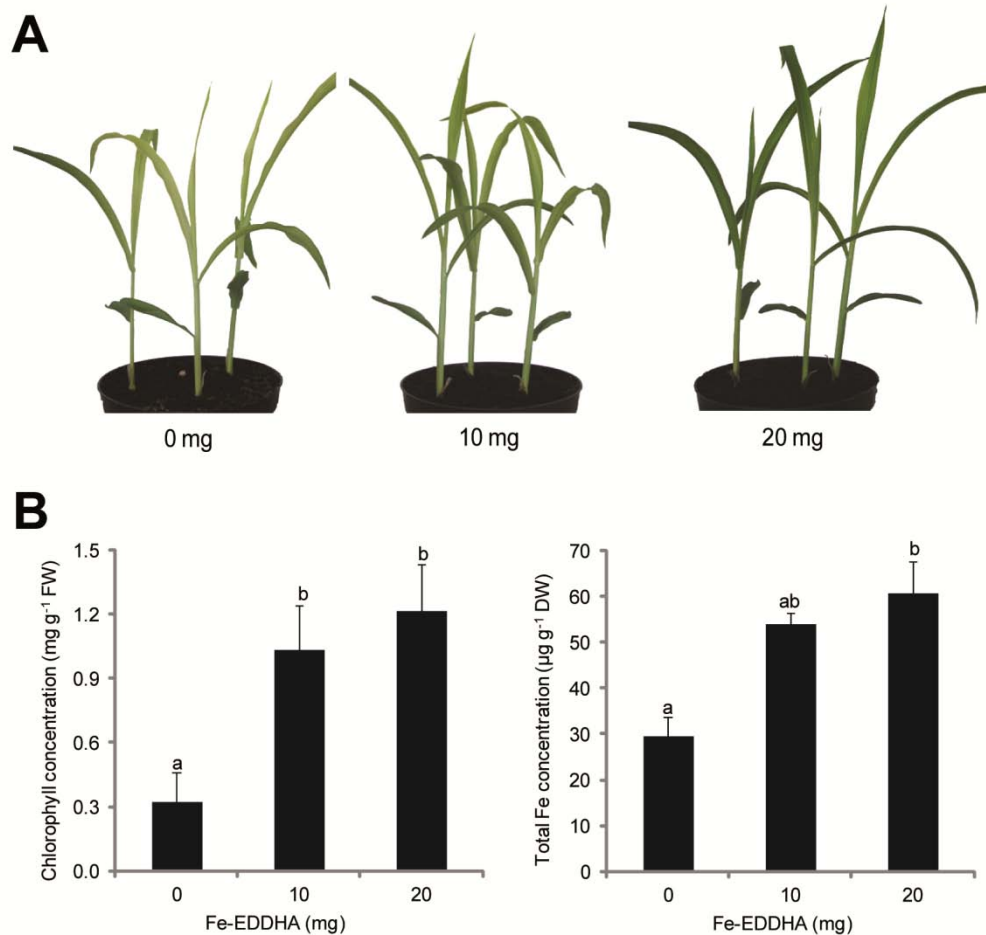


**Fig. 8. Characterization of the Fe nutritional status in the maize mutant *ys1*.** (A) Phenotype of two week-old maize plants grown in soil with supply of 0, 10 or 20 mg Fe-EDDHA per pot. (B) Chlorophyll and total Fe concentrations of youngest fully expanded leaves. Bars indicate means  $\pm$  SD,  $n = 4$ , and significant differences are indicated by different letters.

Infection assays were conducted also with wounded and non-wounded leaves. On non-wounded leaves, the severity of infection symptoms was lower when Fe-EDDHA was supplied (Fig. 9A). There were no significant differences among Fe treatments when leaves were wounded, as indicated by the quantitative analysis of lesion area and fungal DNA (Fig. 9B). Thus, the results confirmed that Fe deficiency increases the susceptibility of maize plants to *C. graminicola* infection.

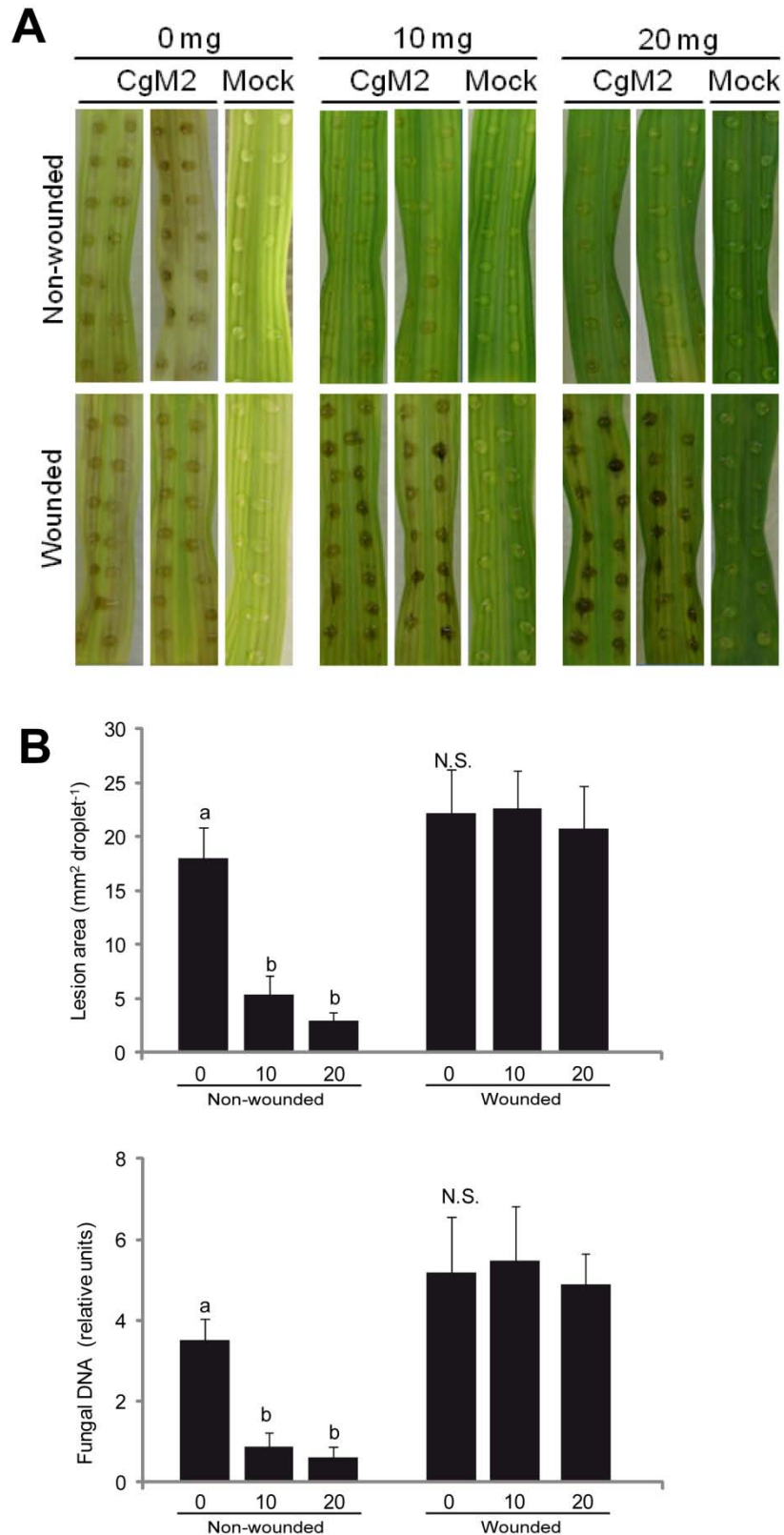


**Fig. 9. Influence of the Fe nutritional status of the maize mutant *ys1* on its susceptibility to *C. graminicola*.** (A) Infection assay. Plants were grown in soil with supply of 0, 10 or 20 mg Fe-EDDHA per pot. Excised leaf blades were either wounded or not wounded and inoculated with  $10^5$  spores ml<sup>-1</sup> of *C. graminicola* suspension containing either  $10^5$  spores ml<sup>-1</sup> (CgM2) or no spores (Mock). (B) Lesion area and fungal DNA amount. At 96 hpi lesion areas were measured by using ImageJ software and fungal DNA was quantified by qPCR. Bars indicate means  $\pm$  SD, n = 4, and significant differences are indicated by different letters. N.S., not significant.

## 2.2.2 Iron resupply restores the tolerance of Fe-deficient maize plants to *C. graminicola*

To verify whether there is also an immediate effect of the Fe nutritional status on the susceptibility of maize plants to *C. graminicola* infection, exogenous Fe was resupplied to Fe-deficient WT plants. Two days before the infection assay, Fe-deficient plants were transferred either to 10  $\mu\text{M}$  (-Fe) or to 100  $\mu\text{M}$  Fe(III)-EDTA (-Fe 100), while control plants were continuously cultivated on 100  $\mu\text{M}$  Fe (+Fe) (Fig. 10A). As indicated by infection symptoms, the lesion area and fungal DNA analysis, Fe-deficient leaves were more severely infected by the fungus than Fe-sufficient leaves (Fig. 10B, C). Compared to Fe-deficient leaves, the leaves in plants which were resupplied with 100  $\mu\text{M}$  Fe (-Fe 100) were less infected (Fig. 10B, C). These observations suggested that the tolerance of Fe-deficient maize plants can be restored by the resupply of Fe.

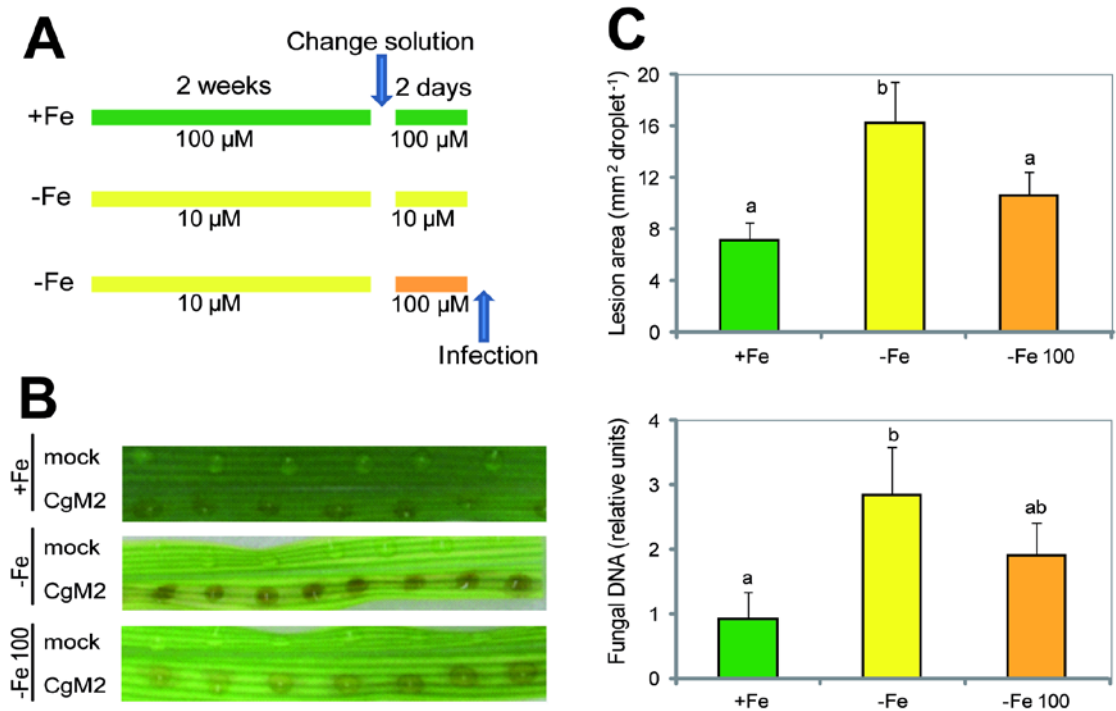


**Fig. 10. Fe resupply restores the tolerance of Fe-deficient plants to *C. graminicola*.** (A) Schematic view of the experimental design: maize plants were precultured with 100  $\mu\text{M}$  Fe (Fe-sufficient) or 10  $\mu\text{M}$  Fe (-Fe) for two weeks. Two days before infection, nutrient solutions were changed and -Fe plants were transferred either to 10 or to 100  $\mu\text{M}$  Fe-EDTA (-Fe 100). (B) Infection assay. Excised leaf blades were inoculated with 10  $\mu\text{l}$  of *C. graminicola* suspension containing either  $10^5$  spores  $\text{ml}^{-1}$  (CgM2) or no spores (Mock). (C) Lesion area and amount of fungal DNA. At 96 hpi lesion areas were measured by using ImageJ software and fungal DNA was quantified by using qPCR. Bars indicate means  $\pm$  SD,  $n = 4$ , and significant difference at  $p < 0.001$  for lesion areas and at  $p < 0.05$  for fungal DNA analysis are indicated by different letters.



### 2.2.3 Fungal growth and development in dependence of the Fe nutritional status of maize leaves

The different susceptibilities of Fe-sufficient and Fe-deficient maize leaves to *C. graminicola* infection suggested that fungal development might vary on both maize leaves. To examine the influence of the Fe nutritional status on fungal development, the following five time points, as previously characterized by Vargas et al. (2012), were chosen as they coincide with relevant changes in fungal development and lifestyle: 12 hpi, germination and appressorial formation; 24 hpi, penetration; 36 hpi, primary hyphae formation (biotrophic growth); 48 hpi, secondary hyphae formation (switch from bio- to necrotrophic growth); 72 hpi, necrotrophic growth. In this experiment, conidia germinated and formed appressoria on both Fe-sufficient and Fe-deficient leaves at 12 hpi (Fig. 11A). However, both germination and appressorial formation were significantly faster on Fe-deficient leaves (Fig. 11B). At 24 hpi, fungal germination and appressorial formation reached almost the same level on Fe-sufficient as on Fe-deficient leaves. At this time point primary hyphae appeared on both, Fe-sufficient and Fe-deficient leaves. However, on Fe-deficient leaves 14% of germinated conidia had already formed primary hyphae while on Fe-sufficient leaves those were only 2.7% (Fig. 11B). At 36 hpi the first secondary hyphae were found on Fe-deficient leaves, while these structures were still absent from Fe-sufficient leaves. From 36 hpi onwards, the rate of secondary hyphae formation on Fe-deficient leaves progressed faster than on Fe-sufficient leaves (Fig. 11B). Thus, these results showed that fungal growth and development, right away from germination and appressorial formation is accelerated on maize leaves suffering from Fe deficiency.

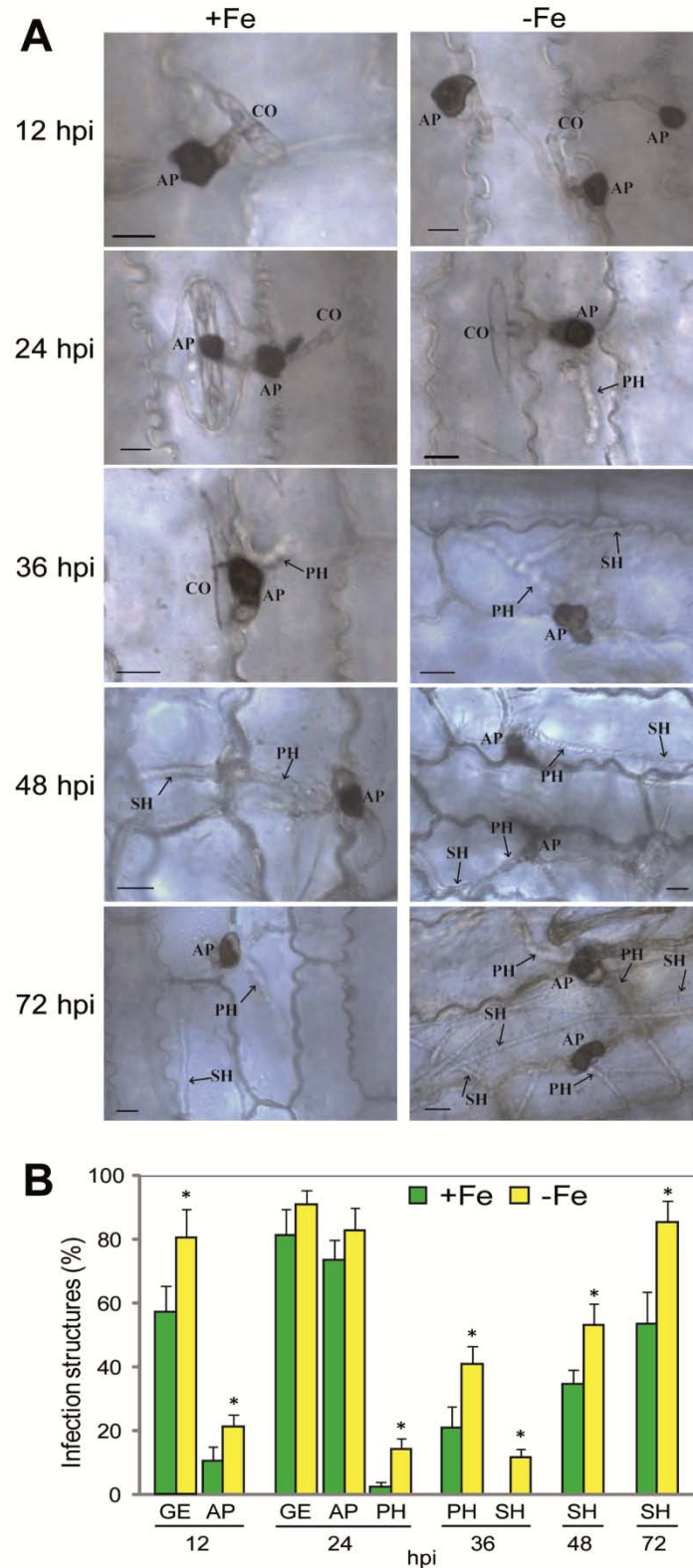


**Fig. 11. Development of infection structures by *Colletotrichum graminicola* on Fe-sufficient and Fe-deficient maize leaves.** (A) Microscopic analysis of *C. graminicola* development on Fe-sufficient (+Fe) and Fe-deficient (-Fe) maize leaves in a time course from 12 to 72 hpi. CO, conidia; AP, appressoria; PH, primary hyphae; SH, secondary hyphae. Bars =10  $\mu$ m. (B) From 12 to 72 hpi the following measures were taken under the microscope and expressed in %: no. of germinated spores per total no. of spores (GE), no. of appressoria per total no. of spores (AP), primary hyphae per total no. of appressoria (PH), and no. of secondary hyphae per total no. of appressoria (SH). Bars indicate means  $\pm$  SD from three biological replicates each with 100 analyzed infection sites; significant differences at  $p < 0.05$  are indicated by \*.

## **2.2.4 Influence of the Fe nutritional status on Fe distribution in maize leaves during *C. graminicola* infection**

### **2.2.4.1 Fe accumulation at infection sites of *C. graminicola***

Prussian blue staining has been widely used to specifically visualize the cellular and even intracellular localization of Fe in animal or plant tissues (Smith et al., 1997; Liu et al., 2007; Roschztardt et al., 2009; Cvitanich et al., 2010). In order to determine changes in cellular Fe distribution during fungal infection, Prussian blue staining was performed on infected leaf tissue in the same time course as before. While there was no particular difference in stained Fe between Fe-sufficient and Fe-deficient leaves 12 hpi, blue staining accumulated on Fe-sufficient leaves 24 hpi around the appressoria of infection sites (Fig. 12A, indicated by arrows). In contrast, on Fe-deficient leaves Fe staining events appeared only at 36 hpi. With the progression of infection, Fe staining events increased at a similar rate on both Fe-sufficient and Fe-deficient leaves up to 48 hpi (Fig. 12B). At 72 hpi, Fe-stained appressoria declined in both treatments, but fungal hyphae, mostly likely representing the thin, secondary hyphae, apparently contained more Fe than the surrounding plant tissue. These data indicated that Fe is recruited to the penetration sites subjacent to appressoria and that Fe accumulates earlier at the infection sites on Fe-sufficient leaves, which are also more tolerant to *C. graminicola* infection than Fe-deficient leaves.

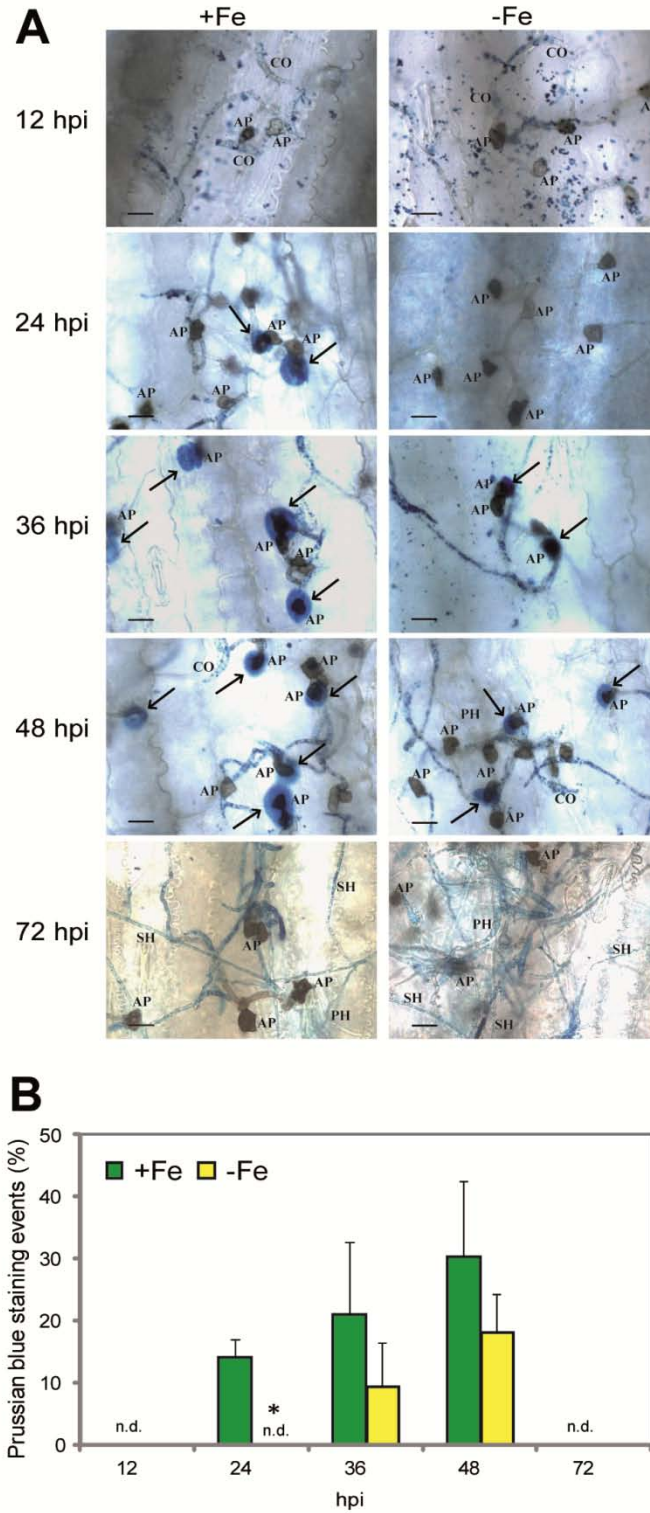


**Fig. 12. Fe accumulation at infection sites of Fe-sufficient and Fe-deficient maize leaves after *Colletotrichum graminicola* infection.** (A) Microscopic images of Prussian blue stained Fe-sufficient (+Fe) and Fe-deficient (-Fe) maize leaves after *C. graminicola* infection. Arrows indicate local Fe accumulation at infection sites. CO, conidia; AP, appressoria; PH, primary hyphae; SH, secondary hyphae. Bars = 10  $\mu$ m. (B) Quantitative analysis of Prussian blue staining events. The no. of Prussian blue-stained appressoria per 100 analyzed appressoria was counted from three biological replicates of each treatment; n.d.: not detected. Bars indicate means  $\pm$  SD, and significant differences at  $p < 0.05$  are indicated by \*.

#### 2.2.4.2 Analysis of different Fe fractions in maize leaves during *C. graminicola* infection

The results from Prussian blue staining indicated that *C. graminicola* infection causes a redistribution of Fe in maize leaves. In order to investigate dynamic changes in the Fe distribution in maize leaves during fungal infection, three different Fe fractions (total Fe, water-soluble and -insoluble Fe) were analyzed in a time course from 0 to 72 hpi. As expected, the concentration of total Fe, water-soluble and -insoluble Fe in Fe-sufficient leaves were significantly higher than in Fe-deficient leaves, regardless of whether the leaves were infected or not (Fig. 13A, B, C). The water-soluble Fe concentrations were higher than the total Fe concentrations (Fig. 13A, C). This might be due to the water-soluble Fe extraction procedure which changed the biomass of samples. Surprisingly, the total Fe concentrations in inoculated Fe-sufficient (+Fe CgM2) leaves at 48 and 72 hpi were higher than in uninfected leaves, whereas no significant differences in total leaf Fe were found during the entire infection period when plants were grown under Fe deficiency (Fig. 13A). Unlike the total Fe, water-soluble Fe increased significantly not only in inoculated Fe-sufficient (+Fe CgM2), but also in inoculated Fe-deficient (-Fe CgM2) leaves during the late necrotrophic growth stages (72 hpi) compared to mock treatments (Fig. 13B). In contrast, the water-insoluble Fe concentrations in both, infected Fe-sufficient (+Fe CgM2) and Fe-deficient (-Fe CgM2) leaves, remained relatively constant during the entire infection period and showed no significant difference between infection and mock treatments (Fig. 13C). These results suggested that *C. graminicola* infection may cause changes mainly in the water-soluble Fe fraction during the late necrotrophic growth phase.

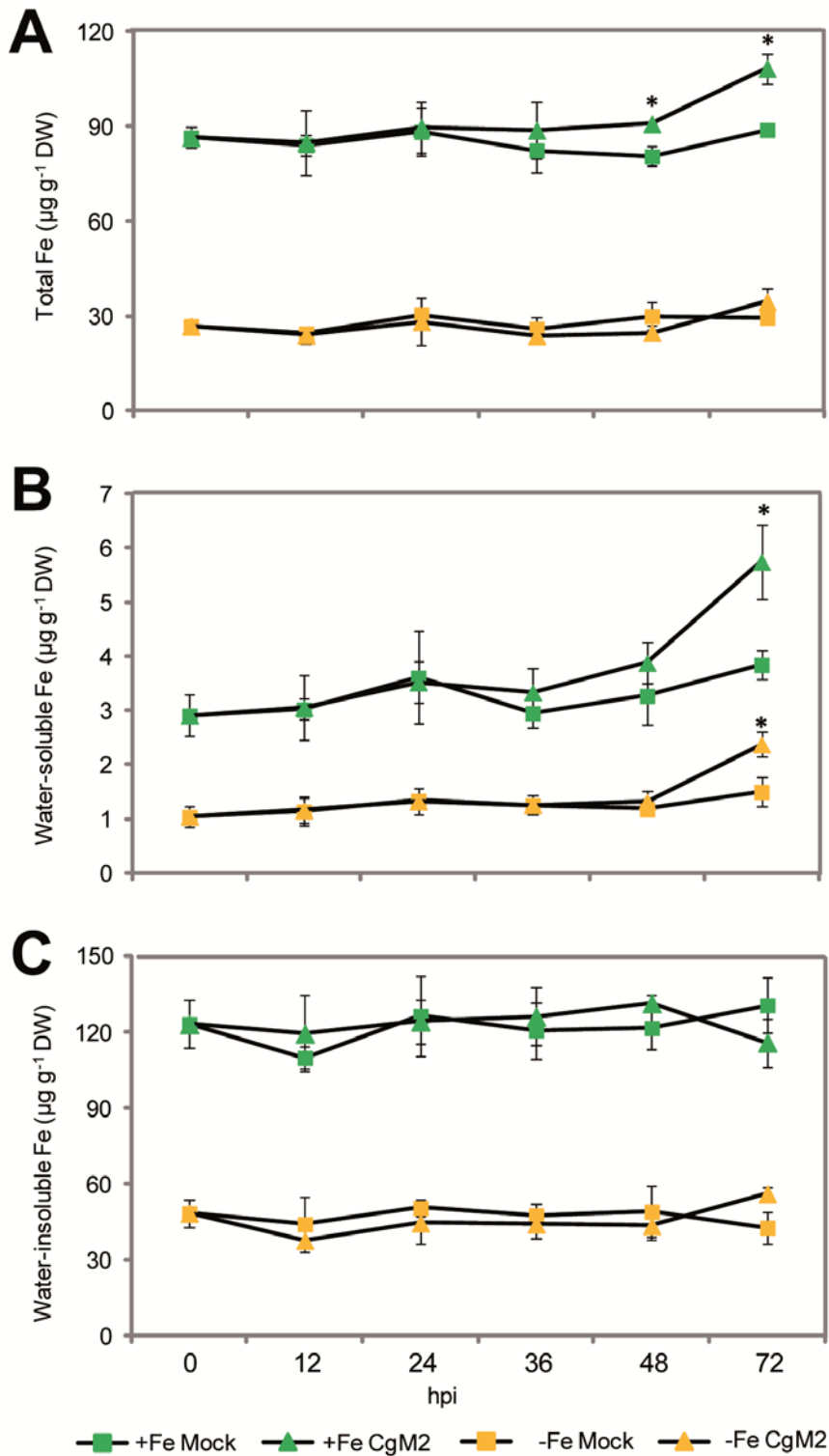


**Fig. 13. Changes in Fe pools of Fe-sufficient and Fe-deficient maize leaves during *Colletotrichum graminicola* infection.** (A) Total Fe concentration in Fe-sufficient and Fe-deficient leaves. (B) Water-soluble Fe concentration in maize leaves. (C) Water-insoluble Fe concentration in Fe-sufficient and Fe-deficient leaves. Bars indicate means  $\pm$  SD, and significant differences at  $p < 0.05$  are indicated by an asterisk \*.

### **2.2.5 The Fe nutritional status of maize leaves affects H<sub>2</sub>O<sub>2</sub> production during *C. graminicola* infection**

The production of ROS is a common active plant defense response to pathogen infection (Apel and Hirt, 2004; Trujillo et al., 2004; Jones and Dangl, 2006). H<sub>2</sub>O<sub>2</sub> has been reported as the major form of ROS produced in maize leaves infected with *C. graminicola* (Vargas et al., 2012). In order to investigate how the Fe nutritional status affects this plant defense response, H<sub>2</sub>O<sub>2</sub> production in Fe-sufficient and Fe-deficient maize leaves at different time points after fungal infection was visualized by staining with DAB (Thordal-Christensen et al., 1997). Whereas DAB staining events, shown as brown-reddish rings surrounding appressoria (Fig. 14A, arrows), were detected in Fe-sufficient leaves already at 24 hpi, they appeared only later, i.e. at 36 hpi, in Fe-deficient leaves. With the progression of fungal infection, H<sub>2</sub>O<sub>2</sub> production increased in both, but although it started earlier in Fe-sufficient leaves, DAB staining events increased less dramatically than in Fe-deficient leaves. At the late necrotrophic growth phase (72 hpi) Fe-deficient leaves were more strongly affected by H<sub>2</sub>O<sub>2</sub> production than Fe-sufficient leaves (Fig. 14B). Taken together, these results showed that i) Fe-sufficient leaves responded earlier to fungal infection with H<sub>2</sub>O<sub>2</sub> formation, and ii) H<sub>2</sub>O<sub>2</sub> production spread more quickly over Fe-deficient leaves when the necrotrophic growth phase had set in.

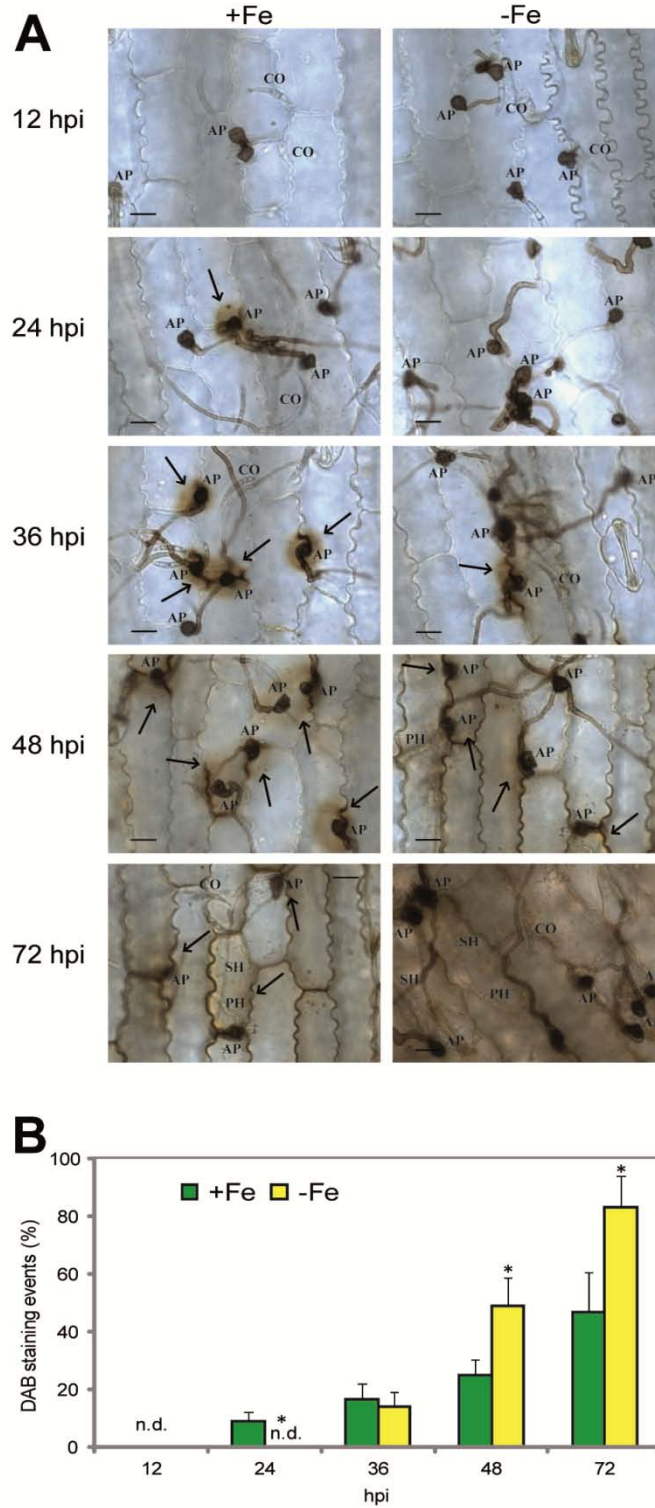


**Fig. 14. H<sub>2</sub>O<sub>2</sub> production in Fe-sufficient and Fe-deficient maize leaves after *Colletotrichum graminicola* infection.** (A) Microscopy analysis of 3,3'-diaminobenzidine (DAB)-stained Fe-sufficient (+Fe) and Fe-deficient (-Fe) maize leaves after *C. graminicola* infection. Arrows indicate local H<sub>2</sub>O<sub>2</sub> production at infection sites. CO, conidia; AP, appressoria; PH, primary hyphae; SH, secondary hyphae. Bars = 10  $\mu$ m. (B) Quantitative analysis of DAB staining events. The no. of DAB staining events per 100 analyzed appressoria was counted from three biological replicates of each treatment. Bars indicate means  $\pm$  SD, and significant differences at  $p < 0.05$  are indicated by \*, n.d.: not detected.



### **2.2.6 The Fe nutritional status in maize influences Fe homeostasis-related gene expression during *C. graminicola* infection**

Many pathogenesis-related (PR) genes are induced upon pathogen attacks and therefore are widely used as marker genes for defense responses in plant-pathogen interactions. To examine the effects of the Fe nutritional status in maize plants on defense responses to *C. graminicola* infection, the expression of *ZmPR-1*, *ZmPR-5*, *ZmPR-4b* and *ZmWind* genes which have already been reported as marker genes in the maize-*C. graminicola* pathosystem (Vargas et al., 2012), were analyzed in a time course. In general, the expression of all PR genes increased with the progression of infection. As expected, all four PR genes were induced in both Fe-sufficient and Fe-deficient leaves already during the early biotrophic growth phase at 12 or 24 hpi (Fig. 15). However, the expression levels of *ZmPR-1* were higher in Fe-sufficient leaves during entire infection period, whereas the levels of *ZmPR-4b* and *ZmWind* showed an opposite response and were higher in Fe-deficient leaves. These data suggested that the Fe nutritional status may differently influence the expression of PR genes during *C. graminicola* infection.

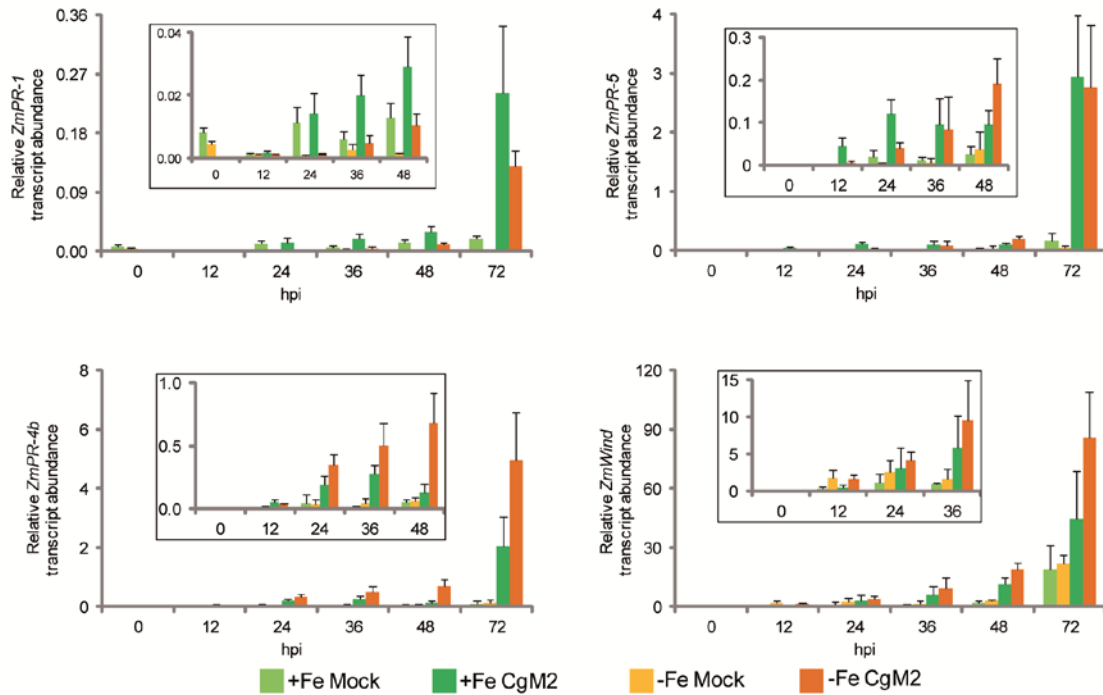


**Fig. 15. Influence of the Fe nutritional status of maize leaves on the expression of pathogenesis-related (PR) genes during *Colletotrichum graminicola* infection.** qRT-PCR analysis of the defense markers *PR-1*, *PR-5*, *PR-4b* and *Wind* in Fe-sufficient and Fe-deficient leaves during fungal infection. Bars indicate means  $\pm$  SD,  $n = 4$ .

Then, the relative expression levels of several Fe homeostasis-related genes involved either in Fe acquisition (*ZmYS1*, *ZmDMAS1* and *ZmIDEF1*), Fe storage (*ZmFER1*, *ZmFER2*, *ZmVIT1* and *ZmNRAMP3*) or in internal Fe allocation (*ZmNAS3*) were determined in a time course during *C. graminicola* infection of Fe-sufficient and -deficient leaves (Fig. 16). In general, changes in transcript abundance during the infection process were low with the exception of *ZmYS1* which increased  $> 3$ -fold in Fe-deficient leaves after 72 hpi. However, no striking differences were found in gene expression in dependence of the Fe nutritional status except for higher transcript levels of *ZmVIT1* and *ZmNAS3* in Fe-sufficient leaves 36 and 48 hpi. Thus, there was no consistent response to *Colletotrichum* infection in the transcriptional regulation of genes involved in Fe homeostasis, suggesting that the fungal infection did not yet disturb Fe homeostasis at the tissue level.

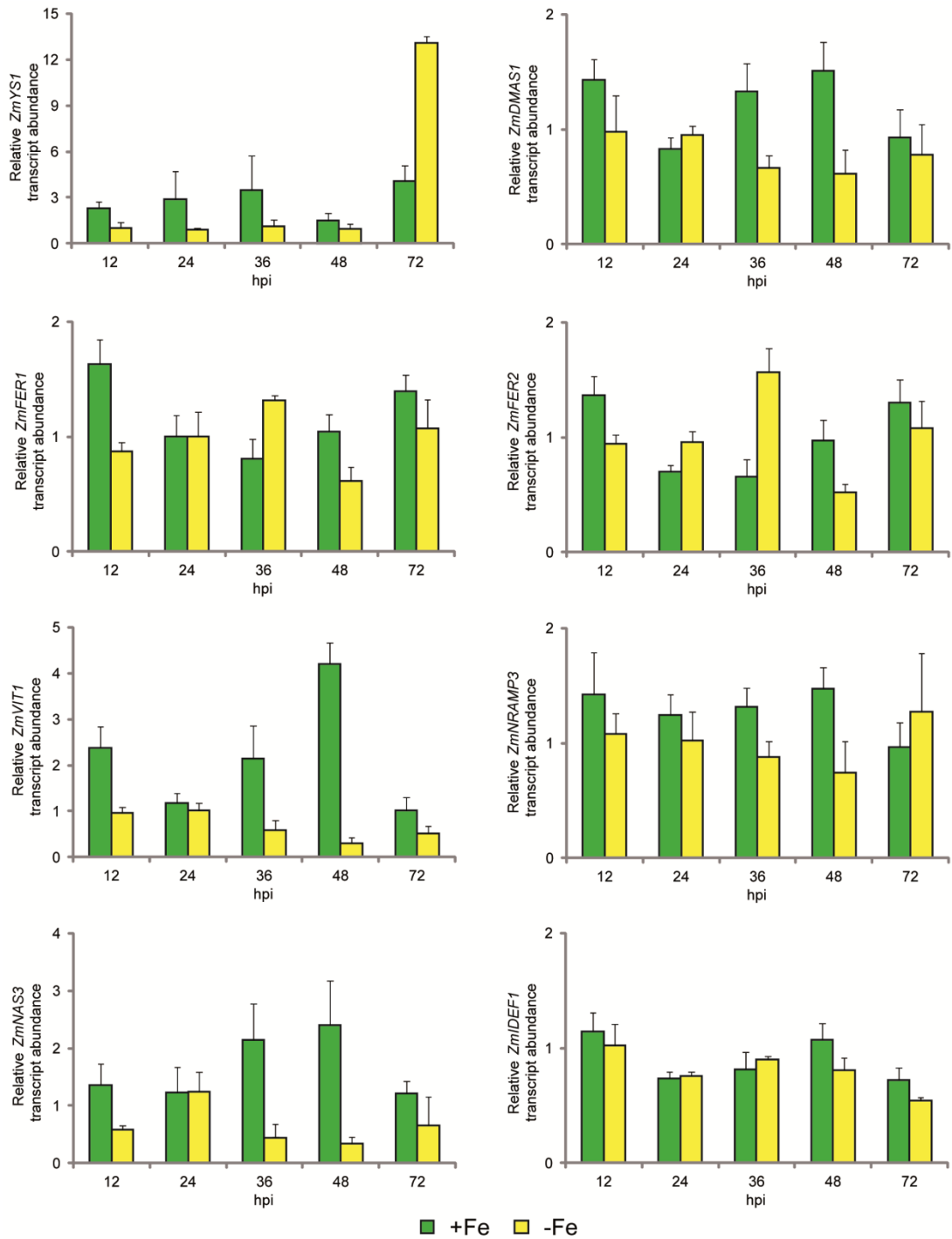


**Fig. 16. Influence of the Fe nutritional status of maize leaves on the expression of the Fe-homeostasis related genes during *Colletotrichum graminicola* infection.** qRT-PCR analysis of the Fe homeostasis-related genes (*ZmYS1*, *ZmDMAS1*, *ZmIDEF1*, *ZmFER1*, *ZmFER2*, *ZmVIT1*, *ZmNRAMP3* and *ZmNAS3*) in Fe-sufficient and Fe-deficient leaves during fungal infection. The values are the ratio of CgM2/Mock. Bars indicate means  $\pm$  SD, n = 4.

## 2.2.7 Influence of the Fe nutritional status of maize plants on the infection by fungal mutants defective in Fe acquisition

### 2.2.7.1 Infection assay with fungal mutants

*C. graminicola* mutants defective in either reductive Fe acquisition by deletion of one ( $\Delta fet3-1$ ) or two ( $\Delta fet3-1/2$ ) ferroxidase genes or defective in siderophore biosynthesis ( $\Delta nps6$  or  $\Delta sid1$ ) were previously employed to study the role of fungal Fe acquisition pathways in pathogenesis (Albarouki and Deising, 2013; Albarouki et al., 2014). In order to investigate the importance of the two fungal Fe acquisition strategies for the infection of maize leaves, wounded or non-wounded leaves were infected with a *C. graminicola* WT strain and the above-mentioned mutants. In agreement with the previous experiments, non-wounded Fe-deficient maize leaves were more severely infected by *C. graminicola* WT than Fe-sufficient leaves (Fig. 17A, B). As observed before (Fig. 17A, B), this difference largely disappeared when leaves were wounded before infection. In agreement with previous studies (Albarouki and Deising, 2013; Albarouki., 2014), *C. graminicola* mutants defective in siderophore biosynthesis ( $\Delta nps6$  and  $\Delta sid1$ ) or in Fe reduction ( $\Delta fet3-1$  and  $\Delta fet3-1/2$ ) were hampered in pathogenesis and led to less lesion symptoms and fungal proliferation (Fig. 17A, B). This reduced infectiousness of the mutants held true for Fe-sufficient as well as for Fe-deficient leaves, although Fe deficiency was of advantage for fungal proliferation. However, when maize leaves were wounded before, all *C. graminicola* mutants tested showed similar levels of infection irrespective of whether leaves were Fe deficient or not. This observation suggested that in particular the necrotrophic growth phase of *C. graminicola* is largely independent of the Fe nutritional status of maize leaves.

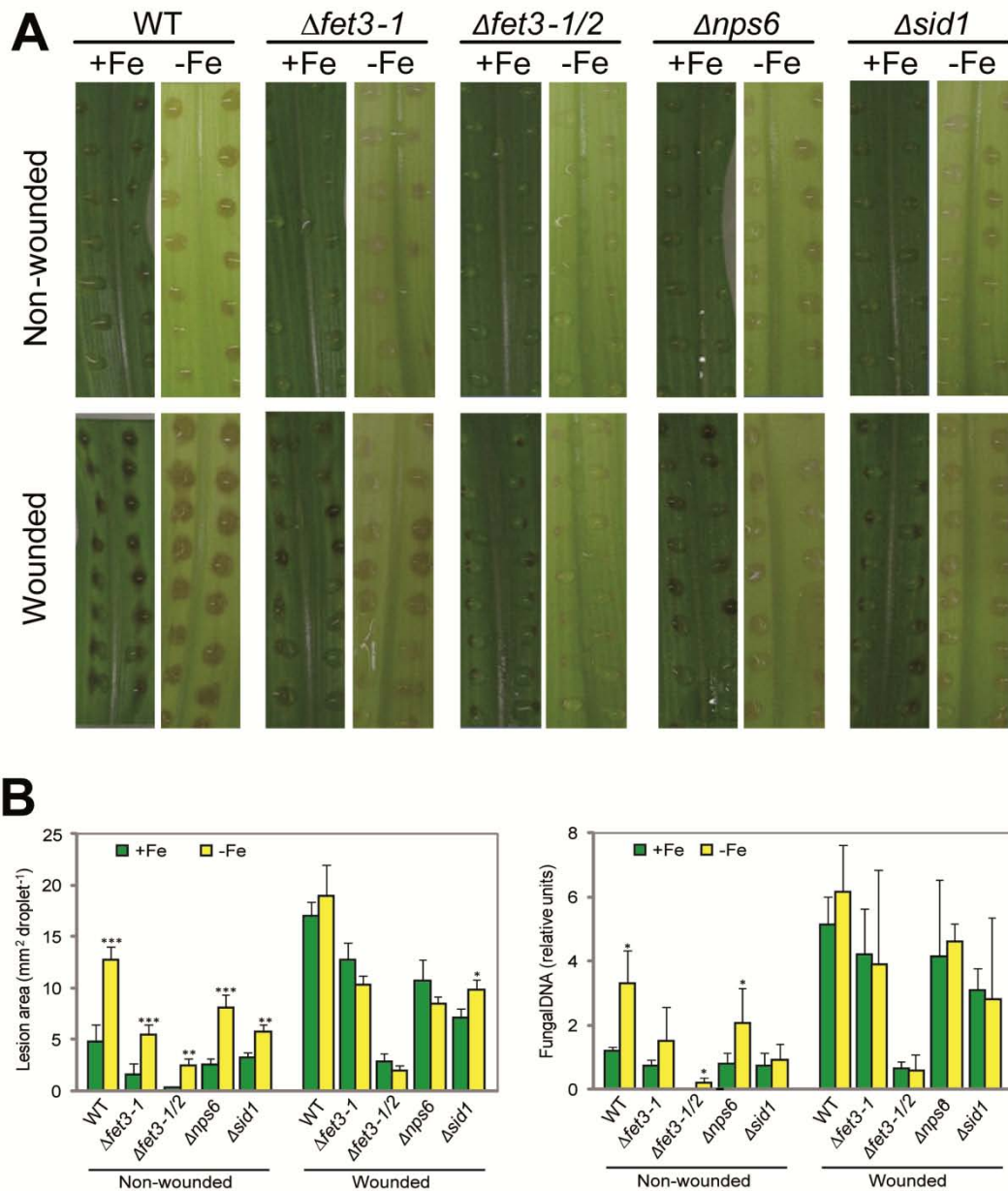


**Fig. 17. Influence of the Fe nutritional status of maize leaves on the infection by *Colletotrichum graminicola* mutants defective in Fe acquisition.** (A) Infection assay of *C. graminicola* WT and mutant strains defective either in reduction-based ( $\Delta fet3-1$  and  $\Delta fet3-1/2$ ) or siderophore-based ( $\Delta nps6$  and  $\Delta sid1$ ) Fe acquisition. Excised leaf blades were either wounded or not wounded and inoculated with 10  $\mu$ l of *C. graminicola* suspension containing either 10<sup>5</sup> spores ml<sup>-1</sup> or no spores. (B) At 96 hpi lesion areas were measured by using ImageJ software and fungal DNA was quantified by qPCR. Bars indicate means  $\pm$  SD, n = 4, and significant differences between Fe-sufficient and Fe-deficient at p < 0.05, 0.01 or 0.001 are indicated by \*, \*\* or \*\*\*.

### **2.2.7.2 Influence of the Fe nutritional status of maize leaves on the development of *Colletotrichum* mutants with disabled Fe acquisition**

The development of fungal mutants on non-wounded Fe-sufficient and Fe-deficient maize leaves was also investigated microscopically in a time course during infection. Compared to the wild-type strain, all fungal mutants showed weaker growth and delayed development at all critical time points (Fig. 18A-E). However, similar to the wild type, all fungal mutants showed a faster development on Fe-deficient leaves. There were no significant differences between mutants defective in reduction-based ( $\Delta fet3-1$  and  $\Delta fet3-1/2$ ) or the siderophore-based pathway ( $\Delta nps6$  and  $\Delta sid1$ ). Thus, a defect in either Fe acquisition pathway impaired fungal development.

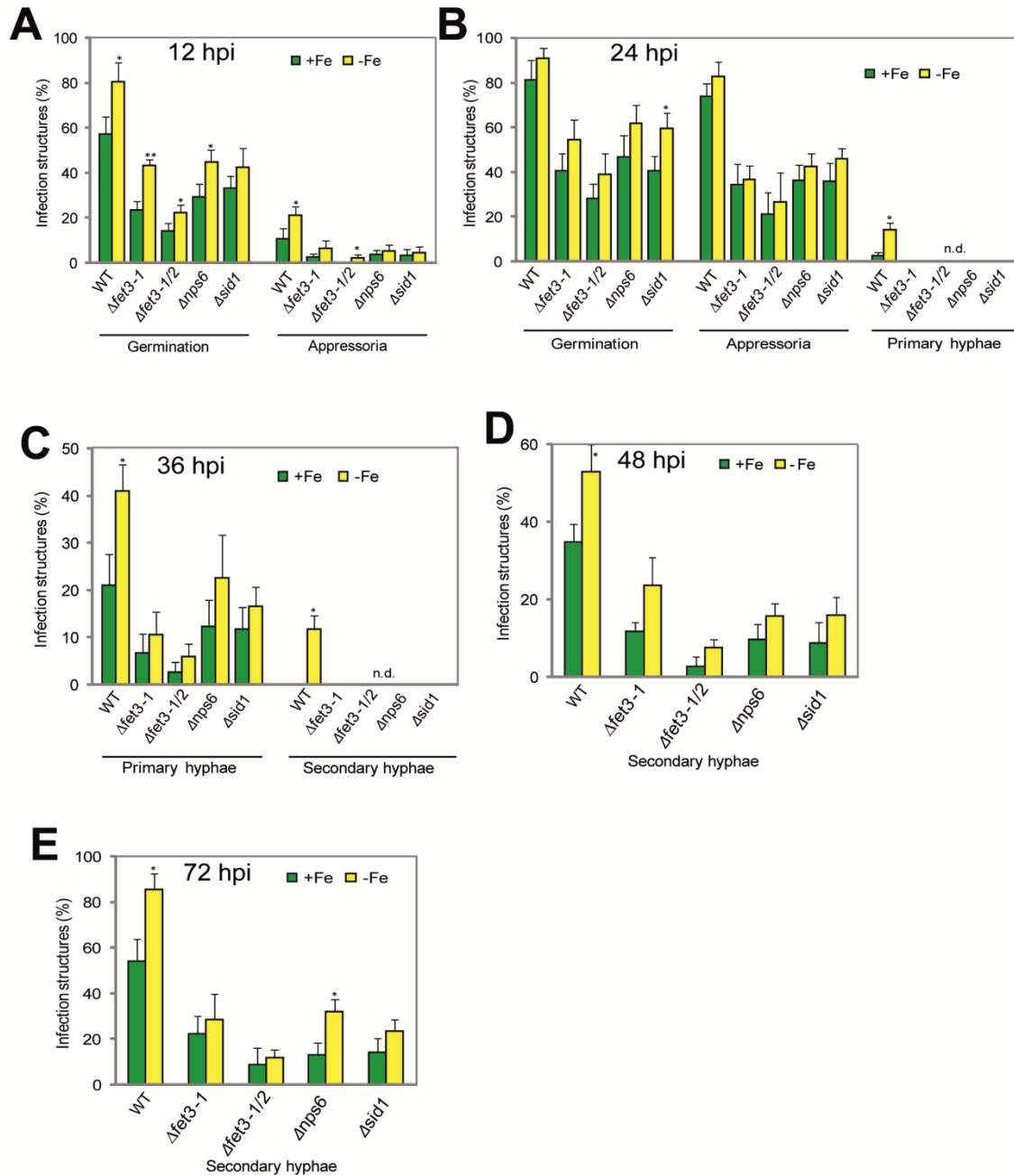


**Fig. 18. Quantitative analysis of infection structures of *Colletotrichum graminicola* wild-type and mutant strains on Fe-sufficient and Fe-deficient maize leaves.** From 12 to 72 hpi (A to E) the following measures were taken under the microscope and expressed in (%): no. of germinated spores per total no. of spores (GE), no. of appressoria per total no. of spores (AP), primary hyphae per total no. of appressoria (PH), and no. of secondary hyphae per total no. of appressoria (SH). n.d.: not detected. Bars indicate means  $\pm$  SD from three biological replicates each with 100 analyzed infection sites; significant differences at  $p < 0.05$  or  $0.001$  are indicated by \* or \*\*.

### 2.2.7.3 Influence of fungal Fe acquisition pathways on local Fe accumulation at the infection site

Prussian blue staining was employed to investigate the influence of the Fe nutritional status in maize leaves on Fe accumulation at the infection sites during fungal infection. In general, Fe staining appeared first in Fe-supplied leaves already at 24 hpi wild-type leaves showed a considerable number of staining events while only in *sid1* but not in the other mutants Fe could be stained at the infection sites (Fig. 19). Also at later time points, Prussian blue staining events appeared later or to a lower extent in particular in the *Colletotrichum* mutants affected in reduction-based Fe acquisition ( $\Delta fet3-1$  and  $\Delta fet3-1/2$ ). These data suggested that there was at least in tendency an influence of the fungal Fe acquisition pathways on the Fe accumulation in infected maize leaves in a way that reduction-based Fe acquisition of the fungus contributed to a local accumulation of Fe around the infection sites.

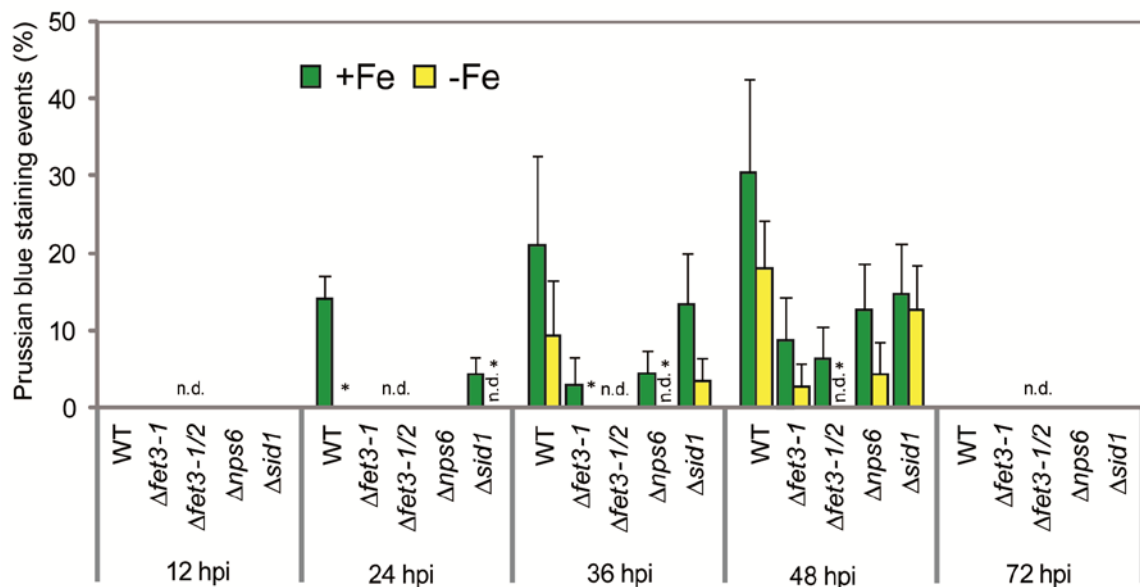


**Fig. 19. Quantitative analysis of Prussian blue-stained appressoria of *Colletotrichum graminicola* wild-type and mutant strains on Fe-sufficient and Fe-deficient maize leaves.** The no. of Prussian blue-stained appressoria per 100 analyzed appressoria was counted from three biological replicates of each treatment; n.d.: not detected. Bars indicate means  $\pm$  SD, and significant differences at  $p < 0.05$  are indicated by \*.



#### 2.2.7.4 Influence of fungal Fe acquisition pathways on local Fe accumulation H<sub>2</sub>O<sub>2</sub> formation at the infection site

To assess the influence of fungal Fe acquisition pathways on H<sub>2</sub>O<sub>2</sub> production of maize leaves of different Fe nutritional status, DAB staining was performed after maize leaves were infected with *Colletotrichum* wild-type and mutant strains defective either in the reduction-based ( $\Delta fet3-1$  and  $\Delta fet3-1/2$ ) or the siderophore-based pathway ( $\Delta nps6$  and  $\Delta sid1$ ). H<sub>2</sub>O<sub>2</sub> formation appeared first on Fe-sufficient leaves infected with wild-type and  $\Delta fet3-1$  but was detected soon after also in the leaves infected with the other mutants. With a delay of 12 h DAB-stained H<sub>2</sub>O<sub>2</sub> also appeared in Fe-deficient leaves, but there increased to a higher level. In general, H<sub>2</sub>O<sub>2</sub> staining tended to remain at higher levels in wild-type infected leaves during the entire infection period (Fig. 20). However, there were no significant differences in H<sub>2</sub>O<sub>2</sub> formation between the leaves infected by strains disabled in reduction-based ( $\Delta fet3-1$  and  $\Delta fet3-1/2$ ) or siderophore-based ( $\Delta nps6$  and  $\Delta sid1$ ) Fe acquisition. These data indicated that H<sub>2</sub>O<sub>2</sub> formation is slightly lower and delayed when maize leaves are infected by mutants with defective Fe acquisition.

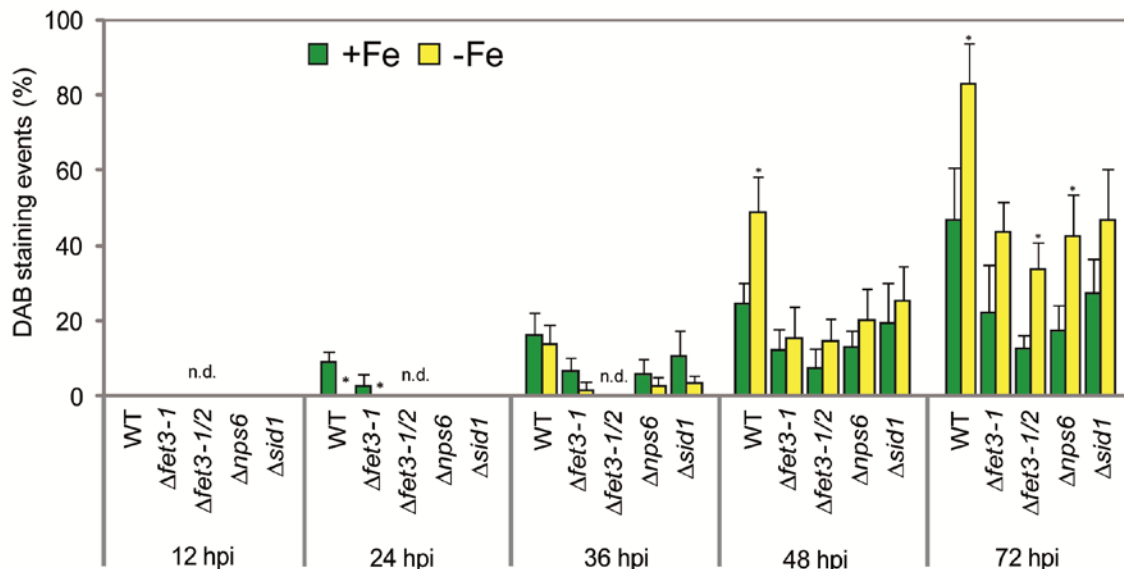


**Fig. 20. Quantitative analysis of DAB-stained appressoria of *Colletotrichum graminicola* wild-type and mutant strains on Fe-sufficient and Fe-deficient maize leaves.** The no. of DAB-stained appressoria per 100 analyzed appressoria was counted from three biological replicates of each treatment; n.d.: not detected. Bars indicate means  $\pm$  SD, and significant differences at  $p < 0.05$  are indicated by \*.

### 2.2.8 Fe deficiency affects maize leaf structure

Fe deficiency induces not only physiological but also morphological changes in plants (Fernandez et al., 2008; Eichert et al., 2010; Rellan-Alvarez et al., 2011), some of which might subsequently influence the susceptibility to pathogen infections. As shown in the previous experiment (3.2.3.) there was a delay in germination and formation of appressoria by *C. graminicola* when conidia were placed on Fe-sufficient maize leaves. This observation prompted to compare the ultrastructure of the surface of Fe-sufficient and Fe-deficient maize leaves using scanning electron microscopy (SEM) and transmission electron microscopy (TEM). The SEM analysis showed that the adaxial surface of Fe-deficient leaves appeared to have a thinner layer of epicuticular waxes as compared to Fe-sufficient leaves (Fig. 21A, B). Further, ultrastructural changes in the adaxial epidermal cell wall and cuticle were analyzed by TEM. The cell wall and the cuticle of Fe-deficient epidermis cells were significantly thinner than those of Fe-sufficient leaves (Fig. 21C, D). This was also reflected in a quantitative analysis measuring the thickness of epidermal cell walls (Fig. 21E). Fe deficiency decreased the thickness of the epidermal cell wall and cuticle approximately by 20% and 25%, respectively. Taken together, these data suggested that Fe deficiency impairs the ultrastructure of epidermal cells of maize leaves, which may contribute to a more rapid germination and formation of appressoria and finally lead to a higher susceptibility of maize plants to fungal infection.

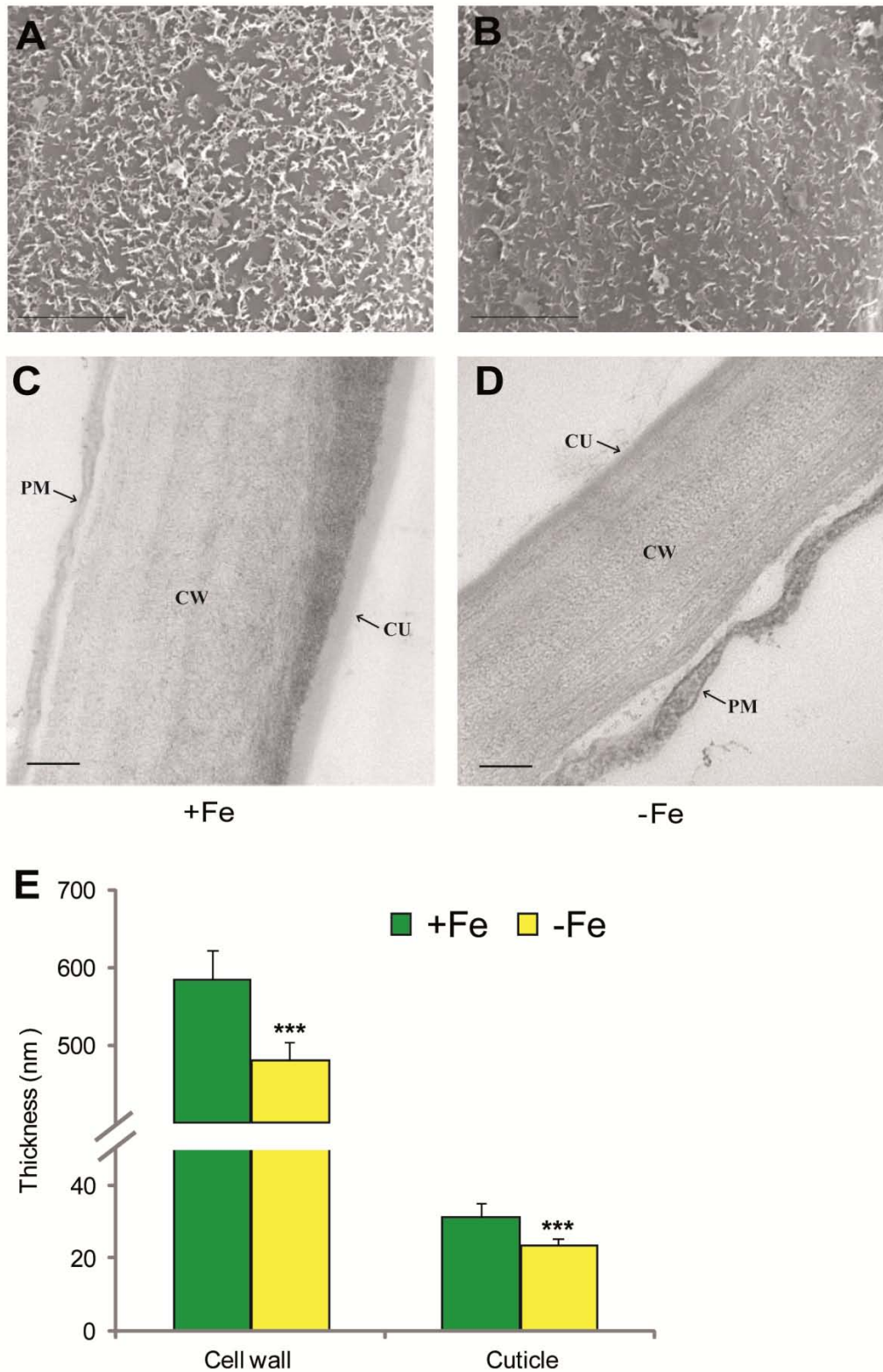


**Fig. 21. Influence of the Fe nutritional status of maize on the ultrastructure of leaf epidermal cells.** (A, B) SEM micrographs of the adaxial leaf surface of a Fe-sufficient and Fe-deficient leaf. Bars = 5  $\mu$ m. (C, D) TEM micrographs of the adaxial epidermal cell wall of a Fe-sufficient and Fe-deficient leaf. CU, cuticle; CW, cell wall; PM, plasma membrane. Bars = 100 nm. (E) Thickness of the adaxial epidermal cell wall and cuticle of Fe-sufficient and Fe-deficient maize leaves. Bars indicate means  $\pm$  SD, and significant differences between both treatments at  $p \leq 0.001$  are indicated by \*\*\*.

## 3 Fe in *Arabidopsis-Colletotrichum higginsianum* interaction

### 3.1 Material and methods

#### 3.1.1 Plant material and growth conditions

In the present study, the *Arabidopsis thaliana* accession line Columbia-0 (Col-0) was used as wild type. The following T-DNA insertion and mutant lines in the Col-0 genetic background were used: *f6'h1-1* (At3g13610; SALK\_132418C), *fer1* (At5g01600; SALK\_020482AZ), *frd3 (man1)* (Delhaize, 1996), *myb72-1* (At1g56160; SAIL\_713\_G10 Syngenta), *pye1* (At3g47640; SALK\_021217C), *vit1-1*, *vit1-1 x mtp8-1* (kindly provided by Prof. Dr. Edgar Peiter's lab (Plant Nutrition, Halle University, Germany)), *35S:FER1* (Duc et al., 2009), *35S:FIT1* (Jakoby et al., 2004), *35S:F6'H1 #3b*, *35S:MYB72* (Van der Ent et al., 2008), *35S:NAS k8* (Pianelli et al., 2005).

##### 3.1.1.1 Hydroponic culture

*Arabidopsis* seeds were placed on rockwool (Rockwool Mineralwool GmbH, Gladbeck, Germany), which was put in Eppendorf tubes of which the bottom was cut off. The tubes were placed on a polystyrene plate, floating on tap water in a 10 l basin. After one week, tap water was replaced by half-strength nutrient solution containing 25  $\mu\text{M}$  Fe-EDTA. Another week later full-strength nutrient solution containing 25  $\mu\text{M}$  Fe-EDTA was supplied. Two weeks after full-strength nutrient solution was supplied, seedlings were transferred in 5 l pots with aerated full-strength nutrient solution containing 50  $\mu\text{M}$  Fe-EDTA. The full-strength nutrient solution contained 1 mM  $\text{KH}_2\text{PO}_4$ , 1 mM  $\text{MgSO}_4$ , 0.25 mM  $\text{K}_2\text{SO}_4$ , 1 mM  $\text{Ca}(\text{NO}_3)_2$ , 50  $\mu\text{M}$  Fe-EDTA, 50  $\mu\text{M}$  KCl, 30  $\mu\text{M}$   $\text{H}_3\text{BO}_3$ , 5  $\mu\text{M}$   $\text{MnSO}_4$ , 1  $\mu\text{M}$   $\text{ZnSO}_4$ , 1  $\mu\text{M}$   $\text{CuSO}_4$ , 0.7  $\mu\text{M}$   $\text{NaMoO}_4$  and the pH was adjusted to 5.8. Nutrient solutions were changed every 4 days. Plants were precultured in a climate chamber under controlled environmental conditions with a 22/18°C and 10/14 h light/dark regime, a light intensity of 240  $\mu\text{mol photons m}^{-2} \text{s}^{-1}$  and at 70% relative humidity. Two weeks after transfer, a part of the plants was exposed to 0  $\mu\text{M}$  Fe-EDTA to

provoke Fe deficiency (-Fe), while the other plants were continuously supplied with 50  $\mu\text{M}$  Fe-EDTA and considered as Fe sufficient (+Fe). After 6 days youngest and fully expanded leaves were excised for the determination of Fe, and infection assays with *C. higginsianum* were conducted.

### 3.1.1.2 Soil culture

Plants were grown in a substrate (Substrat 1, Klasmann-Deilmann, Geeste, Germany) in a climate chamber at 60% humidity and a light intensity of 250  $\mu\text{mol photons m}^{-2} \text{ s}^{-1}$  and a 9/15 hours (20/18°C) day-night regime for 25 days. The youngest and fully expanded leaves were used for infection assays with *C. higginsianum*.

### 3.1.2 Fungal culture and plant inoculation

*Colletotrichum higginsianum* wild type strain IMI 349063A was kindly provided by O'Connell's lab (Max Planck-Institute for Plant Breeding Research, Cologne, Germany). The fungus was cultured on Mathur's medium at room temperature. The Mathur's medium contained (per 500 ml): glucose, 1.4 g,  $\text{MgSO}_4$ , 0.61 g,  $\text{KH}_2\text{PO}_4$ , 1.36 g, oxioid mycological peptone, 1.09 g and 15 g agar (Mathur et al., 1950). Fungal spores were harvested from a 2-4 week-old culture using sterile water. After 3 times of washing, conidia suspensions were adjusted to desired concentrations with a hemocytometer.

To infect plants grown with hydroponic culture, leaves were excised and placed on Petri dishes (23 x 23 cm, Corning, NY, USA) containing two layers of moist filter paper. Leaves were inoculated with 5  $\mu\text{l}$  droplets either containing  $10^5$  spores  $\text{ml}^{-1}$  (Ch) or no spores as mock control. Alternatively, a sterile pipette tip was used to wound the leaves immediately before inoculation. The dishes were incubated in darkness at 25°C. At 3, 4 and 5 dpi, symptoms were photographed for determination of lesion areas. Infected areas were collected at 4 dpi using a cork borer (diameter 0.4 cm) for fungal RNA analysis.

To infect the plants grown in substrate, intact leaves were inoculated with either 10  $\mu\text{l}$  suspension containing  $5 \times 10^5$  spores  $\text{ml}^{-1}$  or no spores as mock control. After inoculation, plants were placed in trays sealed in a plastic bag to maintain high

humidity and incubated in the same growth chamber. Plastic bags were removed after 24 hours. At 5 dpi, symptoms were either estimated along a disease score (DS) or photographed for quantitative determination of lesion areas, and infected areas were collected using a cork borer (diameter 0.5 cm) for fungal RNA analysis.

### **3.1.3 Infection assays**

#### **3.1.3.1 Determination of disease scores**

Disease scores (DS) were estimated based on numerical ratings from 0 to 3 of the extent of pathogen colonization on the host and the severity of host symptoms. DS 0 describes an intact plant with no symptoms or small pin-point brown flecks; DS 1 plants have mostly intact leaves with necrotic flecks or limited lesions. DS 2 referred to plants with partially collapsed leaves and with large brown necrotic lesions, some tissue maceration and water-soaked regions on the inoculated surface; partially, plants were collapsed. DS 3 indicates completely collapsed, macerated and water-soaked tissue (Birker et al., 2008).

#### **3.1.3.2 Determination of lesion areas**

Symptoms were photographed and lesion areas were measured using the ImageJ software (<http://rsbweb.nih.gov/ij/>).

#### **3.1.3.3 Quantification of fungal RNA**

Quantitative reverse transcription PCR (qRT-PCR) was employed for quantifying fungal RNA mass as described by Narusaka et al. (2010). Briefly, samples were homogenized using a mixer mill (MM400, Retsch, Haan, Germany) for 1 min at 30 Hz. The RNA was extracted with Trizol (Life Technologies, Darmstadt, Germany). After removing genomic DNA, RNA samples were reverse transcribed to cDNA with the RevertAid First Strand cDNA Synthesis Kit (Fermentas, St. Leon-Rot, Germany). qPCR was performed with a Mastercycler realplex (Eppendorf, Hamburg, Germany) and the IQ SYBR Green Supermix (Bio-RAd Laboratories, Hercules, CA, USA) using the specific primers for *AtCBP20* (At5g44200, nuclear

cap-binding protein subunit 20) and for *ChACT* (*C. higginsianum* actin; supplemental Table 1, page 98).

### **3.1.4 Quantification of the plant Fe nutritional status in Arabidopsis plants**

#### **3.1.4.1 Determination of chlorophyll concentrations**

Chlorophyll concentrations in Arabidopsis leaves were determined after extraction of fresh leaf material grinded in liquid N<sub>2</sub> with *N,N*-dimethylformamid (Sigma-Aldrich, Steinheim, Germany) at 4°C for 48 h. The absorbance at 647 and 664 nm was then measured in extracts according to Moran and Porath (1980) and Moran (1982).

#### **3.1.4.2 Determination of total Fe concentration**

After homogenization by a mixer mill (2.1.3.2.), the samples were dried at 65°C for 3 days. The Fe concentrations were measured by Inductively-Coupled Plasma Optic Emission Spectrometry (ICP-OES; iCAP, Thermo Scientific, Dreieich, Germany) after wet digestion of grinded leaf material in HNO<sub>3</sub> in a microwave (Eggert and von Wirén, 2013).

### **3.1.5 Histological staining and microscopy**

#### **3.1.5.1 Light microscopy**

Light microscopy was performed using a Zeiss Axio Imager M2 microscope (Zeiss, Oberkochen, Germany), equipped with a camera (Axio Cam MRC). After removing chlorophyll with 96% ethanol, infected leaves were mounted and directly observed under the microscope.

#### **3.1.5.2 Prussian blue staining**

For Fe staining, leaf segments were taken from sites where fungal suspensions had been placed on. Prussian blue staining was modified from Cvitanich et al. (2010). Briefly, after removing chlorophyll by extraction with methanol: chloroform: acetic acid (6:3:1, v/v/v), samples were stained with 1 volume of 4% HCl mixed with 1 volume of 8% (w/v) fresh potassium hexacyanoferrate (II) trihydrate (Merck,

Darmstadt, Germany) at 28°C for 24 h. After washing several times with bidestilled water, samples were mounted and observed under a light microscope.

### **3.1.5.3 DAB staining**

To localize the occurrence of hydrogen peroxide, 3,3'-diaminobenzidine (DAB) (Sigma-Aldrich, Steinheim, Germany) staining was conducted according to Hüchelhoven et al. (1999). After briefly dipping leaf samples in 0.1% (v/v) Tween 20, they were vacuum infiltrated with freshly prepared 0.1% (w/v) DAB solution (pH 3.8, HCl) and incubated overnight in the dark at room temperature. After removing chlorophyll with 96% ethanol, samples were mounted and observed under a light microscope.



## 3.2 Results

### 3.2.1 Influence of the iron nutritional status on the susceptibility of Arabidopsis plants to *C. higginsianum*

To examine the influence of the Fe nutritional status on the susceptibility of Arabidopsis plants to *C. higginsianum*, plants were first precultured hydroponically for 6 weeks. Then, a part of the plants were exposed to 0  $\mu\text{M}$  Fe-EDTA to achieve Fe deficiency (-Fe), while the other plants were continuously supplied with 50  $\mu\text{M}$  Fe-EDTA and considered as Fe sufficient (+Fe). Six days after exposure to 0  $\mu\text{M}$  Fe, Fe-deficiency symptoms expressed as chlorosis in younger leaves, whereas Fe-supplied plants did not show any chlorosis (Fig. 22A). As expected, Fe-deficient plants showed significantly lower concentrations of chlorophyll and total Fe in younger and fully expanded leaves compared to Fe-sufficient plants (Fig. 22B).

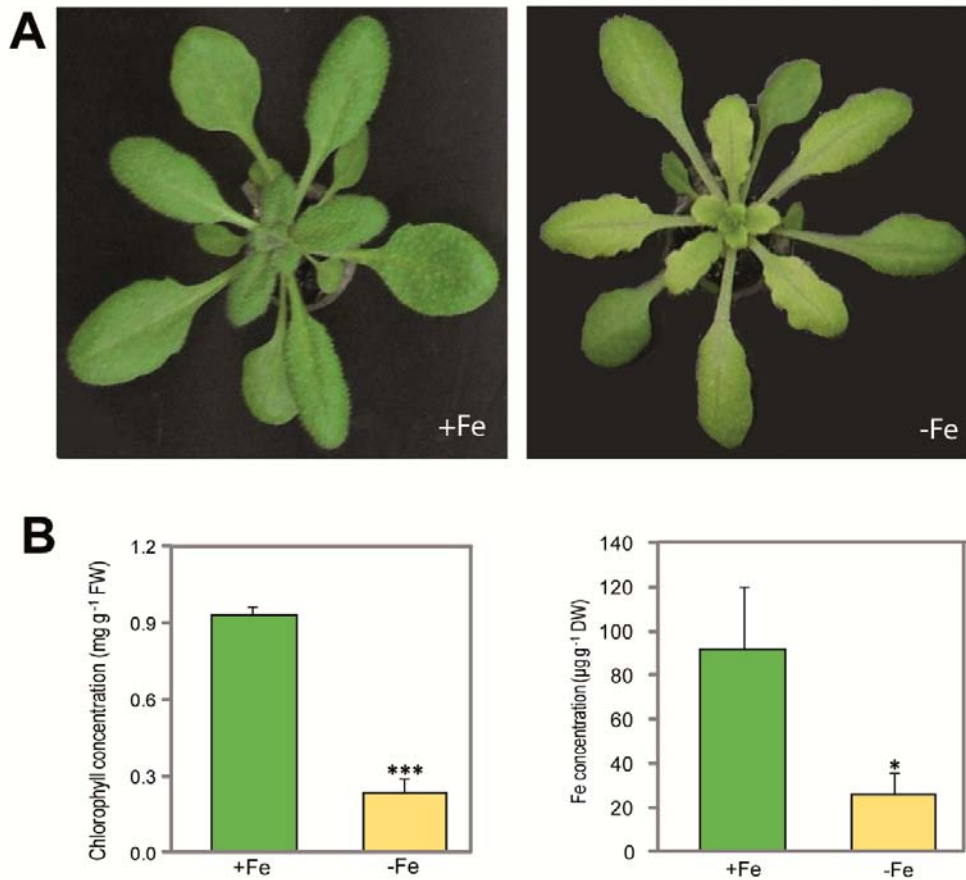


**Fig. 22. Iron nutritional status in Arabidopsis plants.** (A) Phenotype of Fe-sufficient and Fe-deficient Arabidopsis plants after transfer for 6 days to nutrient solution with (+Fe) or without (-Fe) 50  $\mu\text{M}$  Fe. (B) Chlorophyll and total Fe concentrations of younger fully expanded leaves. Bars indicate means  $\pm$  SD,  $n = 4$ , and significant differences at  $p < 0.05$ , 0.01 or 0.001 are indicated by \*, \*\* or \*\*\*.

Subsequently, an infection assay was conducted on wounded and non-wounded leaf segments, and symptoms were photographed 3, 4 and 5 dpi (Fig. 23A). With increasing incubation time the severity of the infection increased on both Fe-sufficient and Fe-deficient leaf segments. On non-wounded leaves, the severity of disease symptoms was lower on Fe-sufficient than on Fe-deficient leaves, as indicated by significantly larger lesion areas (Fig. 23B) and higher levels of fungal RNA mass (Fig. 23C). In contrast, on wounded leaves the severity of disease symptoms was similar in Fe-sufficient and Fe-deficient leaves suggesting that the plant Fe nutritional status has no more impact on fungal infection and proliferation. Taken together, this experiment showed that the Fe nutritional status strongly affects the susceptibility of non-wounded *Arabidopsis* plants to *C. higginsianum* in a way that Fe-deficient *Arabidopsis* plants are more susceptible than Fe-sufficient plants.

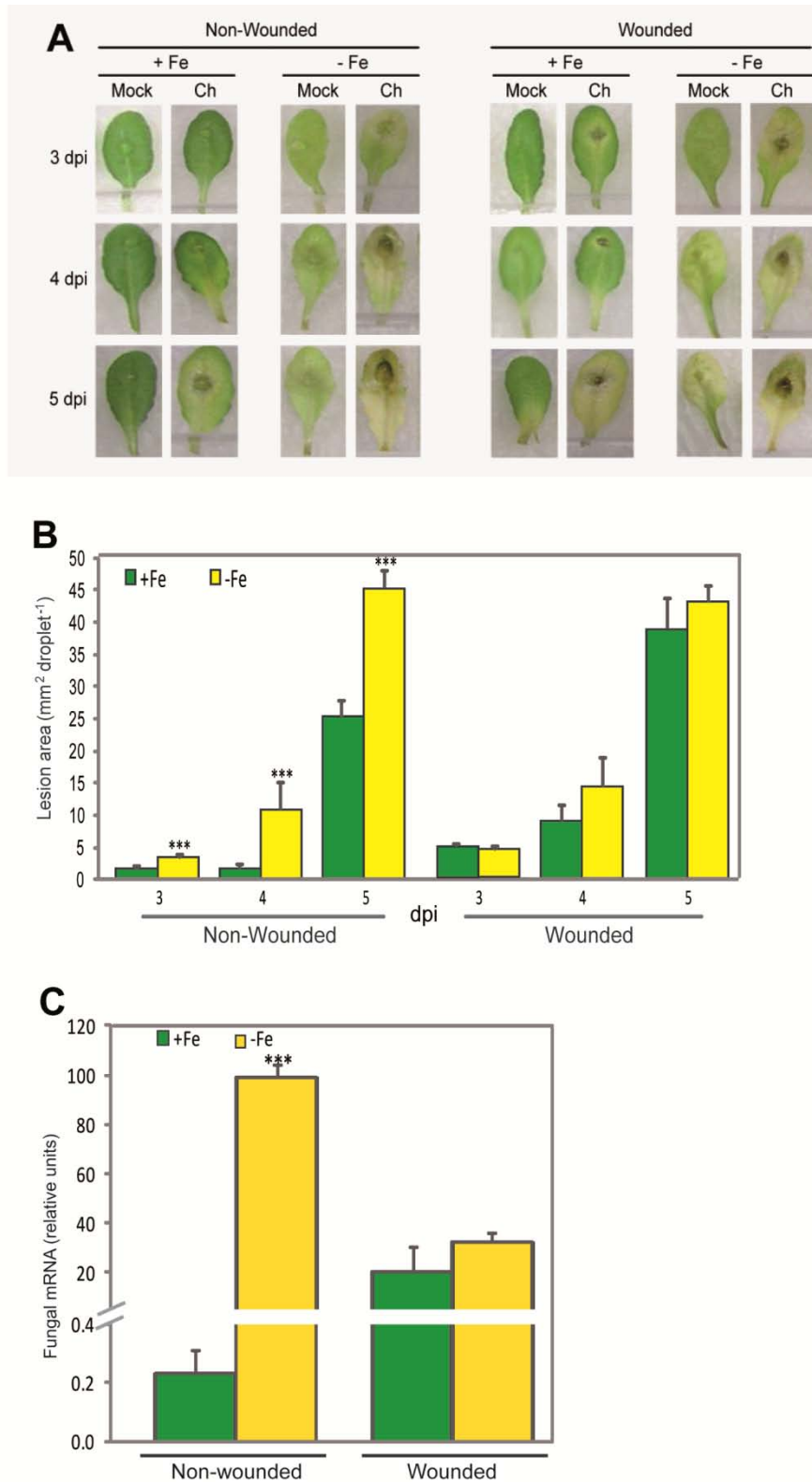


**Fig. 23. Influence of the Fe nutritional status of Arabidopsis on *C. higginsianum* infection.** (A) Infection assay. Excised leaf blades were either wounded or not wounded and inoculated with 5  $\mu$ l of *C. higginsianum* suspension containing either  $10^5$  spores/ml (Ch) or no spores (Mock). (B) Lesion area measurement (3, 4 and 5 dpi) and fungal RNA quantification (4 dpi). Lesion areas were measured using the ImageJ software and fungal RNA was quantified by qRT-PCR. Bars indicate means  $\pm$  SD, n = 4, and significant differences between Fe treatments at p < 0.05, 0.01 or 0.001 are indicated by \*, \*\* or \*\*\*.

### **3.2.2 Fungal growth and development are accelerated on Fe-deficient Arabidopsis leaves**

The influence of the Fe nutritional status on fungal development was examined on Fe-sufficient and Fe-deficient Arabidopsis leaves in a time course from 12 to 96 hpi which are characterized by the following fungal development: 12 hpi, germination and appressorial formation; 24 to 36 hpi, penetration; 48 hpi, primary hyphae formation (biotrophic growth); 72 hpi, secondary hyphae formation (switch from bio- to necrotrophic growth); 96 hpi, necrotrophic growth. At 12 hpi, conidia already germinated and formed appressoria on both Fe-sufficient and Fe-deficient leaves (Fig. 24A). However, the germination rate and appressorium formation rate was twofold higher on Fe-deficient leaves than on Fe-sufficient leaves (Fig. 24B). At 36 hpi, the fungus already formed primary hyphae on Fe-deficient leaves whereas this structure was still absent from Fe-sufficient leaves (Fig. 24A). From this time point onwards, the rate of secondary hyphae formation on Fe-deficient leaves progressed faster than on Fe-sufficient leaves, as indicated by quantitative analysis of infection structures (Fig. 24B). These results showed that *C. higginsianum* grows and develops faster on Fe-deficient Arabidopsis leaves than on Fe-sufficient leaves.

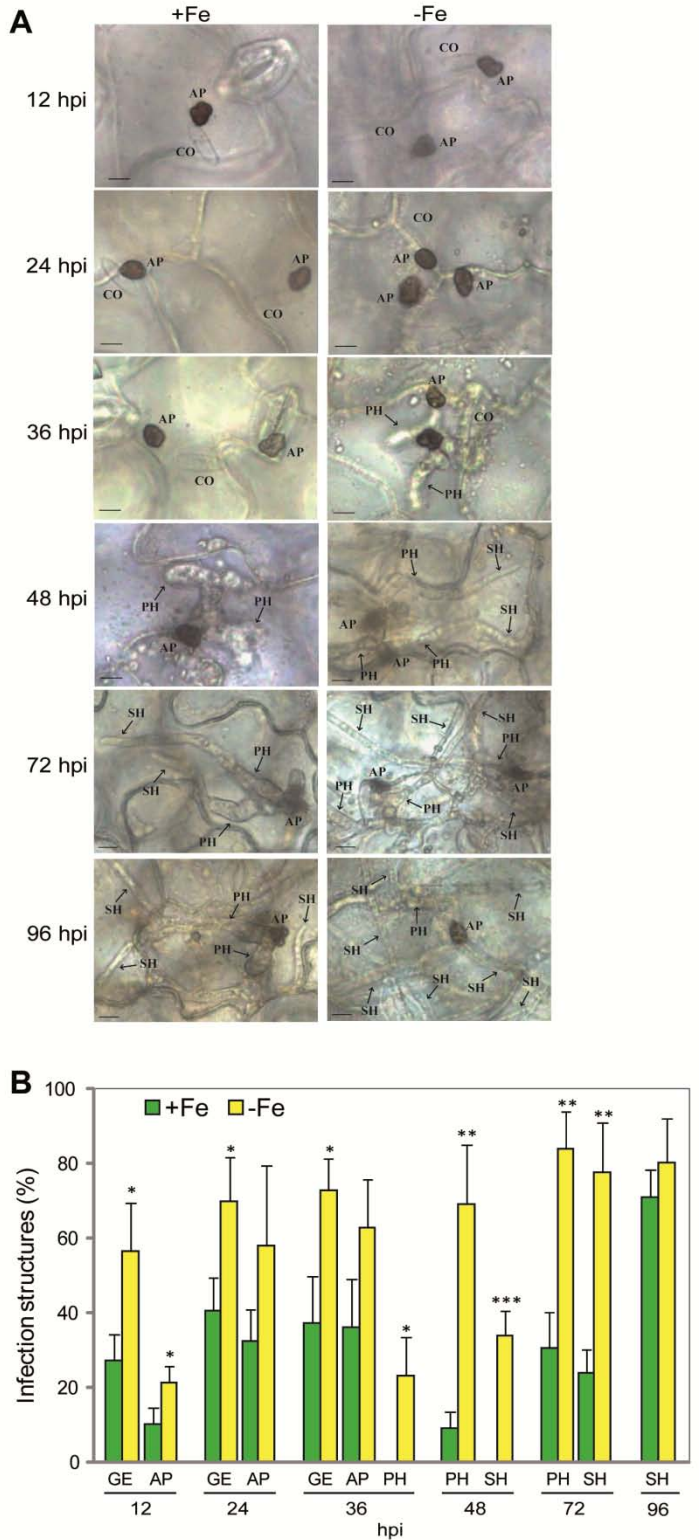


**Fig. 24. Development of infection structures by *Colletotrichum higginsianum* on Fe-sufficient and Fe-deficient Arabidopsis leaves.** (A) Microscopic analysis of *C. higginsianum* development on Fe-sufficient and Fe-deficient Arabidopsis leaves in a time course from 12 to 96 hpi. CO, conidia; AP, appressoria; PH, primary hyphae; SH, secondary hyphae. Bars =10  $\mu$ m. (B) From 12 to 96 hpi the following measures were taken under the microscope and expressed in %: no. of germinated spores per total no. of spores (GE), no. of appressoria per total no. of spores (AP), primary hyphae per total no. of appressoria (PH), and no. of secondary hyphae per total no. of appressoria (SH). Bars indicate means  $\pm$  SD from three biological replicates each with 100 analyzed infection sites; significant differences between Fe treatments at  $p < 0.05$ ,  $0.01$  or  $0.001$  are indicated by \*, \*\* or \*\*\*.

### 3.2.3 Assessment of the sensitivity to *C. higginsianum* in Arabidopsis lines affected in the expression of Fe homeostasis-related genes

To examine the influence of individual physiological processes on the susceptibility of Arabidopsis plants to *C. higginsianum*, transgenic Arabidopsis lines with modulated expression of Fe homeostasis-related genes were used. The genes of these mutants are involved either in Fe acquisition (*35S:FIT1*, *myb72-1*, *35S:MYB72*, *f6'h1-1*, *35S:F6'H1 #3b* and *frd3*), in Fe storage (*fer1*, *35S:FER1*, *vit1-1* and *vit1-1 x mpt8-1*), or in internal Fe allocation (*35S:NAS k8* and *pye1*). At 4 dpi, symptoms were photographed and the severity of disease symptoms was assessed by visual rating of the necrotic areas formed at the inoculation sites (Fig. 25A). As indicated by the disease score, *35S:FIT1*, *fer1* and *f6'h1-1* tended to be less severely infected by the fungus compared to Col-0, whereas the rest of the Arabidopsis lines were more severely infected (Fig. 25B). The disease scores of *pye1*, *35S:F6'H1 #3b*, *vit1-1* and *35S:FER1* were significantly higher than that of Col-0. On the other hand, fungal mRNA mass was significantly lower in *35S:FIT1*, and significantly higher in *vit1-1*, *35S:F6'H1 #3b*, *35S:NAS k8* and *35S:FER1* than in Col-0 (Fig. 25C). Together, these results suggested that certain Fe homeostasis-related genes indeed influence the susceptibility of Arabidopsis plants to *C. higginsianum*. In particular the lines *35S:FIT1*, *35S:FER1*, *35S:F6'H1 #3b*, *35S:NAS k8* and *vit1-1* were considered to modulate plant susceptibility to the fungus and were thus selected for further experiments.

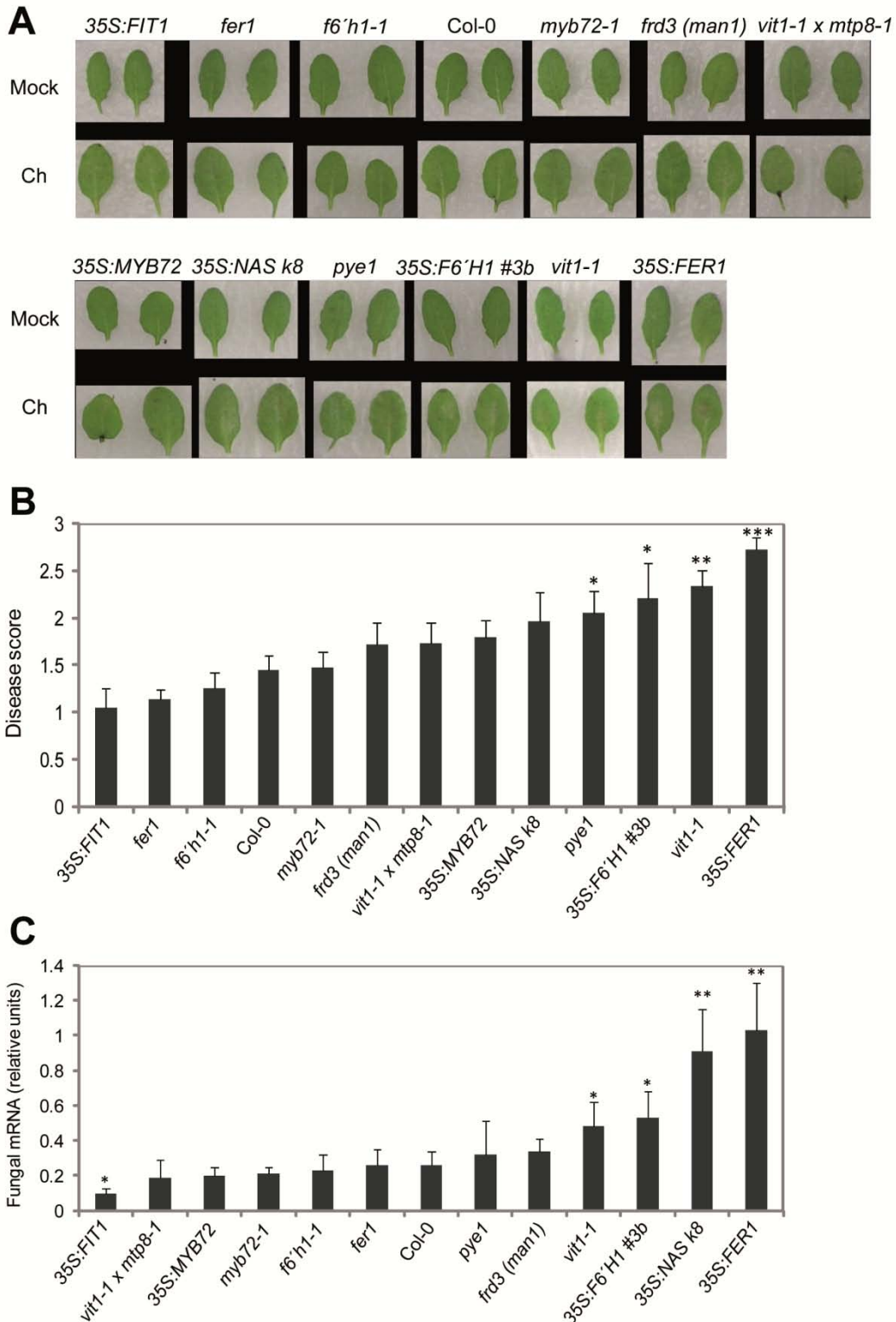


**Fig. 25. Sensitivity of different Arabidopsis lines to *C. higginsianum* infection.** (A) Infection assay. Excised leaf blades were inoculated with 5  $\mu$ l of *C. higginsianum* suspension containing either  $10^5$  spores  $\text{ml}^{-1}$  (Ch) or no spores (Mock). (B) Disease score and fungal RNA quantification. Disease scores were rated based on the severity of symptoms, and fungal RNA was quantified by qRT-PCR. Bars indicate means  $\pm$  SD,  $n = 4$ , and significant differences at  $p < 0.05$ ,  $0.01$  or  $0.001$  are indicated by \*, \*\* or \*\*\*.

### **3.2.4 Influence of the expression of Fe homeostasis-related genes on Fe accumulation and H<sub>2</sub>O<sub>2</sub> production after infection with *C. higginsianum***

#### **3.2.4.1 Confirmation of disease susceptibility of the lines *35S:FIT1*, *35S:FER1*, *35S:F6'H1 #3b*, *35S:NAS k8* and *vit1-1***

Five lines (*35S:FIT1*, *35S:FER1*, *35S:F6'H1 #3b*, *35S:NAS k8* and *vit1-1*) from the previous screening experiment were selected for further investigation by using Prussian blue and DAB staining. First, the infection assay of the selected Arabidopsis lines was repeated to confirm the susceptibility of these lines to *C. higginsianum*. At 4 dpi, symptoms were photographed for lesion area measurements, and infected leaf tissues were collected for fungal RNA analysis (Fig. 26A). According to lesion area analysis (Fig. 26B) and fungal RNA analysis (Fig. 26C) *35S:FIT1* showed a lower susceptibility to *C. higginsianum* than Col-0, whereas the other four lines, *35S:FER1*, *35S:F6'H1 #3b*, *35S:NAS k8* and *vit1-1*, were more severely infected as shown by larger necrotic areas (Fig. 26A). According to fungal RNA mass the extent of the susceptibility was slightly different among these four lines when compared to the results of the previous experiment (Fig. 25C). Nevertheless, this experiment confirmed that *35S:FIT1* plants are more resistant to *C. higginsianum* whereas *35S:FER1*, *35S:F6'H1 #3b*, *35S:NAS k8* and *vit1-1* plants are more susceptible than WT plants.



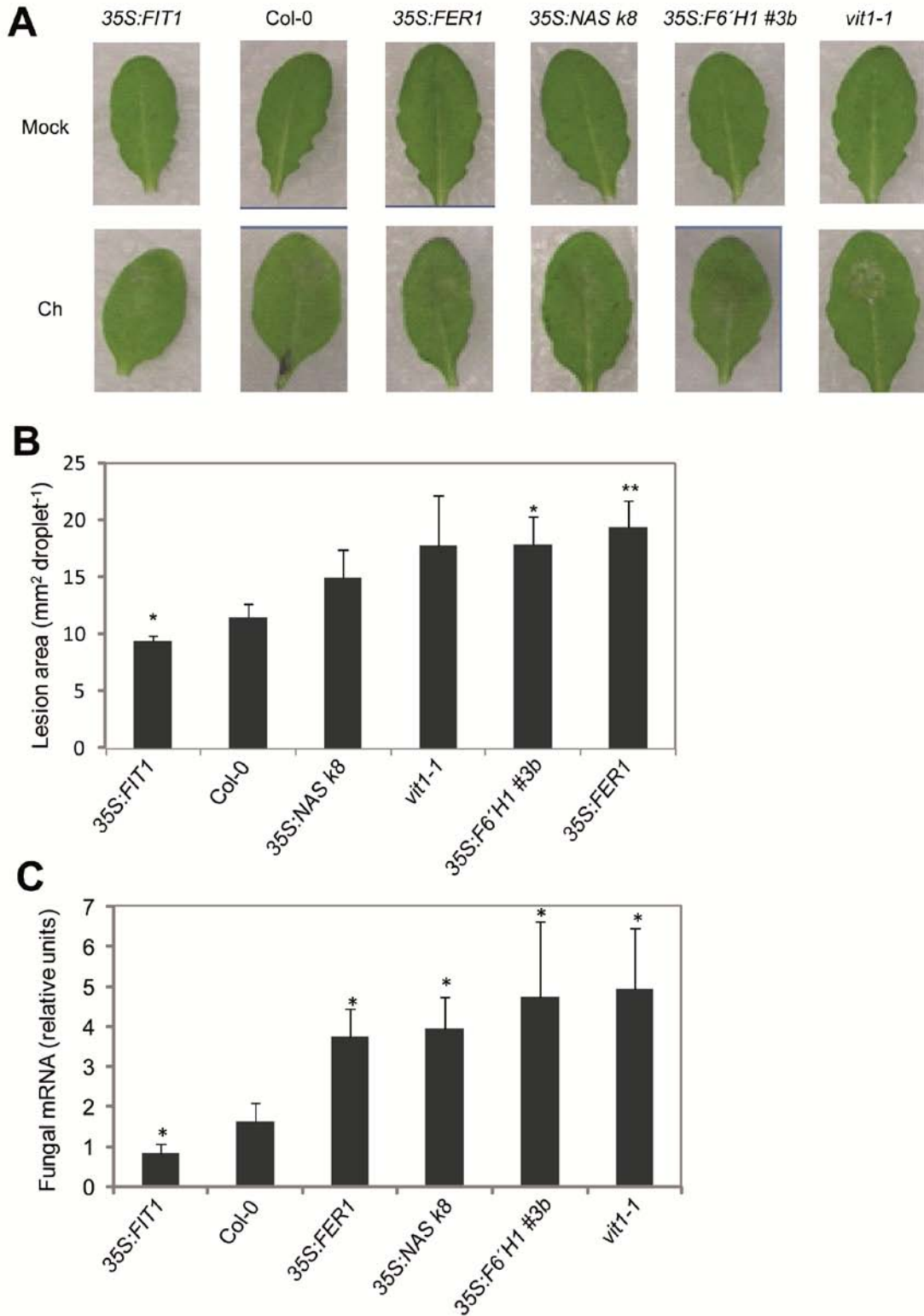


**Fig. 26. Confirmation of the susceptibility to *C. higginsianum* in different Arabidopsis lines.** (A) Infection assay. Excised leaf blades were inoculated with 5  $\mu$ l of *C. higginsianum* suspension containing either  $10^5$  spores  $\text{ml}^{-1}$  (Ch) or no spores (Mock). (B) Lesion area measurement and fungal RNA quantification. Lesion areas were measured using the ImageJ software and fungal RNA was quantified by qRT-PCR. Bars indicate means  $\pm$  SD,  $n = 4$ , and significant differences at  $p < 0.05$ ,  $0.01$  or  $0.001$  are indicated by \*, \*\* or \*\*\*.

### 3.2.4.2 Influence of the expression of Fe homeostasis-related genes on Fe accumulation after infection with *C. higginsianum*

In order to investigate the influence of Fe homeostasis-related genes on Fe accumulation at infection sites, Prussian blue staining was performed with infected Arabidopsis leaves in a time course from 12 to 96 hpi after *C. higginsianum* infection. At 24 hpi Prussian blue stained Fe only in conidia. While blue rings of Prussian blue-stained Fe surrounding the infection sites appeared on wild-type leaves not before 72 hpi, they were observed earlier in leaf tissues of *35S:FER1* and *vit1-1* leaves, i.e. already at 48 hpi (Fig. 27A). At 72 hpi all the four lines *35S:FER1*, *vit1-1*, *35S:NAS k8* and *35S:F6'H1 #3b* showed blue-stained fungal structures under the epidermal surface, which appeared to be strongest on *vit1-1* leaves. By contrast, on *35S:FIT1* leaves only conidia residing on the leaf surface were stained, while Fe staining around hyphal structures appeared only at 96 hpi. With progressing duration after the infection, Prussian blue-stained Fe increased in all Arabidopsis leaves, which was confirmed by the quantitative analysis of Fe staining events (Fig. 27B). At the final time point (96 hpi), the lines *35S:FER1*, *35S:F6'H1 #3b*, and *vit1-1* showed a significantly higher number of Prussian blue staining events than Col-0 (Fig. 27B), indicating that these lines favour Fe accumulation at fungal infection sites.

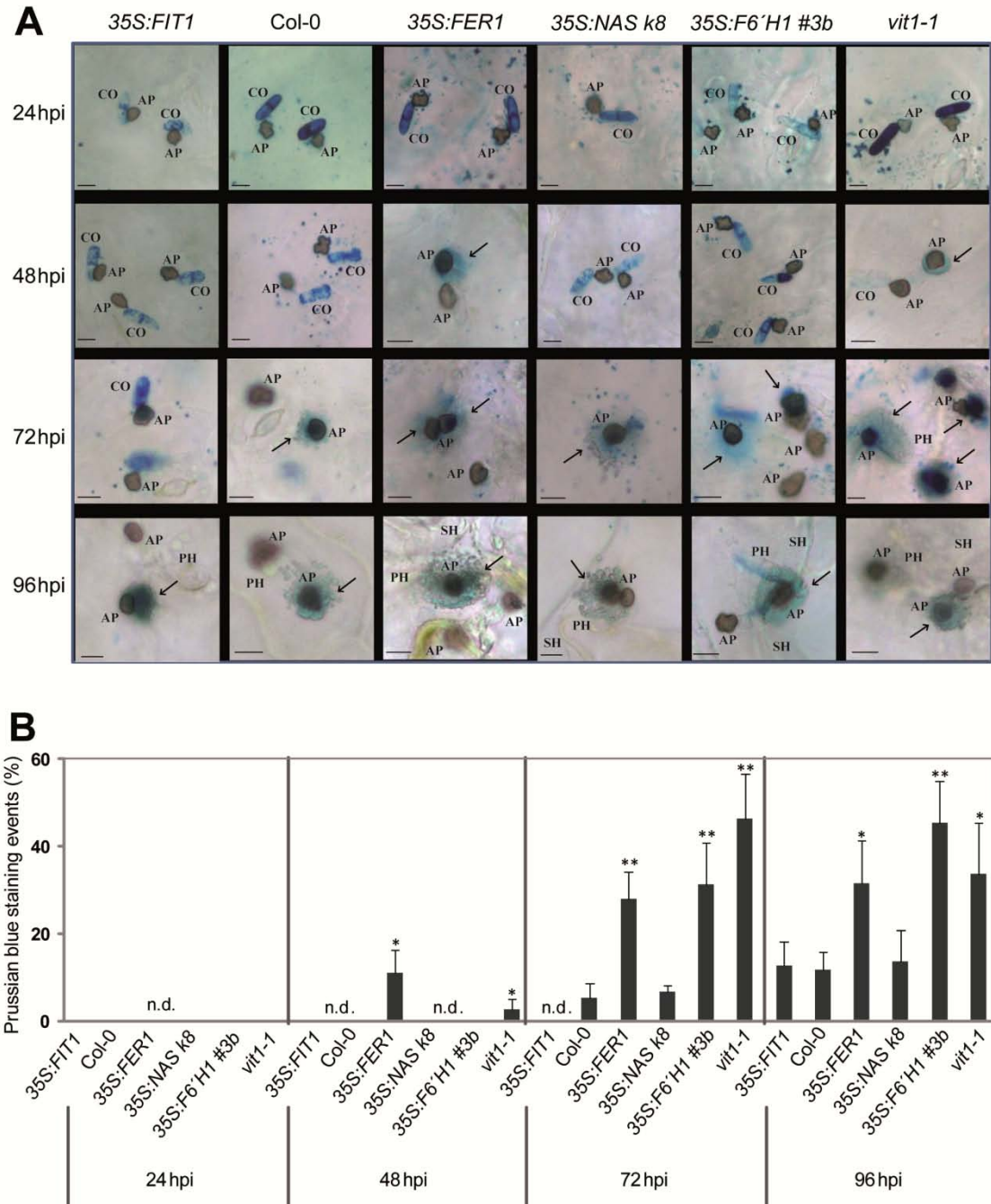


**Fig. 27. Fe accumulation at infection sites of *Colletotrichum higginsianum* in different Arabidopsis lines.** (A) Microscopic images of Prussian blue-stained Arabidopsis leaves after *C. higginsianum* infection. Arrows indicate local Fe accumulation at infection sites. CO, conidia; AP, appressoria; PH, primary hyphae; SH, secondary hyphae. Bars = 10  $\mu$ m. (B) Quantitative analysis of Prussian blue staining events. The no. of Prussian blue-stained appressoria per 100 analyzed appressoria was counted from three biological replicates of each treatment; n.d.: not detected. Bars indicate means  $\pm$  SD, and significant differences at  $p < 0.05$  or  $0.01$  are indicated by \* or \*\*.

### **3.2.4.3 Influence of the expression of Fe homeostasis-related genes on H<sub>2</sub>O<sub>2</sub> production after infection with *C. higginsianum***

In parallel to the Prussian blue staining for Fe, DAB staining was performed with all selected Arabidopsis lines in a time course after *C. higginsianum* infection to assess the influence of the Fe homeostasis-related genes on H<sub>2</sub>O<sub>2</sub> production. Up to 48 hpi, no DAB-stained cells were detected in any of the Arabidopsis lines (Fig. 28A). Only at 72 hpi DAB staining appeared as brown-reddish coloured spots surrounding the appressoria, which increased in number with progressing infection. As shown by the quantitative assessment of DAB staining events, there was no significant difference between 35S:*FIT1* and Col-0 during the entire infection period. In contrast, the H<sub>2</sub>O<sub>2</sub> production levels of 35S:*FER1*, 35S:*F6'H1* #3b, 35S:*NAS k8* and *vit1-1* were significantly lower than Col-0 at 96 hpi (Fig. 28B). These results suggested that *FIT1* and *VIT1-1* positively modulate H<sub>2</sub>O<sub>2</sub> production, which contributes to defence response against *C. higginsianum*, whereas *FER1*, *NAS* and *F6'H1* in contrast negatively modulate H<sub>2</sub>O<sub>2</sub> production.

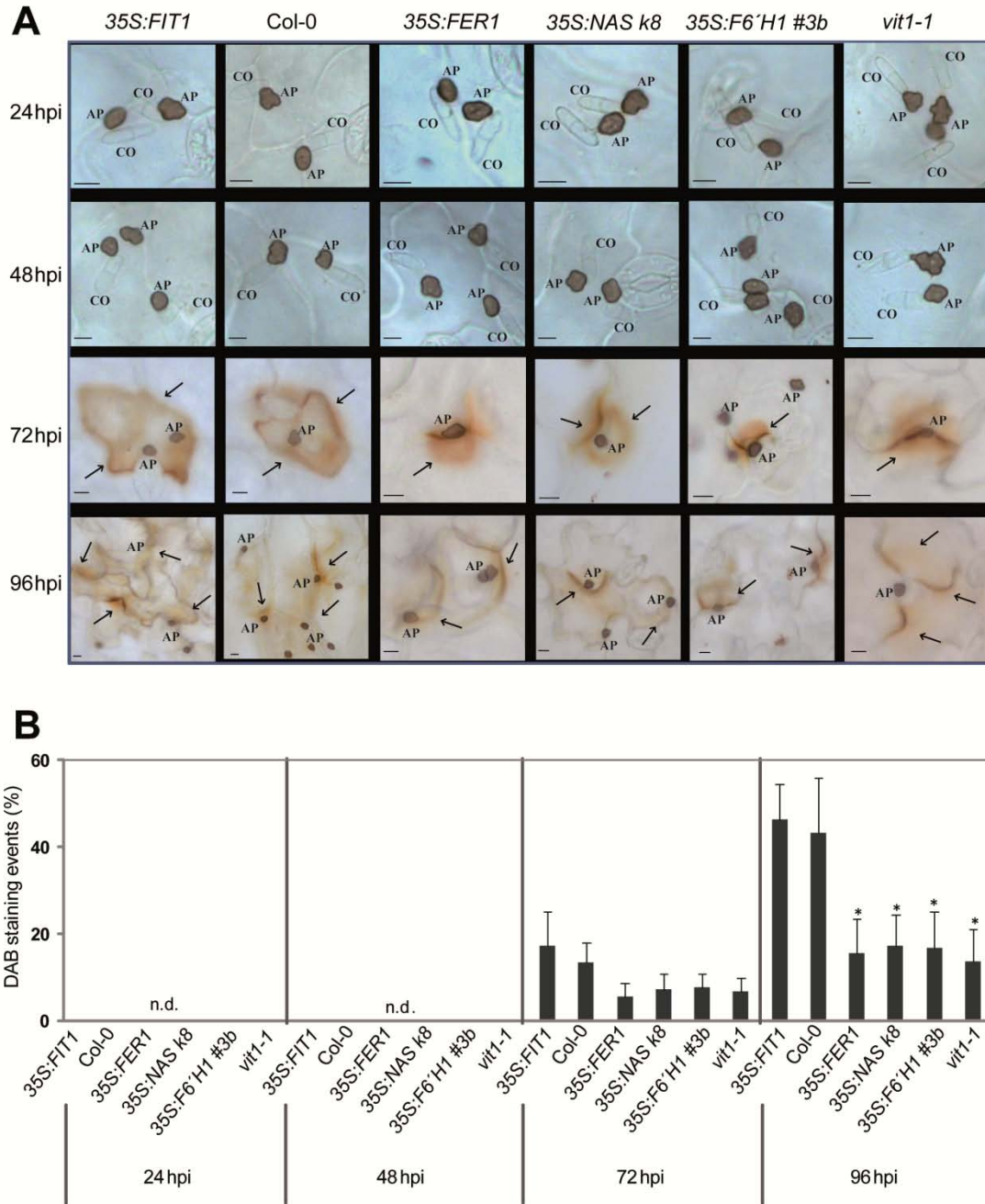


**Fig. 28. H<sub>2</sub>O<sub>2</sub> production at infection sites of *Colletotrichum higginsianum* in different *Arabidopsis* lines.** (A) Microscopy analysis of 3,3'-diaminobenzidine (DAB)-stained *Arabidopsis* leaves after *C. higginsianum* infection. Arrows indicate local H<sub>2</sub>O<sub>2</sub> production at infection sites. CO, conidia; AP, appressoria. Bars = 10  $\mu$ m. (B) Quantitative analysis of DAB staining events. The no. of DAB staining events per 100 analyzed appressoria was counted from three biological replicates of each treatment. Bars indicate means  $\pm$  SD, and significant differences at  $p < 0.05$  are indicated by \*, n.d.: not detected.

## 4 Discussion

Among all plant nutrients, in particular Fe plays a key role in plant-pathogen interactions, as it is required for defense responses protecting plant hosts from bacterial or fungal infections. As the plant tissue provides the only Fe source for leaf pathogens, plants have developed Fe-withholding strategies to exert control over the development and proliferation of attacking pathogens. While there is mounting evidence for Fe-withholding strategies to improve pathogen resistance (Deak et al., 1999; Dellagi et al., 2005), there are contrasting reports on the role of the Fe nutritional status of the host on disease resistance (Graham, 1983; Guerra and Anderson, 1985; Macur et al., 1991). A direct involvement of Fe in the defense response has been reported in *Arabidopsis* (Segond et al., 2009; Chen et al., 2014) and wheat (Liu et al., 2007) by a cellular relocalization of Fe to infection sites which coincided with local ROS production. However, the mechanisms how plants alter their Fe homeostasis and reprogramming their internal Fe trafficking to counteract plant pathogens are still completely unknown. Investigating the role of the plant Fe nutritional status in the maize-*C. graminicola* and *Arabidopsis*-*C. higginsianum* pathosystems was a first approach to address this question and led in the present study to conclude that i) an adequate Fe nutritional status is required to delay and partially suppress the fungal infection process and the biotrophic growth phase of *C. graminicola*, ii) the recruitment of Fe to fungal infection sites coincides with an earlier onset of H<sub>2</sub>O<sub>2</sub> production. Moreover, employing *Arabidopsis* mutants with modified expression of Fe homeostasis-related genes further indicated that iii) individual physiological processes of Fe homeostasis can increase or decrease the plant susceptibility to the pathogen. In the following sections these aspects are elucidated in more detail.

## 4.1 An adequate Fe nutritional status suppresses infection and biotrophic growth of *Colletotrichum*

### 4.1.1 Fe-sufficient maize and Arabidopsis plants are more tolerant than Fe-deficient plants to the hemibiotrophic pathogen *Colletotrichum*

To characterize the overall influence of the plant Fe nutritional status on resistance against the hemibiotrophic pathogen *Colletotrichum*, disease markers were compared in maize plants supplied with a gradient of Fe concentrations reflecting the Fe nutritional status from Fe deficiency to slight Fe excess. Pathogen resistance followed Fe nutrition in an optimum response curve with adequately Fe-supplied plants being most resistant to *C. graminicola* while plants suffering from Fe deficiency or Fe excess showed higher disease scores (Fig. 7). The tendency of maize plants supplied with 250  $\mu\text{M}$  Fe to be more susceptible to *C. graminicola* fully agrees with a promotive function of surplus plant Fe for ROS production and fungal infection (Deak et al., 1999; Liu et al., 2007). In an alternative approach, Fe supply reduced the susceptibility of *ys1* maize mutant, defective in phytosiderophore uptake, to *C. graminicola* (Fig. 9) confirming the results that an adequate Fe nutritional status suppresses fungal infection. In the alternative Arabidopsis-*C. higginsianum* pathosystem, Fe-deficient Arabidopsis plants were also more susceptible than Fe-sufficient plants (Fig. 23), confirming that an adequate Fe nutritional status supports tolerance not only in strategy I but also in strategy II plants against *Colletotrichum*. At a first glance, an increasing susceptibility of Fe-deficient maize and Arabidopsis to *Colletotrichum* may also not be unexpected with regard to previous reports showing that bean or tomato plants grown under low Fe supplies were more susceptible to *Fusarium solani* or *Verticillium dahlia*, respectively (Guerra and Anderson, 1985; Macur et al., 1991). Along the same line, additional foliar application of Fe increased the resistance of apple and pear to *Sphaeropsis malorum* and of cabbage to *Olpidium brassicae* (Graham, 1983). However, these results are in contradiction to those reported by Kieu et al. (2012), who showed that Fe-deficient Arabidopsis plants exhibit increased tolerance to the bacterium *Dickeya dadantii* or to the necrotrophic fungus *Botrytis cinerea*. Such contradictory observations go beyond the general view that a well-balanced nutritional status best protects plants from diseases (Datnoff et al., 2007; Dordas 2008; Marschner, 2012; Gupta et al., 2013), but may

be indicative for a differential effect of an individual nutrient depending on the plant-pathosystem and the lifestyle of the pathogen. For instance, many studies have shown that phosphorous application can reduce powdery mildew in apple, pod and stem blight in soybean, yellow dwarf virus disease in barley, brown stripe disease in sugarcane and blast disease in rice (Huber and Graham, 1999; Kirkegaard et al., 1999; Reuveni et al., 1998; 2000), whereas in other studies application of phosphorous increased the severity of diseases caused by *Sclerotinia* in many garden plants, by *Bremia* in lettuce and by flag smut in wheat (Huber, 1980). With regard to the role of the plant nutritional status, the lifestyle of the pathogen plays an important role. When the disease was caused by biotrophic fungi, e.g. *Puccinia graminis* (Howard et al., 1994) or *Erysiphe graminis* (Bueschbell and Hoffmann, 1992), high nitrogen supply to winter wheat led to an enhanced severity of the infection. However, when the disease was caused by necrotrophic fungi, e.g. *Fusarium oxysporum* (Woltz and Engelhar, 1973), high nitrogen supply to chrysanthemum decreased the severity of the disease. The present observations lead to hypothesize that the tolerance of plants to biotrophy is enhanced under an adequate Fe nutritional status of the host plant, whereas the tolerance of plants to necrotrophy is enhanced by a low or deficient Fe nutritional status. However, this far-reaching hypothesis needs to be confirmed by more investigations in future.

#### **4.1.2 The Fe nutritional status does not affect the severity of *C. graminicola* infection in wounded leaves**

Comparing the infection process of *C. graminicola* in non-wounded versus wounded maize leaves provides the advantage that wounding allows the fungus skipping the biotrophic growth phase and directly entering the necrotrophic growth phase, which accelerates fungal growth and disease spreading (Horbach et al., 2009). In agreement with a previous study by Albarouki and Deising (2013), *C. graminicola* proliferated more rapidly on wounded leaves than on non-wounded leaves irrespective of the supplied Fe level, as indicated by larger lesion areas and higher fungal DNA mass (Fig. 7). This allowed hypothesizing that the Fe nutritional status hardly impacts on necrotrophic fungal growth, but rather on the biotrophic growth phase. However, wounding accelerated the growth of *C. higginsianum* only



on Fe-sufficient *Arabidopsis* leaves (Fig. 23), while necrotic lesion areas were similar in wounded and non-wounded leaves of Fe-deficient plants. By contrast, the fungal RNA mass was even significantly reduced after wounding (Fig. 23B, C). This was most likely the result of a shorter period for fungal proliferation before the plant tissue collapsed and supports the notion that a biotrophic growth phase allows the fungus to develop more vegetative and generative structures. This view supports the general concept that pathogen infection is facilitated by wounding as it provides immediate access to nutrients, allowing the pathogen to rapidly colonize a small area of the host tissue. However, Chassot et al. (2008) reported that wounding can transiently increase the resistance of *Arabidopsis* against *Botrytis* infection, probably due to the fact that physical injury can counter-actively induce plant defense responses, including the induction of defense-related genes (Reymond et al., 2000) and the accumulation of anti-microbial proteins such as proteinase inhibitors or chitinase (Ryan, 1990; Chang et al., 1995).

To verify the above conclusion that the Fe nutritional status hardly impacts on the growth of necrotrophic fungi, but rather on the biotrophic growth phase of hemibiotrophic fungi, a comparative microscopic analysis of infection structures of *Colletotrichum* was conducted in non-wounded leaves of Fe-sufficient or -deficient maize and *Arabidopsis* plants. On Fe-sufficient leaves, significantly lower rates of germination and appressorial formation and of primary hyphae formation apparently delayed the switch from biotrophic to necrotrophic growth of *Colletotrichum* (Figs. 11, 24). Considering the higher rate of secondary hyphae formation on Fe-deficient leaves as a consequence of the accelerated biotrophic development at earlier stages (Figs. 11B, 24B) allowed concluding that in non-wounded leaves Fe plays a protective role against fungal infection and biotrophic growth, but does not impact the necrotrophic growth phase of the fungus. Such a conclusion gains in importance with respect to the recent finding that *C. graminicola* mainly relies on reduction-based Fe acquisition during infection and biotrophic but not during necrotrophic growth (Albarouki and Deising, 2013). This coincidence suggests that the Fe nutritional status of the plant is a determinant for pathogenesis when the fungus acquires Fe(III) by reduction, while it loses impact whenever the fungus employs siderophores for Fe acquisition.

#### **4.1.3 The benefit of an adequate Fe nutritional status in maize leaves is independent on the Fe acquisition pathways of *C. graminicola***

With regard to the outstanding importance of Fe acquisition strategies for the pathogenesis of fungal pathogens (Eichhorn et al., 2006; Greenshields et al., 2007a; Haas et al., 2008; Albarouki and Deising, 2013), *C. graminicola* mutants, which are defective either in reduction-based (i.e.  $\Delta fet3-1$  and  $\Delta fet3-1/2$ ) or siderophore-based (i.e.  $\Delta nps6$  and  $\Delta sid1$ ) Fe acquisition, were employed in an alternative approach to examine the importance of the Fe nutritional status of maize leaves on their susceptibility to *C. graminicola*. Irrespective of leaf wounding all fungal mutants showed lower virulence than the wild type. In particular the double mutant  $\Delta fet3-1/2$  showed a severe loss of virulence (Fig. 17) supporting that the reduction-based Fe acquisition strategy is indispensable for fungal development and full virulence (Albarouki and Deising, 2013). While the leaf Fe nutritional status remained without influence on fungal infection on wounded leaves, Fe deficiency in non-wounded leaves promoted fungal growth and development (Fig. 17). A parallel microscopic analysis revealed that an adequate Fe nutritional status suppressed fungal infection structures already during biotrophic growth (Fig. 18). Thus, maize leaves profited from an adequate Fe nutritional status independently of the fungal Fe acquisition mechanism, indicating that Fe plays a more fundamental protective role in the defense response to *Colletotrichum*.

#### **4.1.4 The impact of Fe deficiency on the ultrastructure of maize leaves**

The importance of nutrients is usually explained in terms of the biochemical functions of these elements in plant metabolism. However, the level of nutrient supply can affect the physiology and especially the structural integrity of cell walls and membranes (Dordas, 2008). Several studies have reported that in particular Fe deficiency can cause not only physiological but also morphological changes in plant cells (Briat, 2007; Eichert et al., 2010; Rellan-Alvarez et al., 2011). For instance, Fe deficiency can lead to a 90% reduction of suberin biosynthesis in bean roots (Sijmons et al., 1985). Suberin is a waxy polymer, consisting of polyaromatic and polyaliphatic chains, which are embedded in the cell walls

(Bernards, 2002). Another study by Fernandez et al. (2008) found that Fe deficiency reduced the amount of soluble cuticular lipids and the weight of the abaxial cuticle in field-grown peach and pear leaves, respectively.

Plant cell walls covered with intact cuticles not only support the mechanical structure to the plant body but also act as first physical barriers against pathogens (Underwood, 2012; Serrano et al., 2014). The impairment of the structure or chemical composition of cell walls usually causes increased susceptibility of plants to pests and pathogens. Maize inbred lines containing lower total contents of cell wall material in the pith, particularly of glucose, xylose and lignin, were more susceptible to corn borers suggesting that cell wall thickness is an important barrier that pathogens must overcome in order to gain access to cytoplasmic nutrients (Barros-Rios et al., 2011). The analysis of mutants has revealed correlations between altered cell wall compositions and an altered susceptibility to pathogens. The Arabidopsis powdery mildew-resistant mutants *pmr5* and *pmr6* display a similar increase in pectin content and decrease in pectin methyl esterification or O-acetylation (Vogel et al., 2002, 2004). With regard to these observations, it is assumed that Fe deficiency-induced morphological changes in leaf structure might subsequently influence the plant susceptibility to pathogen infections. As shown in the previous experiment there was a delay in germination and formation of *Colletotrichum* appressoria when conidia were placed on Fe-sufficient maize (Fig. 11) or Arabidopsis (Fig. 24) leaves. This delay may have been caused by differences in the structure or/and chemical composition of cell walls in Fe-sufficient and Fe-deficient leaves. This assumption prompted to compare the ultrastructure of leaves in dependence of Fe supply. The cell wall and the cuticle of maize epidermis cells were significantly weaker under Fe deficiency as they appeared much thinner than those of Fe-sufficient leaves (Fig. 21C, D). Fe-deficient maize leaves displayed also a thinner layer of epicuticular waxes on the adaxial surface than Fe-sufficient leaves (Fig. 21A, B), suggesting a difference in the amount and/or composition of epicuticular waxes in these leaves. These differences may determine germination rates of *C. graminicola* conidia and finally the susceptibility of the maize leaf tissue to this fungus. Thus, it would be of interest in future to compare the chemical composition of epicuticular waxes in Fe-sufficient and Fe-deficient maize leaves.

However, the cell wall functions not just as a passive barrier limiting the access of pathogens, it is also actively remodeled and reinforced in response to pathogen attacks, referred to as cell wall appositions (CWAs) or papillae, specifically at infection sites of potentially pathogenic microbes (Schulze-Lefert, 2004; Luna et al., 2011; Underwood, 2012). Rapid deposition of papillae is generally correlated with resistance to fungal pathogens that attempt to penetrate plant cell walls for the establishment of feeding structures. To date, there is no study reporting how the Fe nutritional status in plants influences papillae formation under pathogen attack, which therefore might also be of interest to be investigated in future.

## **4.2 A protective role of Fe against fungal infection by H<sub>2</sub>O<sub>2</sub> production**

### **4.2.1 Fe accumulates at infection sites in maize or Arabidopsis leaves infected by *Colletotrichum***

In plant and animal defense responses Fe has been reported to mediate ROS production at the site of infection indicating a protective role of Fe against pathogens (Collins et al., 2002; Liu et al., 2007; Nairz et al., 2010). Infection of wheat leaves by the biotrophic fungus *Blumeria graminis* f. sp. *tritici* (*Bgt*) triggered the recruitment of Fe to the infection sites which coincided with the local production of ROS (Liu et al., 2007). Interestingly, the authors also found a similar Fe accumulation at infected sites by *Bgt* in other strategy II plants like barley, maize, millet, oat and sorghum, but not in the strategy I plant Arabidopsis (Greenshields et al., 2007) suggesting that such a kind of Fe recruitment for defense responses may only exist in strategy II, but not in strategy I plants. In the present study, Fe recruitment to the infection sites was visualized by Prussian blue staining and not only observed in *C. graminicola*-infected maize leaves (Fig. 12A), but also in Arabidopsis leaves infected by *C. higginsanum* (Fig. 27A). This Fe accumulation at the infection site is reported for the first time here in a strategy I plant, indicating that such kind of Fe recruitment may represent a more general feature of plants attacked by pathogens. Interestingly, Fe accumulation in *C. graminicola*-infected maize leaves was however only occurred in the biotrophic

phase up to 48 hpi, but not in the necrotrophic growth phase (Fig. 12A). This observation together with the other investigations with biotrophic fungi (Greenshields et al., 2007; Liu et al., 2007) tempt to hypothesize that such kind of defense response in form of Fe recruitment to the infection sites probably depends on the lifestyle of the pathogen, i.e. being restricted to biotrophy but not to necrotrophy. Therefore, it would be interesting in future to test this hypothesis with plants infected by necrotrophic fungi.

The increased Fe accumulation at infection sites in wheat epidermis cells 24 hpi after *Bgt* infection led to the assumption that this pathogen triggers Fe relocation at the tissue level from the mesophyll towards the epidermis (Liu et al., 2007). However, the authors did not find a decrease of Fe in mesophyll cells. In their working model, they suggested that Fe recruitment to infection sites depended on Fe retranslocation only at the cellular level, which lead to Fe depletion and subsequently to Fe deficiency in the cytosol. Along the same lines, the upregulation of vacuolar Fe export by NRAMP3 in *Arabidopsis* infected with *Erwinia chrysanthemi* suggested that a pathogen invasion triggers Fe depletion in the cytosol and induces the mobilization of vacuolar Fe stores by NRAMP3 (Segond et al., 2009). In the present study, different Fe fractions were analyzed in Fe-sufficient and Fe-deficient maize leaves during *C. graminicola* infection. In fact, Fe concentrations particularly in Fe-sufficient and *Colletotrichum*-infected leaves increased at later stages of the infection process. This was also reflected in a larger pool of water-soluble Fe in infected than in control leaves. However, no significant changes were found in any of the Fe fractions between infected and non-infected leaves at early biotrophic growth, i.e. when Fe was recruited to the infection sites (Fig. 13,). This suggested that there was no conversion from water-insoluble to water-soluble Fe and all Fe recruited to the infection sites originally came from the water-soluble fraction. Together, these data lead to the assumption that the Fe recruitment caused an Fe relocation towards infection sites most likely only in epidermal cells, where it subsequently mediates a ROS burst at the infection sites. Interestingly, the Fe-deficiency marker genes *IRT1* and *FRO2* were induced in roots of *Erwinia chrysanthemi*-infected *Arabidopsis* plants, suggesting the existence of a shoot-to-root Fe-deficiency signaling pathway activated by pathogen infection in the leaves (Segond et al., 2009). However, the mechanisms

how Fe is transported from the cytosol to the infection sites at the cellular level, and how the whole-plant signaling pathway is constituted still remains unknown and requires further investigations in future.

#### **4.2.2 The relation between Fe recruitment and H<sub>2</sub>O<sub>2</sub> production at pathogen infection sites**

In *C. graminicola*-infected maize leaves, the Fe relocation to the infection sites set in later under Fe deficiency, i.e. at 36 hpi (Fig. 12), when secondary hyphae had been formed and necrotrophic growth had begun (Fig. 11). This observation prompted to investigate ROS production as an early component of the basal plant defense response against pathogens (Jones and Dangl, 2006; He et al., 2007). DAB staining revealed an earlier and stronger local H<sub>2</sub>O<sub>2</sub> production in Fe-sufficient maize leaves at 24 hpi, i.e. during the biotrophic growth phase (Fig. 14). At the same time, H<sub>2</sub>O<sub>2</sub> production in Fe-deficient leaves was still negligible, although the formation of fungal infection structures was already more progressed (Fig. 11B). The situation turned into the opposite 48 and 72 hpi, when DAB staining indicated ROS production throughout the whole Fe-deficient leaf tissue (Fig. 14A), which was most likely a consequence of vigorous necrotrophic growth of *C. graminicola*. There was a strong temporal and spatial coincidence between DAB staining and Prussian blue staining until the fungus switched to necrotrophic growth 36 hpi (Figs. 12, 14), indicating that free Fe was involved in local H<sub>2</sub>O<sub>2</sub> production at the infection sites (Liu et al., 2007). Likewise, a highly similar coincidence in local Fe accumulation and H<sub>2</sub>O<sub>2</sub> production was found in a parallel approach when examining *C. graminicola* mutants defective in Fe acquisition and infectious to maize leaves to different degrees. Those mutants which were most compromised in the formation of infection structures (Fig. 18) showed delayed Fe and DAB staining during the biotrophic growth phase (Figs. 19, 20). Thus, these observations lead to conclude that in Fe-deficient leaves the delayed and less intense recruitment of Fe to the infection sites at early fungal growth stages was a major cause for a weaker oxidative burst, and hence, allowed more rapid fungal development and progression to the necrotrophic lifestyle. This scenario provides an explanation for the beneficial role of an adequate Fe nutritional status in

resistance to *C. graminicola*. Recently, it has been proposed that the switch from biotrophic to necrotrophic growth of *C. graminicola* represents an escape strategy of the fungus to avoid exposure to ROS-containing vesicles produced by plant cells and delivered to the infection sites (Vargas et al., 2012). In present study with maize, such vesicles were not observed so far. However, it may be of interest in future to investigate whether Fe deficiency promotes the formation of ROS-containing vesicles.

#### **4.3 Fe homeostasis-related genes influence the susceptibility of maize and Arabidopsis to *Colletotrichum***

Plant pathogens invade hosts to explore nutrients that sustain their growth and proliferation. During the invasion, pathogens secrete a range of molecules (toxins, enzymes, effectors) into extracellular and intracellular compartments in order to induce cellular disintegration, to suppress host immunity or to manipulate host cells such that nutrients are delivered to the pathogen (Faulkner and Robatzek, 2012). Such manipulation is usually coupled with a reprogramming of the expression of nutrient-related genes in host cells and allows the pathogen to modify nutrient homeostasis and metabolism in the host. For example, *Botrytis cinerea* infection can enhance the expression of several genes involved in nutrient recycling, proteolysis and sugar, amino acid, or nutrient uptake in Arabidopsis (AbuQamar et al., 2006). Several fungal and bacterial pathogens induce the expression of Arabidopsis *SWEET* genes encoding plant sugar exporters, indicating that the SWEETs are probably targeted by pathogens for an efficient assimilate transfer from the host to the pathogen (Chen et al., 2010). As an indispensable element for growth and proliferation, pathogens have to acquire Fe from the plant tissue. However, the bioavailability of Fe is very low in the plant tissue. Thus, pathogens have developed two high-affinity Fe acquisition systems based either on Fe(III) reduction or Fe(III) chelation by siderophores. Both reduction-based and siderophore-based Fe acquisition strategies (Eichhorn et al., 2006; Albarouki and Deising, 2013) have been proven capable of modulating the oxidative stress response and the Fe homeostasis of the plant (Mei et al., 1993; Dellagi et al., 2005; Greenshields et al., 2007; Haas et al., 2008; Calla et al., 2013;

Albarouki et al., 2014). On the other hand, to resist to pathogen attacks, plants have evolved besides their pre-formed mechanical defense structures (cell walls, epidermal cuticles and bark) and basal defense responses (CWAs, ROS production and pathogen-related (PR) gene expression), also defense responses related to the reprogramming of their nutrient homeostasis in a way to either reduce the availability of nutrients to the pathogen or to directly employ nutrients for the restriction of pathogen growth (Datnoff et al., 2007; Fagard et al., 2014).

In planta, a balanced Fe homeostasis requires a tight coordination of many genes involved in Fe uptake, storage and intracellular allocation. Any changes in the expression of Fe homeostasis-related genes may therefore cause an imbalance in Fe allocation or in cytosolic Fe pools and thereby influence the susceptibility to pathogens. In order to systematically examine the influence of Fe homeostasis-related genes on the plant susceptibility to *Colletotrichum*, studies either using transgenic Arabidopsis lines with modulated expression of Fe homeostasis-related genes or transcripts analyses in maize were conducted. Compared to Arabidopsis wild-type plants, some mutants had a modulated expression of genes involved in Fe acquisition (*35S:FIT1* and *35S:F6'H1 #3b*), in Fe storage (*35S:FER1* and *vit1-1*), or in internal Fe allocation (*35S:NAS k8*) and showed significant alterations in their susceptibility to *C. higginsianum* (Figs. 25, 26), suggesting that individual physiological processes of Fe homeostasis can influence the plant susceptibility to pathogens. As discussed before, Fe bioavailability is a very important factor that determines the susceptibility of hosts to certain pathogens. The lower susceptibility of Fe-sufficient maize (Fig. 7) and Arabidopsis (Fig. 23) plants to *Colletotrichum* infection suggested that a higher Fe bioavailability in the plant cell is correlated to a higher production of H<sub>2</sub>O<sub>2</sub> (Fig. 14) and finally to a higher tolerance to *Colletotrichum*. This assumption may imply that changes in the expression of certain Fe homeostasis-related genes can increase of Fe bioavailability within plant cells and may thereby contribute to a higher tolerance to pathogen infection. This assumption is also supported by the studies from Liu et al. (2007) and Segond et al. (2009) which suggested that plants can redistribute Fe to the apoplast during pathogen attack, where an oxidative burst takes place. However, Fe relocation to the apoplast causes Fe deficiency in the cytosol of infected cells which provokes a reprogramming of Fe homeostasis involving Fe storage, internal



Fe allocation and Fe uptake. In line with this view, DAB staining indicated higher H<sub>2</sub>O<sub>2</sub> accumulation in the more resistant line *35S:FIT1* and lower H<sub>2</sub>O<sub>2</sub> levels in the more susceptible lines *35S:FER1*, *35S:NAS k8*, *35S:F6'H1 #3b* and *vit1-1* during *C. higginsianum* infection (Fig. 28). Unexpectedly, the H<sub>2</sub>O<sub>2</sub> production in those mutants did not coincide with Fe accumulation levels as indicated by Prussian blue staining during fungal infection (Fig. 27). The biological cause for this lacking coincidence between localized Fe and H<sub>2</sub>O<sub>2</sub> accumulation at the infection sites across different Arabidopsis mutant and transgenic lines requires further investigation. In contrast, in maize plants H<sub>2</sub>O<sub>2</sub> production coincided with a higher Fe accumulation at infection sites and with a higher tolerance to *C. graminicola* (Figs. 12, 14). However, no consistent response to *C. graminicola* infection was found in the transcriptional regulation of genes involved in Fe homeostasis in maize (Fig. 15).

Due to its high Fe-storage capacity (up to 4000 ions), ferritin plays an important role in Fe storage and in buffering of Fe homeostasis in plants as well as in animals. The upregulation of *FER* expression during infection mediated by the bacterial or fungal siderophores suggested that plant ferritin functions as a good competitor for Fe to siderophores and is able to reduce the Fe availability to the pathogen (Dellagi et al., 2005; Segond et al., 2009; Djennane et al., 2011; Kieu et al., 2012). Many studies have shown that over-expression of ferritin (Deak et al., 1999) or mammalian lactoferrin (Zhang et al., 1998; Malnoy et al., 2003) in different plant species confers resistance to viral, bacterial or necrotrophic fungal pathogens. On the other hand, ferritin is also known to accumulate in response to Fe overload (Gaymard et al., 1996) or to an excess of ROS (Petit et al., 2001; Murgia et al., 2002). The over-expression of ferritin may thus counteract ROS production and cause plant cells to become more susceptible to pathogen infection. As shown in the present study, Arabidopsis plants over-expressing *FER1* exhibited a low level of H<sub>2</sub>O<sub>2</sub> production during *C. higginsianum* infection (Fig. 28) and were thus more susceptible to this fungus (Figs. 25, 26), although a high level of Fe accumulated at the infection sites (Fig. 27). This suggested that Fe accumulating at the infection sites might have been captured by ferritin and therefore was inactive in ROS formation via the Fenton reaction. Interestingly, no upregulation of *FER* genes in maize (Fig. 16) or wheat (Liu et al., 2007) was found

during infection with the hemibiotrophic fungus *C. graminicola* or the biotrophic fungus *Bgt*, respectively (Fig. 16), suggesting that ferritin might only be induced in response to infection by necrotrophic pathogens.

Another gene involved in intracellular Fe storage in plants is the vacuolar iron transporter 1 (*VIT1*), which functions as an Fe importer into vacuoles (Kim et al., 2006). One may assume that defective expression of *VIT1* might cause an increase of Fe in cytosol. However, no differences in the Fe content of shoots were determined between *vit1-1* and wild-type *Arabidopsis* plants (Kim et al., 2006). Interestingly, the *vit1-1* mutant was more susceptible to the hemibiotrophic fungus *C. higginsianum* (Figs. 25, 26) suggesting a role of vacuolar Fe in plant-pathogen interactions. At the same line, the *Arabidopsis* mutant *nramp3*, which is defective in vacuolar Fe export, showed an increased susceptibility to *Erwinia chrysanthemi* infection, and the over expression of this gene inversely decreased the susceptibility to this bacteria (Segond et al., 2009). Again, this differential role of Fe in pathogen susceptibility may be due to the lifestyle of the pathogen.

The ligand nicotianamine (NA) is able to bind both Fe<sup>(II)</sup> and Fe<sup>(III)</sup>. It functions in intracellular and long-distance Fe trafficking (Briat et al., 2007) and in protecting plants from oxidative damage (von Wirén et al., 1999). Over-expression of nicotianamine synthase (NAS) in *Arabidopsis* conferred a higher accumulation of NA and decreased the water-soluble Fe fraction in shoots (Cassin et al., 2009). This suggested that the higher susceptibility of *Arabidopsis* plants over-expressing *NAS* may have caused a higher NA accumulation which induced a lower Fe availability than in wild-type plants (Figs. 25, 26). This assumption is supported by the study that wheat *TmNAS1* was downregulated 24 hours after *Bgt* infection (Liu et al., 2007). The present study is the first to show that NA is involved in plant-pathogen interactions. However, the mechanism how NA accumulation in plant influences the susceptibility to pathogens is still unknown and needs more investigation. Interestingly, the *Arabidopsis ys13* mutant, defective in a putative metal-NA transporter involved in Fe, Zn, and Cu translocation, exhibited a higher susceptibility to *Pseudomonas syringe*, supporting a biological function of this metal transporter in plant pathogen defense responses (Chen et al., 2014).

In conclusion, the present work may be of agronomic significance as it improves the understanding of the role of Fe nutritional status in plant-pathogen interactions. This knowledge could eventually contribute to an improved management of Fe nutrition in agricultural plant production to better control plant diseases. A deeper analysis of the cause for improved *Colletotrichum* resistance by over-expression of *FIT* might ultimately be even of interest for the breeding of lines with enhanced resistance to hemibiotrophic fungal pathogens.

## 5 Summary

The plant nutritional status is known to have a strong impact on a plant's resistance against pathogens. In particular Fe appears as a determinant of plant resistance as both, the pathogen and the host compete for Fe during plant-pathogen interactions. However, there have been contradictory reports on whether a Fe-sufficient or Fe-deficient nutritional status of the plant is more beneficial for plant resistance. To address this question, the present study investigated the role of Fe in the defense response of plants against fungal pathogens in the maize-*Colletotrichum graminicola* and Arabidopsis-*Colletotrichum higginsianum* pathosystems.

First, maize and Arabidopsis plants with different Fe nutritional status were assessed for the susceptibility to *Colletotrichum*. Fe-sufficient maize and Arabidopsis plants were more tolerant to *Colletotrichum* infection than Fe-deficient plants, indicating that Fe plays a positive role in the plant defense against these pathogens. Microscopic studies showed that the development of *Colletotrichum* on Fe-sufficient maize and Arabidopsis leaves was slower than on Fe-deficient leaves from the beginning of fungal spore germination and appressorium formation, which determined in the end the differences in the susceptibility between plants. One Fe-dependent component contributing to enhanced resistance may lie in the leaf surface ultrastructure. Using scanning electron microscopy and transmission electron microscopy revealed that Fe-deficient leaves appeared to have less cuticle wax on their surface than Fe-sufficient leaves, and that Fe-deficient leaves had significantly thinner cell walls and cuticle layers compared to Fe-sufficient leaves.

Iron recruitment to the infection site coincides with the local production of H<sub>2</sub>O<sub>2</sub> and is one of the plant defense responses against pathogens. Therefore, Prussian blue and DAB staining procedures were used to visualize the Fe recruitment and H<sub>2</sub>O<sub>2</sub> production on both Fe-sufficient and -deficient maize leaves infected by *C. graminicola* WT and mutant strains defective in Fe acquisition pathways. There was a strong temporal and spatial coincidence between DAB staining and Prussian blue staining until the fungus switched from biotrophic to necrotrophic growth. Likewise, a highly similar coincidence in local Fe accumulation and H<sub>2</sub>O<sub>2</sub> production was found when examining *C. graminicola* mutants. Those mutants

which were most compromised in the formation of infection structures showed delayed Fe and DAB staining during the biotrophic growth phase. It was therefore concluded that in Fe-deficient leaves the delayed and less intense recruitment of Fe to the infection sites at early fungal growth stages was a major cause for a weaker oxidative burst, and hence, allowed more rapid fungal development and progression to the necrotrophic growth phase. This scenario provides an explanation for the beneficial role of an adequate Fe nutritional status in resistance to *Colletotrichum graminicola*.

In order to systematically examine the influence of Fe homeostasis-related genes on the susceptibility of Arabidopsis plants to *Colletotrichum higginsianum*, studies using transgenic Arabidopsis lines with modulated expression of Fe homeostasis-related genes were conducted. While only one line over-expressing the transcription factor *FIT* showed an enhanced resistance, other Arabidopsis lines or mutants involved either in Fe acquisition, storage or internal allocation showed a significantly higher susceptibility to *Colletotrichum higginsianum*. Moreover, here plant resistance again coincided with an earlier and higher accumulation of H<sub>2</sub>O<sub>2</sub> but not with an earlier recruitment of Fe to the infection sites. These studies reveal a strong involvement of the Fe nutritional status in lifestyle changes of hemibiotrophic fungi and of Fe homeostasis-related genes in plant resistance mechanisms against fungal pathogens.

## 6 References

- AbuQamar S, Chen X, Dhawan R, Bluhm B, Salmeron J, Lam S, Dietrich RA, Mengiste T** (2006) Expression profiling and mutant analysis reveals complex regulatory networks involved in Arabidopsis response to *Botrytis* infection. *Plant Journal* **48**: 28-44
- Albarouki E, Deising HB** (2013) Infection structure-specific reductive iron assimilation is required for cell wall integrity and full virulence of the maize pathogen *Colletotrichum graminicola*. *Mol Plant Microbe Interact* **26**: 695-708
- Albarouki E, Schaffner L, Ye F, von Wirén N, Haas H, Deising HB** (2014) Biotrophy-specific downregulation of siderophore biosynthesis in *Colletotrichum graminicola* is required for modulation of immune responses of maize. *Molecular Microbiology* **92**: 338-355
- Anderson DW, Nicholson RL** (1996) Characterization of a laccase in the conidial mucilage of *Colletotrichum graminicola*. *Mycologia* **88**: 996-1002
- Apel K, Hirt H** (2004) Reactive oxygen species: metabolism, oxidative stress, and signal transduction. *Annual Review of Plant Biology* **55**: 373-399
- Apostol I, Heinsteins PF, Low PS** (1989) Rapid stimulation of an oxidative burst during elicitation of cultured plant cells : role in defense and signal transduction. *Plant Physiology* **90**: 109-116
- Arosio P, Levi S** (2002) Ferritin, iron homeostasis, and oxidative damage. *Free Radic Biol Med* **33**: 457-463
- Askwith C, Eide D, Van Ho A, Bernard PS, Li L, Davis-Kaplan S, Sipe DM, Kaplan J** (1994) The *FET3* gene of *S. cerevisiae* encodes a multicopper oxidase required for ferrous iron uptake. *Cell* **76**: 403-410
- Barros-Rios J, Malvar RA, Jung HJG, Santiago R** (2011) Cell wall composition as a maize defense mechanism against corn borers. *Phytochemistry* **72**: 365-371
- Bashir K, Inoue H, Nagasaka S, Takahashi M, Nakanishi H, Mori S, Nishizawa NK** (2006) Cloning and characterization of deoxymugineic acid synthase genes from graminaceous plants. *Journal of Biological Chemistry* **281**: 32395-32402
- Bauer P, Ling HQ, Guerinot ML** (2007) FIT, the FER-LIKE IRON DEFICIENCY INDUCED TRANSCRIPTION FACTOR in Arabidopsis. *Plant Physiol Biochem* **45**: 260-261
- Bechinger C, Giebel KF, Schnell M, Leiderer P, Deising HB, Bastmeyer M** (1999) Optical measurements of invasive forces exerted by appressoria of a plant pathogenic fungus. *Science* **285**: 1896-1899
- Bergstrom GC, Nicholson RL** (1999) The biology of corn anthracnose - Knowledge to exploit for improved management. *Plant Disease* **83**: 596-608
- Bernards MA** (2002) Demystifying suberin. *Canadian Journal of Botany-Revue Canadienne De Botanique* **80**: 227-240
- Birker D, Heidrich K, Takahara H, Narusaka M, Deslandes L, Narusaka Y, Reymond M, Parker JE, O'Connell R** (2009) A locus conferring resistance to *Colletotrichum higginsianum* is shared by four geographically distinct Arabidopsis accessions. *Plant Journal* **60**: 602-613
- Boukhalfa H, Crumbliss AL** (2002) Chemical aspects of siderophore mediated iron transport. *Biometals* **15**: 325-339

- Briat J** (2002) Metal ion-activated oxidative stress and its control. In “Oxidative Stress in Plants” (D. Inze´ and M. Van Montagu, ed.) **Taylor & Francis, London, NewYork: 171-190**
- Briat JF, Curie C, Gaymard F** (2007) Iron utilization and metabolism in plants. *Current Opinion in Plant Biology* **10**: 276-282
- Briat JF, Ravet K, Arnaud N, Duc C, Boucherez J, Touraine B, Cellier F, Gaymard F** (2010) New insights into ferritin synthesis and function highlight a link between iron homeostasis and oxidative stress in plants. *Ann Bot* **105**: 811-822
- Brown JC, Chaney RL** (1971) Effect of iron on the transport of citrate into the xylem of soybeans and tomatoes. *Plant Physiology* **47**: 836-840
- Buschbell T, Hoffmann GM** (1992) The effects of different nitrogen regimes on the epidemiologic development of pathogens on winter-wheat and their control. *Zeitschrift Fuer Pflanzenkrankheiten Und Pflanzenschutz-Journal of Plant Diseases and Protection* **99**: 381-403
- Calla B, Blahut-Beatty L, Koziol L, Simmonds D, Clough SJ** (2013) Transcriptome analyses suggest a disturbance of iron homeostasis in soybean leaves during white mold disease establishment. *Molecular Plant Pathology*
- Cassin G, Mari S, Curie C, Briat JF, Czernic P** (2009) Increased sensitivity to iron deficiency in *Arabidopsis thaliana* overaccumulating nicotianamine. *J Exp Bot* **60**: 1249-1259
- Chang MM, Horovitz D, Culley D, Hadwiger LA** (1995) Molecular-cloning and characterization of a pea chitinase gene expressed in response to wounding, fungal infection and the elicitor chitosan. *Plant Molecular Biology* **28**: 105-111
- Chassot C, Buchala A, Schoonbeek HJ, Metraux JP, Lamotte O** (2008) Wounding of *Arabidopsis* leaves causes a powerful but transient protection against *Botrytis* infection. *Plant Journal* **55**: 555-567
- Chen CC, Chien WF, Lin NC, Yeh KC** (2014) Alternative functions of *Arabidopsis* YELLOW STRIPE-LIKE3: from metal translocation to pathogen defense. *Plos One* **9**: e98008
- Chen LQ, Hou BH, Lalonde S, Takanaga H, Hartung ML, Qu XQ, Guo WJ, Kim JG, Underwood W, Chaudhuri B, Chermak D, Antony G, White FF, Somerville SC, Mudgett MB, Frommer WB** (2010) Sugar transporters for intercellular exchange and nutrition of pathogens. *Nature* **468**: 527-532
- Colangelo EP, Guerinot ML** (2004) The essential basic helix-loop-helix protein FIT1 is required for the iron deficiency response. *Plant Cell* **16**: 3400-3412
- Colangelo EP, Guerinot ML** (2006) Put the metal to the petal: metal uptake and transport throughout plants. *Current Opinion in Plant Biology* **9**: 322-330
- Collins HL, Kaufmann SH, Schaible UE** (2002) Iron chelation via deferoxamine exacerbates experimental *salmonellosis* via inhibition of the nicotinamide adenine dinucleotide phosphate oxidase-dependent respiratory burst. *Journal of Immunology* **168**: 3458-3463
- Curie C, Panaviene Z, Loulergue C, Dellaporta SL, Briat JF, Walker EL** (2001) Maize yellow stripe1 encodes a membrane protein directly involved in Fe(III) uptake. *Nature* **409**: 346-349
- Cvitanich C, Przybylowicz WJ, Urbanski DF, Jurkiewicz AM, Mesjasz-Przybylowicz J, Blair MW, Astudillo C, Jensen EO, Stougaard J** (2010) Iron and ferritin accumulate in separate cellular locations in *Phaseolus* seeds. *Bmc Plant Biology* **10**: 26

- Datnoff LE, Elmer WH, Huber DM** (2007) Mineral nutrition and plant disease. APS Press, St. Paul, MN.
- Daudi A, Cheng Z, O'Brien JA, Mammarella N, Khan S, Ausubel FM, Bolwell GP** (2012) The apoplastic oxidative burst peroxidase in *Arabidopsis* is a major component of pattern-triggered immunity. *Plant Cell* **24**: 275-287
- Deak M, Horvath GV, Davletova S, Torok K, Sass L, Vass I, Barna B, Kiraly Z, Dudits D** (1999) Plants ectopically expressing the iron-binding protein, ferritin, are tolerant to oxidative damage and pathogens. *Nature Biotechnology* **17**: 192-196
- Dean R, JA VANK, Pretorius ZA, Hammond-Kosack KE, A DIP, Spanu PD, Rudd JJ, Dickman M, Kahmann R, Ellis J, Foster GD** (2012) The Top 10 fungal pathogens in molecular plant pathology. *Molecular Plant Pathology*
- Delhaize E** (1996) A metal-accumulator mutant of *Arabidopsis thaliana*. *Plant Physiology* **111**: 849-855
- Dellagi A, Rigault M, Segond D, Roux C, Kraepiel Y, Cellier F, Briat JF, Gaymard F, Expert D** (2005) Siderophore-mediated upregulation of *Arabidopsis* ferritin expression in response to *Erwinia chrysanthemi* infection. *Plant Journal* **43**: 262-272
- DiDonato RJ, Jr., Roberts LA, Sanderson T, Easley RB, Walker EL** (2004) *Arabidopsis* Yellow Stripe-Like2 (YSL2): a metal-regulated gene encoding a plasma membrane transporter of nicotianamine-metal complexes. *Plant Journal* **39**: 403-414
- Djennane S, Cesbron C, Sourice S, Cournol R, Dupuis F, Eychenne M, Loridon K, Chevreau E** (2011) Iron homeostasis and fire blight susceptibility in transgenic pear plants overexpressing a pea ferritin gene. *Plant Science* **180**: 694-701
- Dordas C** (2008) Role of nutrients in controlling plant diseases in sustainable agriculture. A review. *Agronomy for Sustainable Development* **28**: 33-46
- Duc C, Cellier F, Lobreaux S, Briat JF, Gaymard F** (2009) Regulation of iron homeostasis in *Arabidopsis thaliana* by the clock regulator time for coffee. *J Biol Chem* **284**: 36271-36281
- Duy D, Wanner G, Meda AR, von Wirén N, Soll J, Philippar K** (2007) PIC1, an ancient permease in *Arabidopsis* chloroplasts, mediates iron transport. *Plant Cell* **19**: 986-1006
- Eggert K, von Wiren N** (2013) Dynamics and partitioning of the ionome in seeds and germinating seedlings of winter oilseed rape. *Metallomics* **5**: 1316-1325
- Eichert T, Peguero-Pina JJ, Gil-Pelegrin E, Heredia A, Fernandez V** (2010) Effects of iron chlorosis and iron resupply on leaf xylem architecture, water relations, gas exchange and stomatal performance of field-grown peach (*Prunus persica*). *Physiol Plant* **138**: 48-59
- Eichhorn H, Lessing F, Winterberg B, Schirawski J, Kamper J, Muller P, Kahmann R** (2006) A ferroxidation/permeation iron uptake system is required for virulence in *Ustilago maydis*. *Plant Cell* **18**: 3332-3345
- Eide D** (1997) Molecular biology of iron and zinc uptake in eukaryotes. *Curr Opin Cell Biol* **9**: 573-577
- Eisendle M, Schrettl M, Kragl C, Muller D, Illmer P, Haas H** (2006) The intracellular siderophore ferricrocin is involved in iron storage, oxidative-stress resistance, germination, and sexual development in *Aspergillus nidulans*. *Eukaryotic Cell* **5**: 1596-1603



- Expert D** (1999) WITHHOLDING AND EXCHANGING IRON: interactions between *Erwinia spp.* and their plant hosts. *Annual Review of Phytopathology* **37**: 307-334
- Fagard M, Launay A, Clement G, Courtial J, Dellagi A, Farjad M, Krapp A, Soulie MC, Masclaux-Daubresse C** (2014) Nitrogen metabolism meets phytopathology. *J Exp Bot*
- Faulkner C, Robatzek S** (2012) Plants and pathogens: putting infection strategies and defence mechanisms on the map. *Current Opinion in Plant Biology*
- Fernandez V, Eichert T, Del Rio V, Lopez-Casado G, Heredia-Guerrero JA, Abadia A, Heredia A, Abadia J** (2008) Leaf structural changes associated with iron deficiency chlorosis in field-grown pear and peach: physiological implications. *Plant and Soil* **311**: 161-172
- Gaymard F, Boucherez J, Briat JF** (1996) Characterization of a ferritin mRNA from *Arabidopsis thaliana* accumulated in response to iron through an oxidative pathway independent of abscisic acid. *Biochemical Journal* **318**: 67-73
- Gechev TS, Van Breusegem F, Stone JM, Denev I, Laloi C** (2006) Reactive oxygen species as signals that modulate plant stress responses and programmed cell death. *Bioessays* **28**: 1091-1101
- Gendre D, Czernic P, Conejero G, Pianelli K, Briat JF, Lebrun M, Mari S** (2007) *TcYSL3*, a member of the YSL gene family from the hyper-accumulator *Thlaspi caerulescens*, encodes a nicotianamine-Ni/Fe transporter. *Plant Journal* **49**: 1-15
- Gernand D, Rutten T, Pickering R, Houben A** (2006) Elimination of chromosomes in *Hordeum vulgare* x *H. bulbosum* crosses at mitosis and interphase involves micronucleus formation and progressive heterochromatinization. *Cytogenet Genome Res* **114**: 169-174
- Graham DR** (1983) Effects of nutrients stress on susceptibility of plants to disease with particular reference to the trace elements. *Adv. Bot. Res.* **10**: 221-276
- Grant JJ, Loake GJ** (2000) Role of reactive oxygen intermediates and cognate redox signaling in disease resistance. *Plant Physiology* **124**: 21-29
- Greenshields DL, Liu G, Feng J, Selvaraj G, Wei Y** (2007) The siderophore biosynthetic gene *SID1*, but not the ferroxidase gene *FET3*, is required for full *Fusarium graminearum* virulence. *Molecular Plant Pathology* **8**: 411-421
- Greenshields DL, Liu G, Wei Y** (2007) Roles of iron in plant defence and fungal virulence. *Plant Signal Behav* **2**: 300-302
- Guerinot ML, Yi Y** (1994) Iron: nutritious, noxious, and not readily available. *Plant Physiology* **104**: 815-820
- Guerra D, Anderson AJ** (1985) The effect of iron and boron amendments on infection of bean by *Fusarium solani*. *Phytopathology* **75**: 989-991
- Gupta KJ, Brotman Y, Segu S, Zeier T, Zeier J, Persijn ST, Cristescu SM, Harren FJ, Bauwe H, Fernie AR, Kaiser WM, Mur LA** (2013) The form of nitrogen nutrition affects resistance against *Pseudomonas syringae* pv. *phaseolicola* in tobacco. *J Exp Bot* **64**: 553-568
- Haas H, Eisendle M, Turgeon BG** (2008) Siderophores in fungal physiology and virulence. *Annual Review of Phytopathology* **46**: 149-187
- He P, Shan L, Sheen J** (2007) Elicitation and suppression of microbe-associated molecular pattern-triggered immunity in plant-microbe interactions. *Cellular Microbiology* **9**: 1385-1396
- Hell R, Stephan UW** (2003) Iron uptake, trafficking and homeostasis in plants. *Planta* **216**: 541-551

- Hider RC** (1984) Siderophore mediated absorption of iron. *Structure and Bonding* **58**: 25-87
- Higuchi K, Suzuki K, Nakanishi H, Yamaguchi H, Nishizawa NK, Mori S** (1999) Cloning of nicotianamine synthase genes, novel genes involved in the biosynthesis of phytosiderophores. *Plant Physiology* **119**: 471-480
- Hintze KJ, Theil EC** (2006) Cellular regulation and molecular interactions of the ferritins. *Cellular and Molecular Life Sciences* **63**: 591-600
- Hof C, Eisfeld K, Antelo L, Foster AJ, Anke H** (2009) Siderophore synthesis in *Magnaporthe grisea* is essential for vegetative growth, conidiation and resistance to oxidative stress. *Fungal Genetics and Biology* **46**: 321-332
- Horbach R, Graf A, Weihmann F, Antelo L, Mathea S, Liermann JC, Opatz T, Thines E, Aguirre J, Deising HB** (2009) Sfp-type 4'-phosphopantetheinyl transferase is indispensable for fungal pathogenicity. *Plant Cell* **21**: 3379-3396
- Howard DD, Chambers AY, Logan J** (1994) Nitrogen and fungicide effects on yield components and disease severity in wheat. *Journal of Production Agriculture* **7**: 448-454
- Howlett BJ** (2006) Secondary metabolite toxins and nutrition of plant pathogenic fungi. *Current Opinion in Plant Biology* **9**: 371-375
- Huber DM** (1980) The role of mineral nutrition in defense. In *Plant Disease, An Advanced Treatise*, Academic Press, New York **5**: 381-406
- Huber DM, Graham RD** (1999) The role of nutrition in crop resistance and tolerance to disease. Food Product Press, New York: 205-226
- Huckelhoven R, Fodor J, Preis C, Kogel KH** (1999) Hypersensitive cell death and papilla formation in barley attacked by the powdery mildew fungus are associated with hydrogen peroxide but not with salicylic acid accumulation. *Plant Physiology* **119**: 1251-1260
- Inoue H, Kobayashi T, Nozoye T, Takahashi M, Kakei Y, Suzuki K, Nakazono M, Nakanishi H, Mori S, Nishizawa NK** (2009) Rice OsYSL15 is an iron-regulated iron(III)-deoxymugineic acid transporter expressed in the roots and is essential for iron uptake in early growth of the seedlings. *J Biol Chem* **284**: 3470-3479
- Ishimaru Y, Kakei Y, Shimo H, Bashir K, Sato Y, Uozumi N, Nakanishi H, Nishizawa NK** (2011) A rice phenolic efflux transporter is essential for solubilizing precipitated apoplasmic iron in the plant stele. *J Biol Chem* **286**: 24649-24655
- Jakoby M, Wang HY, Reidt W, Weisshaar B, Bauer P** (2004) FRU (BHLH029) is required for induction of iron mobilization genes in *Arabidopsis thaliana*. *Febs Letters* **577**: 528-534
- Jeong J, Cohu C, Kerkeb L, Pilon M, Connolly EL, Guerinot ML** (2008) Chloroplast Fe(III) chelate reductase activity is essential for seedling viability under iron limiting conditions. *Proc Natl Acad Sci U S A* **105**: 10619-10624
- Jeong J, Guerinot ML** (2009) Homing in on iron homeostasis in plants. *Trends in Plant Science* **14**: 280-285
- Jin CW, You GY, He YF, Tang CX, Wu P, Zheng SJ** (2007) Iron deficiency-induced secretion of phenolics facilitates the reutilization of root apoplasmic iron in red clover. *Plant Physiology* **144**: 278-285
- Jones JD, Dangl JL** (2006) The plant immune system. *Nature* **444**: 323-329

- Kawei S, Kamei S, Matsuda Y, Ando R, Kondo S, Ishizawa A, Alam S** (2001) Concentration of iron and phytosiderophores in xylem sap of iron-deficient barley plants. *Soil Science and Plant Nutrition* **47**: 265-272
- Kieu NP, Aznar A, Segond D, Rigault M, Simond-Cote E, Kunz C, Soulie MC, Expert D, Dellagi A** (2012) Iron deficiency affects plant defence responses and confers resistance to *Dickeya dadantii* and *Botrytis cinerea*. *Molecular Plant Pathology* **13**: 816-827
- Kim SA, Guerinot ML** (2007) Mining iron: Iron uptake and transport in plants. *Febs Letters* **581**: 2273-2280
- Kim SA, Punshon T, Lanzirotti A, Li L, Alonso JM, Ecker JR, Kaplan J, Guerinot ML** (2006) Localization of iron in Arabidopsis seed requires the vacuolar membrane transporter VIT1. *Science* **314**: 1295-1298
- Kirkegaard JA, Munns R, James RA, Neate SM** (1999) Does water and phosphorus uptake limit leaf growth of Rhizoctonia-infected wheat seedlings? *Plant and Soil* **209**: 157-166
- Kobayashi T, Nakayama Y, Itai RN, Nakanishi H, Yoshihara T, Mori S, Nishizawa NK** (2003) Identification of novel cis-acting elements, IDE1 and IDE2, of the barley IDS2 gene promoter conferring iron-deficiency-inducible, root-specific expression in heterogeneous tobacco plants. *Plant Journal* **36**: 780-793
- Kobayashi T, Nishizawa NK** (2012) Iron uptake, translocation, and regulation in higher plants. *Annu. Rev. Plant Biol.* **63**: 131-152
- Kobayashi T, Ogo Y, Itai RN, Nakanishi H, Takahashi M, Mori S, Nishizawa NK** (2007) The transcription factor IDEF1 regulates the response to and tolerance of iron deficiency in plants. *Proc. Natl. Acad. Sci. USA* **104**: 19150-19155
- Kombrink G, Ancillo G, Büchter R, Dietrich J, Hoegen E, Ponath Y, Schmelzer E, Strömberg A, Wegener S** (2001) The role of chitinases in plant defense and plant development. 6<sup>th</sup> International Workshop on PR-proteins. May 20-24, 2001, Spa, Belgium. **Book of abstract**: p.11
- Kwok EY, Severance S, Kosman DJ** (2006) Evidence for iron channeling in the Fet3p-Ftr1p high-affinity iron uptake complex in the yeast plasma membrane. *Biochemistry* **45**: 6317-6327
- Lanquar V, Lelievre F, Bolte S, Hames C, Alcon C, Neumann D, Vansuyt G, Curie C, Schroder A, Kramer U, Barbier-Brygoo H, Thomine S** (2005) Mobilization of vacuolar iron by AtNRAMP3 and AtNRAMP4 is essential for seed germination on low iron. *Embo Journal* **24**: 4041-4051
- Lindsay WL, Schwab AP** (1982) The chemistry of iron in soils and its availability to plants. *Journal of Plant Nutrition* **5**: 821-840
- Liu GS, Greenshields DL, Sammynaiken R, Hirji RN, Selvaraj G, Wei YD** (2007) Targeted alterations in iron homeostasis underlie plant defense responses. *Journal of Cell Science* **120**: 596-605
- Long TA, Tsukagoshi H, Busch W, Lahner B, Salt DE, Benfey PN** (2010) The bHLH transcription factor POPEYE regulates response to iron deficiency in Arabidopsis roots. *Plant Cell* **22**: 2219-2236
- Luna E, Pastor V, Robert J, Flors V, Mauch-Mani B, Ton J** (2011) Callose deposition: a multifaceted plant defense response. *Mol Plant Microbe Interact* **24**: 183-193
- Macur RE, Mathre DE, Olsen RA** (1991) Interactions between iron nutrition and *Verticillium* wilt resistance in tomato. *Plant and Soil* **134**: 281-286

- Malnoy M, Venisse JS, Brisset MN, Chevreau E** (2003) Expression of bovine lactoferrin cDNA confers resistance to *Erwinia amylovora* in transgenic pear. *Molecular Breeding* **12**: 231-244
- Marschner H** (1995) Mineral nutrition of higher plants. Academic Press, London
- Marschner H, Romheld V** (1994) Strategies of plants for acquisition of iron. *Plant and Soil* **165**: 261-274
- Marschner P** (2012) Mineral Nutrition of Higher Plants, Third Edition. Academic Press, London
- Mata CG, Lamattina L, Cassia RO** (2001) Involvement of iron and ferritin in the potato - *Phytophthora infestans* interaction. *European Journal of Plant Pathology* **107**: 557-562
- Mathur RS, Barnett HL, Lilly VG** (1950) Sporulation of *Colletotrichum lindemuthianum* in culture. *Phytopathology* **40**: 104-114
- Mei BG, Budde AD, Leong SA** (1993) *Sid1*, a gene initiating siderophore biosynthesis in *Ustilago maydis* - molecular characterization, regulation by iron, and role in phytopathogenicity. *Proceedings of the National Academy of Sciences of the United States of America* **90**: 903-907
- Mellersh DG, Foulds IV, Higgins VJ, Heath MC** (2002) H<sub>2</sub>O<sub>2</sub> plays different roles in determining penetration failure in three diverse plant-fungal interactions. *Plant Journal* **29**: 257-268
- Miethke M, Marahiel MA** (2007) Siderophore-based iron acquisition and pathogen control. *Microbiol Mol Biol Rev* **71**: 413-451
- Mila I, Scalbert A, Expert D** (1996) Iron withholding by plant polyphenols and resistance to pathogens and rots. *Phytochemistry* **42**: 1551-1555
- Mims CW, Vaillancourt LJ** (2002) Ultrastructural characterization of infection and colonization of maize leaves by *Colletotrichum graminicola*, and by a *C. graminicola* pathogenicity mutant. *Phytopathology* **92**: 803-812
- Mino Y, Ishida T, Ota N, Inoue M, Nomoto K, Takemoto T, Tanaka H, Sugiura Y** (1983) Mugineic acid iron(III) complex and its structurally analogous cobalt(III) complex - characterization and implication for absorption and transport of iron in gramineous plants. *Journal of the American Chemical Society* **105**: 4671-4676
- Moran R** (1982) Formulae for determination of chlorophyllous pigments extracted with *N,N*-dimethylformamide. *Plant Physiology* **69**: 1376-1381
- Moran R, Porath D** (1980) Chlorophyll determination in intact tissues using *n,n*-dimethylformamide. *Plant Physiology* **65**: 478-479
- Mori S** (1999) Iron acquisition by plants. *Current Opinion in Plant Biology* **2**: 250-253
- Munch S, Lingner U, Floss DS, Ludwig N, Sauer N, Deising HB** (2008) The hemibiotrophic lifestyle of *Colletotrichum* species. *Journal of Plant Physiology* **165**: 41-51
- Murata Y, Ma JF, Yamaji N, Ueno D, Nomoto K, Iwashita T** (2006) A specific transporter for iron(III)-phytosiderophore in barley roots. *Plant Journal* **46**: 563-572
- Murgia I, Delledonne M, Soave C** (2002) Nitric oxide mediates iron-induced ferritin accumulation in Arabidopsis. *Plant Journal* **30**: 521-528
- Nairz M, Schroll A, Sonnweber T, Weiss G** (2010) The struggle for iron - a metal at the host-pathogen interface. *Cellular Microbiology* **12**: 1691-1702
- Narusaka M, Shiraishi T, Iwabuchi M, Narusaka Y** (2010) Monitoring fungal viability and development in plants infected with *Colletotrichum*

- higginsianum* by quantitative reverse transcription-polymerase chain reaction. *Journal of General Plant Pathology* **76**: 1-6
- Narusaka Y, Narusaka M, Park P, Kubo Y, Hirayama T, Seki M, Shiraishi T, Ishida J, Nakashima M, Enju A, Sakurai T, Satou M, Kobayashi M, Shinozaki K** (2004) RCH1, a locus in *Arabidopsis* That confers resistance to the hemibiotrophic fungal pathogen *Colletotrichum higginsianum*. *Molecular Plant-Microbe Interactions* **17**: 749-762
- Neilands JB** (1995) Siderophores: structure and function of microbial iron transport compounds. *J Biol Chem* **270**: 26723-26726
- Nikolic M, Romheld V** (2002) Does high bicarbonate supply to roots change availability of iron in the leaf apoplast? *Plant and Soil* **241**: 67-74
- Nikolic M, Romheld V** (2003) Nitrate does not result in iron inactivation in the apoplast of sunflower leaves. *Plant Physiology* **132**: 1303-1314
- Nozoye T, Nagasaka S, Kobayashi T, Takahashi M, Sato Y, Uozumi N, Nakanishi H, Nishizawa NK** (2011) Phytosiderophore efflux transporters are crucial for iron acquisition in graminaceous plants. *Journal of Biological Chemistry* **286**: 5446-5454
- O'Connell R, Herbert C, Sreenivasaprasad S, Khatib M, Esquerre-Tugaye MT, Dumas B** (2004) A novel *Arabidopsis-Colletotrichum* pathosystem for the molecular dissection of plant-fungal interactions. *Molecular Plant-Microbe Interactions* **17**: 272-282
- O'Connell RJ, Thon MR, Hacquard S, Amyotte SG, Kleemann J, Torres MF, Damm U, Buiate EA, Epstein L, Alkan N, Altmuller J, Alvarado-Balderrama L, Bauser CA, Becker C, Birren BW, Chen Z, Choi J, Crouch JA, Duvick JP, Farman MA, Gan P, Heiman D, Henrissat B, Howard RJ, Kabbage M, Koch C, Kracher B, Kubo Y, Law AD, Lebrun MH, Lee YH, Miyara I, Moore N, Neumann U, Nordstrom K, Panaccione DG, Panstruga R, Place M, Proctor RH, Prusky D, Rech G, Reinhardt R, Rollins JA, Rounsley S, Schardl CL, Schwartz DC, Shenoy N, Shirasu K, Siskakolli UR, Stuber K, Sukno SA, Sweigard JA, Takano Y, Takahara H, Trail F, van der Does HC, Voll LM, Will I, Young S, Zeng Q, Zhang J, Zhou S, Dickman MB, Schulze-Lefert P, Ver Loren van Themaat E, Ma LJ, Vaillancourt LJ** (2012) Lifestyle transitions in plant pathogenic *Colletotrichum* fungi deciphered by genome and transcriptome analyses. *Nat Genet* **44**: 1060-1065
- Ogo Y, Kobayashi T, Nakanishi Itai R, Nakanishi H, Kakei Y, Takahashi M, Toki S, Mori S, Nishizawa NK** (2008) A novel NAC transcription factor, IDEF2, that recognizes the iron deficiency-responsive element 2 regulates the genes involved in iron homeostasis in plants. *J Biol Chem* **283**: 13407-13417
- Oide S, Moeder W, Krasnoff S, Gibson D, Haas H, Yoshioka K, Turgeon BG** (2006) NPS6, encoding a nonribosomal peptide synthetase involved in siderophore-mediated iron metabolism, is a conserved virulence determinant of plant pathogenic ascomycetes. *Plant Cell* **18**: 2836-2853
- Olsen RA, Bennett JH, Blume D, Brown JC** (1981) Chemical aspects of the Fe stress response mechanism in tomatoes. *Journal of Plant Nutrition* **3**: 905-921
- Pao SS, Paulsen IT, Saier MH, Jr.** (1998) Major facilitator superfamily. *Microbiol Mol Biol Rev* **62**: 1-34
- Perpetua NS, Kubo Y, Takano Y, Furusawa I** (1996) Cloning and characterization of a melanin biosynthetic *THR1* reductase gene essential

- for appressorial penetration of *Colletotrichum lagenarium*. *Molecular Plant-Microbe Interactions* **9**: 323-329
- Petit JM, Briat JF, Lobreaux S** (2001) Structure and differential expression of the four members of the *Arabidopsis thaliana* ferritin gene family. *Biochemical Journal* **359**: 575-582
- Philpott CC** (2006) Iron uptake in fungi: a system for every source. *Biochim Biophys Acta* **1763**: 636-645
- Pianelli K, Mari S, Marques L, Lebrun M, Czernic P** (2005) Nicotianamine over-accumulation confers resistance to nickel in *Arabidopsis thaliana*. *Transgenic Res* **14**: 739-748
- Ramanan N, Wang Y** (2000) A high-affinity iron permease essential for *Candida albicans* virulence. *Science* **288**: 1062-1064
- Ratledge C, Dover LG** (2000) Iron metabolism in pathogenic bacteria. *Annual Review of Microbiology* **54**: 881-941
- Ravet K, Touraine B, Boucherez J, Briat JF, Gaymard F, Cellier F** (2009) Ferritins control interaction between iron homeostasis and oxidative stress in *Arabidopsis*. *Plant Journal* **57**: 400-412
- Ray PD, Huang BW, Tsuji Y** (2012) Reactive oxygen species (ROS) homeostasis and redox regulation in cellular signaling. *Cell Signal* **24**: 981-990
- Rellan-Alvarez R, El-Jendoubi H, Wohlgemuth G, Abadia A, Fiehn O, Abadia J, Alvarez-Fernandez A** (2011) Metabolite profile changes in xylem sap and leaf extracts of strategy I plants in response to iron deficiency and resupply. *Front Plant Sci* **2**: 66
- Reuveni M, Oppenheim D, Reuveni R** (1998) Integrated control of powdery mildew on apple trees by foliar sprays of mono-potassium phosphate fertilizer and sterol inhibiting fungicides. *Crop Protection* **17**: 563-568
- Reuveni R, Dor G, Raviv M, Reuveni M, Tuzun S** (2000) Systemic resistance against *Sphaerotheca fuliginea* in cucumber plants exposed to phosphate in hydroponics system, and its control by foliar spray of mono-potassium phosphate. *Crop Protection* **19**: 355-361
- Reymond P, Weber H, Damond M, Farmer EE** (2000) Differential gene expression in response to mechanical wounding and insect feeding in *Arabidopsis*. *Plant Cell* **12**: 707-719
- Robinson NJ, Procter CM, Connolly EL, Guerinot ML** (1999) A ferric-chelate reductase for iron uptake from soils. *Nature* **397**: 694-697
- Rogers EE, Guerinot ML** (2002) FRD3, a member of the multidrug and toxin efflux family, controls iron deficiency responses in *Arabidopsis*. *Plant Cell* **14**: 1787-1799
- Romheld V, Marschner H** (1986) Evidence for a specific uptake system for iron phytosiderophores in roots of grasses. *Plant Physiology* **80**: 175-180
- Roschzttardt H, Conejero G, Curie C, Mari S** (2009) Identification of the endodermal vacuole as the iron storage compartment in the *Arabidopsis* embryo. *Plant Physiology* **151**: 1329-1338
- Ryan CA** (1990) Protease inhibitors in plants - genes for improving defenses against insects and pathogens. *Annual Review of Phytopathology* **28**: 425-449
- Schaaf G, Ludewig U, Erenoglu BE, Mori S, Kitahara T, von Wirén N** (2004) ZmYS1 functions as a proton-coupled symporter for phytosiderophore- and nicotianamine-chelated metals. *Journal of Biological Chemistry* **279**: 9091-9096

- Schaible ME, Kaufmann SHE** (2004) Iron and microbial infection. *Nature Reviews Microbiology* **2**: 946-953
- Schmid NB, Giehl RF, Doll S, Mock HP, Strehmel N, Scheel D, Kong X, Hider RC, von Wiren N** (2014) Feruloyl-CoA 6'-Hydroxylase1-dependent coumarins mediate iron acquisition from alkaline substrates in *Arabidopsis*. *Plant Physiology* **164**: 160-172
- Schmidt W** (2003) Iron solutions: acquisition strategies and signaling pathways in plants. *Trends Plant Sci* **8**: 188-193
- Scholz G, Becker R, Pich A, Stephan UW** (1992) Nicotianamine - a common constituent of Strategy-I and Strategy-II of iron acquisition by plants - a review. *Journal of Plant Nutrition* **15**: 1647-1665
- Schrettl M, Bignell E, Kragl C, Sabiha Y, Loss O, Eisendle M, Wallner A, Arst HN, Jr., Haynes K, Haas H** (2007) Distinct roles for intra- and extracellular siderophores during *Aspergillus fumigatus* infection. *Plos Pathogens* **3**: 1195-1207
- Schulze-Lefert P** (2004) Knocking on the heaven's wall: pathogenesis of and resistance to biotrophic fungi at the cell wall. *Current Opinion in Plant Biology* **7**: 377-383
- Seckback J** (1982) Ferreting out the secrets of plant ferritin - a review. *Journal of Plant Nutrition* **5**: 369-394
- Segond D, Dellagi A, Lanquar V, Rigault M, Patrit O, Thomine S, Expert D** (2009) *NRAMP* genes function in *Arabidopsis thaliana* resistance to *Erwinia chrysanthemi* infection. *Plant Journal* **58**: 195-207
- Serrano M, Coluccia F, Torres M, L'Haridon F, Metraux JP** (2014) The cuticle and plant defense to pathogens. *Frontiers in Plant Science* **5**: 274
- Shi R, Weber G, Koster J, Reza-Hajirezaei M, Zou C, Zhang F, von Wiren N** (2012) Senescence-induced iron mobilization in source leaves of barley (*Hordeum vulgare*) plants. *New Phytologist*
- Shi X, Stoj C, Romeo A, Kosman DJ, Zhu Z** (2003) Fre1p Cu<sup>2+</sup> reduction and Fet3p Cu<sup>1+</sup> oxidation modulate copper toxicity in *Saccharomyces cerevisiae*. *J Biol Chem* **278**: 50309-50315
- Shimada C, Lipka V, O'Connell R, Okuno T, Schulze-Lefert P, Takano Y** (2006) Nonhost resistance in *Arabidopsis-Colletotrichum* interactions acts at the cell periphery and requires actin filament function. *Mol Plant Microbe Interact* **19**: 270-279
- Shojima S, Nishizawa NK, Fushiya S, Nozoe S, Irifune T, Mori S** (1990) Biosynthesis of phytosiderophores: in vitro biosynthesis of 2'-Deoxymugineic acid from L-methionine and nicotianamine. *Plant Physiology* **93**: 1497-1503
- Sijmons PC, Kolattukudy PE, Bienfait HF** (1985) Iron deficiency decreases suberization in bean roots through a decrease in suberin-specific peroxidase activity. *Plant Physiology* **78**: 115-120
- Smith MA, Harris PL, Sayre LM, Perry G** (1997) Iron accumulation in Alzheimer disease is a source of redox-generated free radicals. *Proc Natl Acad Sci U S A* **94**: 9866-9868
- Stearman R, Yuan DS, Yamaguchi-Iwai Y, Klausner RD, Dancis A** (1996) A permease-oxidase complex involved in high-affinity iron uptake in yeast. *Science* **271**: 1552-1557
- Sun H, Zhang JZ** (2009) *Colletotrichum destructivum* from cowpea infecting *Arabidopsis thaliana* and its identity to *C. higginsianum*. *European Journal of Plant Pathology* **125**: 459-469

- Takagi S, Nomoto K, Takemoto T** (1984) Physiological aspect of mugineic acid, a possible phytosiderophore of graminaceous plants. *Journal of Plant Nutrition* **7**: 469-477
- Takahashi M, Yamaguchi H, Nakanishi H, Shioiri T, Nishizawa NK, Mori S** (1999) Cloning two genes for nicotianamine aminotransferase, a critical enzyme in iron acquisition (Strategy II) in graminaceous plants. *Plant Physiology* **121**: 947-956
- Trujillo M, Kogel KH, Huckelhoven R** (2004) Superoxide and hydrogen peroxide play different roles in the nonhost interaction of barley and wheat with inappropriate formae speciales of *Blumeria graminis*. *Molecular Plant-Microbe Interactions* **17**: 304-312
- Ueno D, Rombola AD, Iwashita T, Nomoto K, Ma JF** (2007) Identification of two novel phytosiderophores secreted by perennial grasses. *New Phytologist* **174**: 304-310
- Underwood W** (2012) The plant cell wall: a dynamic barrier against pathogen invasion. *Front Plant Sci* **3**: 85
- Vakdevi V, Sashidhar RB, Deshpande V** (2009) Purification and characterization of mycoferritin from *Aspergillus flavus* MTCC 873. *Indian J Biochem Biophys* **46**: 360-365
- Van der Ent S, Verhagen BWM, Van Doorn R, Bakker D, Verlaan MG, Pel MJC, Joosten RG, Proveniers MCG, Van Loon LC, Ton J, Pieterse CMJ** (2008) MYB72 is required in early signaling steps of rhizobacteria-induced systemic resistance in arabidopsis. *Plant Physiology* **146**: 1293-1304
- Van Ho A, Ward DM, Kaplan J** (2002) Transition metal transport in yeast. *Annual Review of Microbiology*, Vol 65 **56**: 237-261
- van Loon LC** (1999) Occurrence and properties of plant pathogenesis-related proteins. *Pathogenesis-related proteins in plants*. Eds. S.K. Datta, S. Muthukrishnan, CRC Press LLC, Boca Raton: 1-19
- van Loon LC, Rep M, Pieterse CM** (2006) Significance of inducible defense-related proteins in infected plants. *Annual Review of Phytopathology* **44**: 135-162
- Vargas WA, Martin JM, Rech GE, Rivera LP, Benito EP, Diaz-Minguez JM, Thon MR, Sukno SA** (2012) Plant defense mechanisms are activated during biotrophic and necrotrophic development of *Colletotricum graminicola* in maize. *Plant Physiology* **158**: 1342-1358
- Vogel JP, Raab TK, Schiff C, Somerville SC** (2002) *PMR6*, a pectate lyase-like gene required for powdery mildew susceptibility in Arabidopsis. *Plant Cell* **14**: 2095-2106
- Vogel JP, Raab TK, Somerville CR, Somerville SC** (2004) Mutations in *PMR5* result in powdery mildew resistance and altered cell wall composition. *Plant Journal* **40**: 968-978
- von Wirén N, Khodr H, Hider RC** (2000) Hydroxylated phytosiderophore species possess an enhanced chelate stability and affinity for iron(III). *Plant Physiology* **124**: 1149-1158
- von Wirén N, Klair S, Bansal S, Briat JF, Khodr H, Shioiri T, Leigh RA, Hider RC** (1999) Nicotianamine chelates both Fe(III) and Fe(II). Implications for metal transport in plants. *Plant Physiology* **119**: 1107-1114
- Von Wirén N, Mori S, Marschner H, Römheld V** (1994) Iron inefficiency in maize mutant *ys1* (*Zea mays* L. cv Yellow-Stripe) is caused by a defect in uptake of iron phytosiderophores. *Plant Physiology* **106**: 71-77



- Wang TP, Quintanar L, Severance S, Solomon EI, Kosman DJ** (2003) Targeted suppression of the ferroxidase and iron trafficking activities of the multicopper oxidase Fet3p from *Saccharomyces cerevisiae*. *Journal of Biological Inorganic Chemistry* **8**: 611-620
- Weinberg ED, Miklossy J** (2008) Iron withholding: a defense against disease. *J Alzheimers Dis* **13**: 451-463
- Werner S, Sugui JA, Steinberg G, Deising HB** (2007) A chitin synthase with a myosin-like motor domain is essential for hyphal growth, appressorium differentiation, and pathogenicity of the maize anthracnose fungus *Colletotrichum graminicola*. *Mol Plant Microbe Interact* **20**: 1555-1567
- Wharton PS, Julian AM, O'Connell RJ** (2001) Ultrastructure of the infection of *Sorghum bicolor* by *Colletotrichum sublineolum*. *Phytopathology* **91**: 149-158
- Woltz SS, Engelhar AW** (1973) Fusarium wilt of chrysanthemum effect of nitrogen source and lime on disease development. *Phytopathology* **63**: 155-157
- Zhang Z, Coyne DP, Vidaver AK, Mitra A** (1998) Expression of human lactoferrin cDNA confers resistance to *Ralstonia solanacearum* in transgenic tobacco plants. *Phytopathology* **88**: 730-734

## 7 Supplementary data

### Supplemental Table 1:

Primers used in this study are listed here.

Primer	Sequence (5' → 3')
ITS2-qPCR-Fw	CGTCGTAGGCCCTTAAAGGTAG
ITS2-qPCR-Rv	TTACGGCAAGAGTCCCTC
M13-qPCR-Fw	GTAAAACGACGGCCAGTGC
M13-qPCR-Rv	CACAGGAAACAGCTATGACC
At-CBP20-Fw	CCTTGTGGCTTTTGTTCGTC
At-CBP20-Rv	ACACGAATAGGCCGGTCATC
Ch-ACT-Fw	GATTCGGTCAAAGACAATCG
Ch-ACT-Rv	CAGCGAGGATTGGAACCTA
ZmDMAS1-Fw	CTCTTCGTCACGTCCAAGGT
ZmDMAS1-Rv	TTCCATCTGGAGATTGCTGA
ZmFER1-Fw	CCTGAGAAAGGAGATGCTCTGTA
ZmFER1-Rv	GATGAAGTCTGTCAGCTGAGGAT
ZmFER2-Fw	GCAATGATCCTCAGCTGATAGAC
ZmFER2-Rv	CTGAAGCAGCATCTGATCAAAG
ZmIDEF1-Fw	TACACCGTGTGGATGGAGAA
ZmIDEF1-Rv	CATGCAATGCAGGACTCAAG
ZmNAS3-Fw	GGTGATCAACTCCGTCATCAT
ZmNAS3-Rv	CCTCCTCCATCTTCTGGTGA
ZmNRAMP3-Fw	ACGCTCGATTGCTTCATCTT
ZmNRAMP3-Rv	CCACCAAACCGATCAGAAGT
ZmPR-1-Fw	ACTGCAAGCTGATCCACTCC

---

ZmPR-1-Rv	CTGTTGGTGTCTGGTTCGTA
ZmPR-4b-Fw	GAACAACCTGGGACCTCAACG
ZmPR-4b-Rv	TTGGTCACCAGGAGACACTG
ZmPR-5-Fw	GCAGCCAGGACTTCTACGAC
ZmPR-5-Rv	ACAGGCATGGGTCTTCATGT
ZmWind-Fw	ACTCGGGCAACAACAAGTTC
ZmWind-Rv	CACAGTACGTGAACCATGCAC
ZmVIT1-Fw	GCTGTTCAGGCGAGGTAGTT
ZmVIT1-Rv	AGATCCCGCGATTAACACTG
ZmYS1-Fw	GAGAATGCGAGATACTGAAGG
ZmYS1-Rv	CATAGGTTGAACCCAACATGAC

---

## 8 Abbreviations

35S	CaMV 35S promoter
-Fe	iron deficient
+Fe	iron sufficient
ALB	anthracnose leaf blight
AP	appressorium
ASR	anthracnose stalk rot
<i>Bgt</i>	<i>Blumeria graminis</i> f. sp. <i>Tritici</i>
CO	conidia
Col-0	Columbia-0, ecotype of <i>Arabidopsis thaliana</i>
CgM2	<i>Colletotrichum graminicola</i> wild-type strain M2
Ch	<i>Colletotrichum higginsianum</i>
CU	cuticle
CW	cell wall
CWA	cell wall apposition
DAB	3,3'-diaminobenzidine
DS	disease score
dpi	days post inoculation
DW	dry weight
EDDHA	ethylenediamine-N,N'-bis(2-hydroxyphenylacetic acid)
EDTA	ethylenediaminetetraacetic acid
Fe	iron (from Latin: ferrum)
FW	fresh weight
GE	germination
hpi	hour post inoculation
ICP-MS	inductively coupled plasma-mass spectrometry
ICP-OES	inductively coupled plasma-optic emission spectrometry
MS	mugineic acid
NA	nicotianamine
n.d.	not detected
n.s.	not significant
PCR	polymerase chain reaction
PH	primary hyphae

---

PM	plasma membrane
PR	pathogenesis-related
PS	phytosiderophore
<i>Pst</i>	<i>Pseudomonas syringae</i> pv. tomato
qPCR	quantitative PCR
qRT-PCR	quantitative real-time PCR
RIA	reductive iron assimilation
ROS	reactive oxygen species
RT	room temperature
SD	standard deviation
SEM	scanning electron microscopy
SIA	siderophore-mediated iron assimilation
SH	secondary hyphae
SP	spore
TEM	transmission electron microscopy
v/v	volume-to-volume ratio
w/v	weight-to-volume ratio
WT	wild type

## 9 Acknowledgements

First of all, I would like to thank Prof. Dr. Nicolaus von Wirén for giving me the opportunity to do my PhD thesis in his research group, all the support and guidance during my work, and also enough freedom to develop as a researcher.

I also would like to thank Prof. Dr. Deising for always being ready for scientific discussions and offering best advices.

Many thanks go to Emad Albarouki for showing me the first step of the wonderful pathomicrobial world, for always kind helping and scientific discussions. Also to Siva for guiding me during the research period and for kind advices.

Of course special thanks to all members of the Molecular Plant Nutrition group. It was great to work together with all of you: Ricardo, Anja, Markus, Ben, Nicole, Diana, Susanne, Bernhard, Claudia, Seckin, Alberto, Elis, Lisa, Julia, Heike, Melanie, Andrea, Seyed, Alex girl and boy, Rongli, Fengying, Polet, Baris, Dima, Sebastian, Zhaojun, Takao, Ying, Ralf, Kai, Stefan, Mo, Dagmar, Christine, Barbara, Cristal, Nunun, Reeza, Wally, Elmarie and everyone else.

I would like to thank Dr. Michael Melzer and his group members Twan, Marion, Kirsten and Monika for their excellent help in microscopy.

I am also very grateful for the support I received in the greenhouse from Mr. Geyer, Mrs. Braun, Mrs. Wackermann, Mrs. Fessel, Mrs. Jacobs, Anke, Andreas and the whole group.

Special thanks to Mrs. Leps for helping in so many administrative issues during my stay at the IPK.

Last but not least, I wish to express my greatest thanks to my wife for all the understanding and patience, to my son for giving me so much fun and happiness.

## 10 Curriculum Vitae

### Personal data

Name: Fanghua Ye  
 Date of birth: 04.05.1975  
 Place of birth: Zhejiang, China  
 Nationality: China  
 Address: Leibniz Institute of Plant Genetics and Crop Plant Research  
 Department of Physiology and Cell Biology  
 Corrensstraße 3, 06466 Gatersleben, Germany  
 Telephone: +49 (0)39482 5798  
 Email: ye@ipk-gatersleben.de

### Education and work experience

05/2010 – now PhD on 'Iron as determinant of virulence and resistance in the maize - *Colletotrichum graminicola* interaction'  
 Molecular Plant Nutrition Group  
 Department of Physiology and Cell Biology  
 Leibniz Institute of Plant Genetics and Crop Plant Research

01/2008 – 04/2010 Project assistant  
 Shanghai Lvle Biotechnology Co., Ltd.

01/2007 – 12/2007 Project assistant  
 Holderhof Produkte AG, Switzerland

04/2002 – 12/2006 Diplom Agrabiologie  
 Diplom thesis in 'Nitrogen use efficiency (NUE) in transgenic tobacco over-expressing the high affinity ammonium transporter AtAMT1;1'  
 Plant Nutrition Institute of the University Hohenheim, Germany

02/2000 – 09/2001 German I, II and DSH  
 Language Center of the University Stuttgart, Germany  
 German College of the University Tongji, Shanghai, China

08/1996 – 01/2000 Teacher and Administrator of laboratory  
 Tashi Center School, Longquan, Zhejiang, China

09/1993 – 07/1996 Bachelor of Biology and Chemistry  
 Lishui Normal University, Lishui, Zhejiang, China

## Publications

**Ye F**, Albarouki E, Lingam B, Deising HB, von Wirén N (2014) An adequate Fe nutritional status of maize suppresses infection and biotrophic growth of *Colletotrichum graminicola*. *Physiologia Plantarum* 151: 280-292

Albarouki E, Schafferer L, **Ye F**, von Wirén N, Haas H, Deising HB (2014) Biotrophy-specific downregulation of siderophore biosynthesis in *Colletotrichum graminicola* is required for modulation of immune responses of maize. *Molecular Microbiology* 92: 338-355

Yuan L, Loque D, **Ye F**, Frommer WB, von Wirén N (2007) Nitrogen-dependent posttranscriptional regulation of the ammonium transporter AtAMT1;1. *Plant Physiology* 143: 732-744

## Participation in scientific conferences during the PhD study

Iron as a determinant of virulence and resistance in the maize–*Colletotrichum graminicola* interaction;  
17<sup>th</sup> International Symposium on Iron Nutrition and Interactions in Plants (ISINIP), Gatersleben, Germany, 06.-10.07.2014

Iron as a determinant of virulence and resistance in the maize–*Colletotrichum graminicola* interaction;  
17<sup>th</sup> International Plant Nutrition Colloquium (IPNC), Istanbul, Turkey 19.-22.08.2013

An adequate Fe nutritional status suppresses the biotrophic growth of *C. graminicola* in maize;  
9<sup>th</sup> Plant Science Student Conference (PSSC), IPB Halle 28.-31.05.2013

Iron in plant-pathogen interaction;  
Interdisciplinary-Center of Crop Plant Research (IZN), Halle Annual Report 11.-12.10. 2012

Iron as a determinant of virulence and resistance in the maize–*Colletotrichum graminicola* interaction;  
Botany Congress, Berlin 19.-22.09.2011

## Supervision activity

Supervision of a bachelor student for research topic 'The influence of iron nutritional status in *Arabidopsis thaliana* on the susceptibility to *Colletotrichum higginsianum*' (10.2013 - 01.2014)



## 11 Affirmation

I hereby declare that the submitted work has been completed by me, the undersigned, and that I have not used any other than permitted reference sources or materials or engaged any plagiarism. All the references and the other sources used in the presented work have been appropriately acknowledged in the work. I further declare that the work has not been previously submitted for the purpose of academic examination, either in its original or similar form, anywhere else.

Hiermit erkläre ich, dass ich diese Arbeit selbständig verfasst und keine anderen als die angegebenen Quellen und Hilfsmittel verwendet habe. Die den benutzten Hilfsmitteln wörtlich oder inhaltlich entnommenen Stellen habe ich unter Quellenangaben kenntlich gemacht. Die vorliegende Arbeit wurde in gleicher oder ähnlicher Form noch keiner anderen Institution oder Prüfungsbehörde vorgelegt.

Fanghua Ye

Gatersleben, 28<sup>th</sup> March, 2015